ACIBADEM MEHMET ALI AYDINLAR UNIVERSITY
INSTITUTE OF HEALTH SCIENCES

DESIGN OF CELL-LOADED MICROCAPSULE FOR CELLULAR THERAPY

MEHMET ALİ KARACA
PH.D. THESIS

DEPARTMENT OF MEDICAL BIOTECHNOLOGY

SUPERVISOR
Assist. Prof. Özgül Gök Özatay

ISTANBUL-2023

ACIBADEM MEHMET ALI AYDINLAR UNIVERSITY
INSTITUTE OF HEALTH SCIENCES

DESIGN OF CELL-LOADED MICROCAPSULE FOR CELLULAR THERAPY

MEHMET ALİ KARACA

PH.D. THESIS

DEPARTMENT OF MEDICAL BIOTECHNOLOGY

SUPERVISOR
Assist. Prof. Özgül Gök Özatay

ISTANBUL-2023

Department:	Institute of Health Science
Program:	Medical Biotechnology Doctorate Program
Thesis Title:	Design of Cell Microcapsule for Cell Therapy
Student's name and Surname:	Mehmet Ali Karaca
Date of Defence:	18 /08/2023

This is to certify that I have examined this copy of Ph.D thesis. I have found that she/he prepared after fulfilling the specified requirements in the associated legislations before the final examining committee whose signatures are below.

Jury Member (Head of the Defense)	Prof. Gamze Torun Köse Yeditepe University	_____
Jury Member (Thesis Supervisor)	Assist. Prof. Özgül Gök Özatay Acıbadem Mehmet Ali Aydınlar University	_____
Jury Member	Prof. Özge Can Acıbadem Mehmet Ali Aydınlar University	_____
Jury Member	Assist. Prof. Ceyhun Ekrem Kırımlı Acıbadem Mehmet Ali Aydınlar University	_____
Jury Member	Assist. Prof. Derya Dilek Kancağı Fenerbahçe University	_____

DECLARATION

I declare that this thesis work is my own work, I had no unethical behavior at any stages from the planning to the writing of the thesis, I obtained all the information in this thesis in accordance with academic and ethical rules, I cited all the information and comments that were not obtained with this thesis work, and I provided resources in the list of references. I also declare that there was no violation of any patents and copyrights during the study and writing of this thesis.

18.08.2023
Mehmet Ali Karaca

PREFACE AND ACKNOWLEDGEMENT

First or foremost, I would like to express my special appreciation and thanks to my academic and industry advisors Assist. Prof. Dr. Özgül Gök Özatay and Prof. Dr. Ercüment Ovalı for their invaluable guidance, continuous support, and motivation, giving a chance to be part of their team throughout my PhD period, supervision of my thesis as well as scientific and personal suggestions. It was great pleasure for me to work with them and with their research groups provided me invaluable experiences and courage to work harder for further achievements. I should also thank Prof. Dr. Ercüment Ovalı to me part in TUBİTAK 2244-Industrial PhD program (Project Code: 118C082). I would like to thank TUSEB (Healthy Institutes of Türkiye), for their financial support (Project Code: 16572) during my PhD thesis.

I acknowledge to Chairman of Board of Truestees of Acıbadem Mehmet Ali Aydınlar University Mr. Mehmet Ali Aydınlar, board of directors in Acıbadem Mehmet Ali Aydınlar University and Chancellor of Acıbadem Mehmet Ali Aydınlar University Prof. Dr. Ahmet Şahin for giving me the opportunities and resources needed to pursue quality doctoral education. I would like to extend my thanks to my jury committee Prof. Dr. Gamze Torun Köse, Prof. Dr. Özge Can, Prof. Dr. Uğur Özbek (previous academic advisors), Assoc. Prof. Dr. Beste Kınıkoğlu (previous committee member), and Assist. Prof. Dr. Derya Dilek Kancağı for their support, advice, and for their careful and constructive review of the final manuscript. I greatly acknowledge Prof. Dr. Gamze Torun Köse from Yeditepe University for providing hFOB 1.19 cell lines.

I would also give my thanks to Prof. Dr. Fatma Yeşim Işıl Ulman, Assoc. Prof. Dr. Gülen Melike Demirpolat, Dr. İnci Kurt Celep, Assist. Prof. Evren Kılınç, Assist. Prof. Timur Hakan Barak, Assoc. Prof. Devrim Öz Arslan, and Assoc. Prof. Günseli Bayram Akçapınar for their professional directions and personal warm contact.

I would like to express my deepest gratitude to MSc. İhsan Yozgat and MSc. Gökhan Kemer for their kind friendship, motivations on me, their endless moral

supports, and patient during PhD education period. I very enjoyed working at Acıbadem Labcell Production Department, and would like to thank Dr. Derya Dilek Kancağı, Dr. Cihan Taştan, Dr. Dilek Turan, Dr. Selen Abanuz Eren, Dr. Sevdican Üstün Yılmaz, MSc. Didem Çakırsoy, MSc. Utku Seyis, MSc. Muhammed Yılancı, MSc. Ömür Selin Günaydın, MSc. Bulut Yurtsever, Dr. Cansu Hemşinlioğlu, MSc. Gözde Karakuş, MSc. Rengim Vural, MSc. Fatma Eyüpoğlu Ünüvar, Muammer Elek, Uğur Kızılsu, Merve Şimşek, Zeynep Torun, Ayzen Özer Elibol, Murat Besdil, and Recai Kuzey for their friendship and technical support. I also would like to thank Gök Research Group members MSc. Elif Gülin Ertuğral, MSc. Ali Murad Özmen, MSc. İrem Soyhan, MSc. İleyna Sevde Üvak, MSc. Rabia Güner, Beyza Dönmüş, Deniz Göl, Emine Durukan, and Berna Ateş, for their support and encourage me.

Last but not least, my deepest heart-felt gratitude my father Ercan Karaca, my mother Asiye Karaca and my sisters Özlem Karaca, Hatice Büşra Karaca, and Hilal Zeynep Karaca for their lifetime support, help and patient. I could not overcome any difficulties without their help and love behind me and I could not finish my educational life without their support. Thank you to be my wonderful family for their unconditional love and support.

This study has been supported by TUSEB (Healthy Institutes of Türkiye) with project number 16572 and TUBITAK (The Scientific and Technological Research Council of Türkiye) with project number 118C082 and 2244-Industry Doctorate Program.

TABLE OF CONTENTS

LIST OF ABBREVIATIONS AND SYMBOLS

Abbreviation	Explanation
Abeta	Amyloid-Beta
AD	Alzheimer Disease
ALP	Alkaline Phosphatase
ASCs	Adult Stem Cells
α-SMA	Alpha Smooth Muscle Actin
BCA	Bicinchoninic Acid Assay
β-cell	Pancreatic Islet Cell
BET	Betulin
BMPs	Bone Morphogenetic Protein
CPC	Calcium Phosphate Cement
CPP	Cell-Penetrating Peptide
CSC	Cardiac Stem Cell
DA	Deacetylation Degree
dECM	Decellularized Extracellular Matrix
EB	Embryonic Body
ELP	Elastine Like Polypeptide
ESC	Embryonic Stem Cell
FGF-2	Fibroblast Growth Factor
GF	Growth Factors
GFP	Green Fluorescence Particles
hMSC	Human Mesenchymal Stem Cell
HSA	Human Serum Albumin
hUCMSC	Human Wharton's Jelly Mesenchymal Stem Cell
IL-6	Interleukin 6
L929	L Strain Clone 929
mESC	Mouse Embryonic Stem Cell
MSC	Mesenchymal Stem Cell
PBS	Phosphate Buffer Saline
PCL	Polycaprolactone

PDGF	Platelet-Derived Growth Factor
PEG	Poly Ethylene Glycol
PEO	Poly Ethylene Oxide
PLA	Polylactic Acid
PLGA	Polylactic-Co-Glycolic Acid
PLL	Poly-L-Lysine
PPO	Polypropylene Glycol
RGD	Arginine-Glycine-Aspargine
SELP	Silk Elastin Like Proteins
SLP	Silk Like Polypeptides
TUBITAK	The Scientific and Technological Research council of Türkiye
TUSEB	Healthy Institutes of Türkiye
VEGF	Vascular Endothelial Growth Factor
VPG	Valine-Proline-Glycine

LIST OF FIGURES

ÖZET

Hücresel Tedavi İçin Hücre Mikrokapsülü Dizaynı

Polimerik malzemeler kullanılarak biyomimetik kapsüllerin oluşturulması, kök hücreleri izole etmenin, onları çevresel etkilerden korumanın, allogreft reddini ortadan kaldırmanın ve hücresel tedavinin etkinliğini artırmanın bir yoludur. Bu çalışmanın ilk bölümünde, fibroblastlar (L929) ve mezenkimal kök hücreler, 12 güne kadar inkübasyon için in vitro koşullar altında aljinat ve aljinat-jelatin mikro boncuklar içine kapsüllendikten sonra gelişmiş canlılıkları ve işlevsellikleri araştırıldı. Bu nedenle, elektrostatik destekli püskürtme tekniği ile üniform ve enjekte edilebilir (<200 um) hücre yüklü mikro boncuklar oluşturulmuştur. Sonuçlar, mikro boncuklar içindeki L929 ve MKH hücrelerinin inkübasyon süresince metabolik aktivitelerini sürdürdüklerini gösterdi. Her iki hücre hattının glikoz tüketimi ve laktik asit üretim seviyeleri tutarlı bir şekilde gözlemlendi. 12. günde salınan hücre sayısının 0. güne göre arttığı bulundu. Kök hücre tedavisinin BET ek tedavisi ile kombinasyonu, kemiğin yeniden şekillenmesi ve yeni kemik dokusu oluşturulması için yeterli tedaviyi sağlayabilir. Aljinat-jelatin ve betulin'in hFOB 1.19 hücresinin canlılığı, işleyişi ve osteojenik farklılaşması üzerindeki etkisi in vitro koşullar altında 12 günlük inkübasyona kadar araştırıldı. Sonuçlara göre, 1 µM'den fazla betulin konsantrasyonu, 2B hücre kültüründe hFOB 1.19 hücreleri üzerinde sitotoksisite göstermektedir. AlJel mikroboncuklarının içindeki hFOB 1.19 hücresi, 1 ve 5 µM BET konsantrasyonunda 12 güne kadar işlevselliklerini sürdürmüştür. Osteogenik belirteçlerin ifadesi, 2B hücre kültüründe hFOB 1.19 ile karşılaştırıldığında betulin'in hFOB 1.19 yüklü AlGel mikroboncukları üzerinde daha fazla osteoindüktif etki göstermiştir.

Anahtar Sözcükler: Mikroenkapsülasyon, Aljinat mikroboncukları, Aljinat-Jelatin mikroboncukları, Osteojenik Farklılaşma, Betulin

ABSTRACT

Design of Cell Microcapsule for Cell Therapy

Construction of biomimetic encapsulates using polymeric materials is way to isolate stem cells, protect them from environmental effects, eliminate allograft rejection, and increase the efficiency of cellular therapy. First part of in this study, fibroblasts (L929) and MSCs were investigated for their improved viability and functionality once encapsulated inside the alginate and alginate-gelatin microbeads under in vitro conditions for up to 12 days of incubation. Thus, uniform and injectable (<200 µm) cell-loaded microbeads were constructed by the electrostatically assisted spraying technique. Results showed that both L929 and MSCs cells continue their metabolic activity inside the microbeads during the incubation periods. Glucose consumption and lactic acid production levels of both cell lines were consistently observed. The released cell number on day 12 was found to be increased compared to day 0. Combination of the stem cell therapy with BET supplement treatment might provide sufficient therapy to bone remodeling and construction new bone tissue. The effect of alginate-gelatin (AlGel) and betulin on viability, functioning, and osteogenic differentiation of hFOB 1.19 cell was investigated under in vitro conditions up to 12 days of incubation. According to result, more than 1 µM concentration of betulin exert cytotoxicity on hFOB 1.19 cells in 2D cell culture. hFOB 1.19 cell inside the AlGel microbeads continue their functionality up to 12 days at 1 and 5 µM concentration of BET. Expression of osteogenic markers indicate more osteoinductive effect of betulin on hFOB 1.19 loaded AlGel microbeads compared with hFOB 1.19 in 2D cell culture.

Keywords: Microencapsulation, Alginate microbeads, Alginate-Gelatin microbeads, Osteogenic Differentiation, Betulin

1 INTRODUCTION AND AIM

Cell therapies are used to regenerate tissue, increase the efficiency of the cancer therapy, and produce specific growth factors (GF) after injection of the cells inside the body. However, direct injection of stem cells presents the syringe needle flow force which disrupt the cell membrane and decrease the viability of transplanted cells ranging from 1% to 32%. Viability of the transplanted cells post injection is crucial for efficiency of injectable cell-based therapies at injured side. Cell viability rate post injection might be improved by encapsulation of cells with hydrogels which protect to cells from damaging effect of extensional forces by direct injection. On the other hand, previous study on effect of alginate hydrogel derivatives on stem cells indicate that composition of alginate hydrogel is not only modifies chemical and physical properties of hydrogel, but also effect to cellular response and efficiency of injectable cell-based therapies. Previous studies showed that the AlGel microbead provides more intact microbead formation compared to the alginate form. In this study, we aim to provide more biomimetic culture conditions for stem cells which potentially ensure more protein secretion and high cell proliferation during the 12 days of incubation time, which would be an enough time for cellular therapies in general.

Bringing biopolymers of alginate and gelatin together enhance performance, and quality of microscaffolds and simulate signaling cascades related to ossification, osteogenic differentiation, and proliferation of the cells. Combinations of biopolymers by addition of gelatin to alginate microbeads makes microbeads more applicable for proliferation and differentiation of osteoblast cells. A recent study showed that adipose-derived stem cells loaded microbeads might be used for cell-based bone tissue regeneration (Leslie et al., 2017). On the other hand, some triterpenoids such as betulin derivatives improve osteogenic differentiation of some murine cells in osteogenic condition in vitro. Moreover, porcine chondrocyte inside the betulin treated scaffolds induce expression of anabolic genes, catabolic genes, and differentiation factors. Although, osteogenic activity of betulin (BET) on murine osteoblast models is confirmed in vitro, there is limited number of studies examined the effect of BET and 3D microenvironments on osteoblast cell models for in vitro research. In this study,

osteogenic differentiation of hFOB 1.19 cell lines inside the combinations of biopolymers of alginate and gelatin microbeads is examined upon treatment with BET.

2 BACKGROUND

Cell therapy is an attractive strategy for the regeneration of tissue and the regulation of growth hormone levels inside the body. Cell transplants are clinically used treatment on various diseases such as neurodegenerative disease, rheumatologic disease, orthopedic disease, endocrine disease, and cardiovascular disease (Kim et al., 2019). Cells that are transplanted via injection into blood veins or target tissue get into body circulation via veins and disperse within the tissue. Cells dispersion within the tissue decrease the cell survival rate and efficiency of the cell therapy. Additionally, cell transplants might be degraded by the patient's immune cells after transplantation inside the patient body. The activity of cell transplants is inhibited, and metabolic activity of the cell transplants is decreased by an immune reaction. Cell dispersion within the tissue and degradation by the immune reaction are the main disadvantages of cell therapy.

Research on encapsulation of cells shows that membrane, used for encapsulation of the cells, acts as a barrier to the immune cell can eliminate the degradation of the cells by the body's immune response. Consequently, cell transplants might be long-term survival inside the patient body after encapsulation (Evron et al., 2018). Previous studies showed that cells might be encapsulated with different kinds of polymeric materials. Polymeric materials might increase the retention time of the cellular population at the target site of the patient body, and provide more effective tissue regeneration therapy, decreasing the time of the therapy.

Biomaterials such as polymeric, ceramic, or composite are commonly used in biomedical applications (Hinderer et al., 2015). Most used biomaterials in medical applications are classified according to types such as natural, synthetic, blended forms of biomaterials.

Naturally sourced biomaterials have a wide range of physical, chemical, and adjustability properties compared with other types (Huang et al., 2019), (Guo et al., 2019). They might be formed in different shapes and structures such as fiber formation.

Fiber formation of polymers mimics the extracellular matrix structure of tissue and cells might be easily attached to fiber formation of polymer which are used as a tissue scaffold (Luo et al., 2019). Construct of tissue-like scaffolds with various polymeric materials is the strategy to replacement of the defect tissue with construct of tissue-like scaffold. Thus, biomaterials in biomedical applications should be biocompatible for biological molecules and shouldn't cause long-term inflammatory responses inside the body post transplantation (Liu vd., 2013).

Regenerative therapy mainly focuses on regeneration of the damaged tissue and reducing the inflammatory response of the patient. Biomaterials in regenerative therapy are be categorized according to their biological properties, chemical properties, and mechanical structure of the tissue. The main aim of regenerative medicine is the construction of the scaffold which mimics to extracellular matrix structure of the target tissue. Various types of polymers might be used to increase regeneration of the damaged tissue and interaction between the cells and tissue. An inflammatory response (inflammation) to biomaterial inside the body varies according to natural and synthetic sources.

2.1 Encapsulation Technology in Cell Therapy

The complexity of the tissue-specific architecture limits the construction of biomimetic scaffolds to induce cellular process in vitro. Biomimetic scaffold should contain many regulatory elements and signaling pathways that have a role in the cellular process in vitro. Cell transplantation to the patient is a more attractive strategy to regenerate tissue. Transplanted cells maintain their functioning and secrete proteins and hormones at specific sides. Transplanted cells might be isolated from the patient's own body (autologous cells) or donor (allogeneic cells) and also these stem cells are capable to differentiate into specific cells by regulation of environmental factors (Shah, 2013). The other classification of stem cells is a source of the cells which are embryonic stem cells (ESCs) or adult stem cells (ASCs) (Liu & Chang, 2010).

Isolation of the autologous stem cells from the patient which requires additional surgery is another challenge for cell therapy. Allogenic and xenogeneic sources for isolation of the stem cell from a donor are alternative strategies in regenerative medicine. In these strategies, allogeneic and xenogeneic sources cells used in cellular therapy cause immunological response inside the patient body after transplantation of cells to a patient. The immunological response inside the body activates the immune cells which degrade the transplanted cells and decrease the efficiency of the cellular therapy. On the other hand, autologous stem cells are isolated from the patient's own body (adipose tissue or bone marrow) might be used for increasing the therapeutic efficiency (Leslie et al., 2017). Thus, autologous stem cells are more applicable cells for therapeutic approaches compared with other cell types and it does not provide any immune response into the patient body. While immunosuppressive and immunosuppressant drugs eliminate the immune response, but long-term usage of immunosuppressive and immunosuppressant drugs causes an undesirable side effect on the patient body (Freimark et al., 2010; Gasperini et al., 2014).

Immobilization of the cells inside the capsule form might overcome the immune reaction post injection. Encapsulated cells with biomaterials are long-term functional and protected from degradation by immune reaction post injection (Song & Roy, 2016). Moreover, diffusion of macromolecules from capsule is illustrated with various encapsulation strategies (Evron et al., 2018). Protein therapy via cell transplantation is a more popular strategy in the clinic. Protection of cells from degradation by immune reaction increases the efficiency of the cell therapeutic approach.

Peripheric fibrosis decrease the efficiency of cell therapy and long-term functionality of the transplanted cells into the patient's body. Peripheric fibrosis block metabolic activity of the transplanted cells into the body. The peripheral fibrotic response might be reduced by applying immunosuppressive drugs to increase the long-term functionality of the transplanted cells. While, presence of peripheral fibrotic growth on the surface of the cell-loaded microbeads is also observed (Ludwig & Ludwig, 2015), cells inside the microbeads can continue to long-term functionality inside the patient body.

The other limitation of cell therapy is that distribution of the cells post injection. Cell transplants distribute at target location and mixed with body circulation. Thus, cell transplant is not effectively regenerate the target side of the patient because of the localization problem. Localization of the transplanted cells at the target tissue might be achieved by various kinds of polymeric scaffolds and strategies especially with microencapsulation of the autologous stem cells. Encapsulation of cells might localize at a specific side of the porous polymeric network. Localization of the autologous stem cells with different kinds of polymeric scaffolds and strategies increases the therapeutic efficiency inside the patient body.

Various polymers were used to construct capsule formation to immobilize the cell inside the capsule. This polymeric formation might be isolated from a natural or synthetic source.

2.2 Polymers Used in Encapsulation Technology

2.2.1 Synthetic polymers

Synthetic polymers are used in a wide variety of applications side in today. They are also used for encapsulation technologies and tissue engineering applications. Synthetic polymers are good mechanical properties, low toxicity inside the body, cheap, and long-term usage when they are compared with natural polymers. Synthetic polymers might be blended with natural polymers to form desired properties of the materials. This blended formation of the polymers displays desired properties in both natural and synthetic biomaterials. Polycaprolactone poly(L-lactide-co-e-caprolactone), polyethylene oxide, and hydroxyapatite are examples of synthetic materials. While some of them contain polyester and organic structure, they are low biocompatibility and biodegradability inside the body.

Synthetic polymers are highly hydrophobic polymers, and their blended formation is commonly used in cell culture research for binding of the cell to the material surface and *in vitro* biocompatibility of the materials (B. Y. Wang vd., 2012). Previous

research showed that blended scaffold (alginate/polyethylene oxide) increases the attachment of the fibroblast cells on scaffolds and proliferation capacity on it (1). Synthetic polymers were classified into 4 different groups such as polyethers, polyesters, poloxamers, recombinant protein-based polymers.

2.2.1.1 Polyether

Polyether contains more than one ether group in its molecular structure. It is a synthetic polymer because of the functionality of the ether group in the main chain. The most used candidate of the polyether is polyethylene glycol (PEG) which is used in the pharmaceutical industry. Polyethylene glycol (PEG) is highly water-soluble, and it might be conjugated with proteins. This procedure is called PEGlyation. Physicochemical properties of the proteins or peptides are altered such as enzymatically degradation, immunogenicity, or residence time after PEGlyation of the proteins or peptides. On the other hand, the copolymer form of PEG (PEG-PLA-based copolymer) exhibits thermo-reversible ability. The other copolymer structure is PEG with polycaprolactone (PCL). PEG-PCL copolymer is formed because of the low degradation rate and high hydrophobicity of the PCL. Moreover, scientists construct the PEG-PCL-PEG which shows sol-gel-sol transition behavior. PEG/PCL ratio regulates the thermo-reversible behavior or the copolymer.

2.2.1.2 Polyesters

Polyesters contain more than one ester group in their molecular structure. It is a type of synthetic polymer because of the functionality of the ester group in their main chain. There are many esters used in drug delivery applications and therapeutic approaches. Polylactic-co-glycolic acid (PLGA) is one of the co-polymer that combination of poly-lactic acid (PLA) and polyglycolic acid (PGA). Degradation of the PLGA has occurred with the hydrolysis of the ester linkages. PLGA is a very biocompatible but easily degradable polymer. Various types of copolymers were designed to overcome the shortcoming of the polymer. These copolymers are PLGA-PEG, PLGA-PEG-PLGA, PEG-PLGA-PEG. These block copolymers are like thermo-

reversible block copolymers. They are gel form at body temperature, and they have flowing properties at or below room temperature. PEG-PLGA-PEG block is generally used for encapsulation of the therapeutic product. Gelation properties of the PEG-PLGA-PEG might be changed with alteration of the PEG-PLGA-PEG copolymer. These designed block copolymers are well biodegradable, and their biodegradability is clearly described with different studies (2), (3). Block copolymeric system is widely used for different therapeutic approaches.

2.2.1.3 Poloxamers

Poloxamers are classified as non-ionic triblock co-polymers compose of polypropylene oxide (PPO), and polyethylene oxide (PEO). Polypropylene oxide (PPO) place's central part and PEO which is hydrophilic surround the PPO. Poloxamers are also called a pluronic in trade (4,5). They have a thermosensitive property, been used in sustained delivery of therapeutic proteins (6–8). Poloxamers which are inert were used to maintain the stability of the incorporated therapeutic proteins and they increase their survival period as compared with sustained-release drug delivery (9) (10). Moreover, poloxamers were used to deliver the therapeutic substance to the target side. Pluronic F127 (PF127) is the most used polymer type for the effective delivery of molecules to the target side.

2.2.1.4 Recombinant protein based polymer

Recombinant Protein-Based Polymers (genetically modified polymers) were used to deliver desired molecules to the target side. In some therapeutic approaches, desired properties of the protein-based polymer might be designed using genetic engineering tools. Target molecules might easily be absorbed in the target side after designing the genetically modified polymers. The most widely used genetically engineering polymer examples are CPPs, transferrin, lectins, and silk-elastin-like protein (SELP) (11,12). These polymers contain repeated amino acid sequences which genetically engineered, and these are produced in a biological organism. Designed genetically engineered polymers are naturally degraded by different pathways.

Targeting of the large molecular weight and poorly permeable therapeutic proteins to the cells might be increased by ***cell-penetrating peptides (CPPs)***. Cell-penetrating peptides might be used in different strategies such as lipid bilayer of the cell to perform the endocytosis process of the therapeutic proteins and peptides into the cytoplasm. Moreover, therapeutic proteins might be delivered with cell-penetrating peptides such as intestinal absorption of the insulin molecule. Delivery of the various macromolecule inside cells was evaluated with different studies (13,14).

2.2.1.5 Transferrin

Transferrin is the type of glycoprotein and receptors. It is highly expressed on the intestinal epithelial cells. It has different properties such as endogenous iron-binding. For this reason, transportation of the iron element via a transferrin receptor might be performed with the endocytosis process within the cells. Additionally, the transferrin receptor on the intestinal epithelial cells might provide absorption of drug molecules. Different molecules such as insulin and human growth hormone might be absorbed via transferrin receptors (15,16).

2.2.1.6 Silk elastin like protein

Silk elastin-like proteins (SELPs) consist of recombinant silk-like proteins obtained from bombyx mori silkworm (GAGAGS) and elastin-like proteins obtained from mammalian trophoblastic (GVGVP) (11). The number and sequence of the repeats organize the physicochemical properties of the SELPs. SELPs ,which is the soluble form in nature, might be densely cross-linked with hydrogels to form an irreversible phase transition state. Each part of the SELPs has a role in the mechanical stability of the gel. The silk part of the SELPs gives viscoelastic properties and the elastin part ensures the viscoelastic behavior of the gel. Mechanical properties of the silk-elastin-like proteins balance the hydrogel network formed by SELPs. SELPs concentration also controls the releasing of some therapeutic proteins which have unique charge on the released agents (17), (18).

2.2.2 Natural polymers

Natural polymers can be used to enhance the efficiency of cellular therapies due to their biocompatibility and biodegradability properties. Source of biomaterials alter the polymeric structure of the natural polymer. Natural polymers are isolated from biological sources such as a microorganism, plants, or animals. The most valuable and remarkable property of a natural polymer is a structural similarity between the human tissue and easy integration with damaged tissue, biocompatibility, and biodegradability (19).

Various types of natural polymers are used in encapsulation technology to fabricate microbeads. Naturally sourced biomaterials mimic extracellular matrix structure and increase the metabolic activity of the cells in cell encapsulation technology. Artificial tissue structures are constructed with natural sources materials such as proteins (collagen, gelatin, silk..), polysaccharide (cellulose, chitin/chitosan, glucose..), and glycosaminoglycans (heparan sulfate, and keratan sulfate). Artificial tissue is commonly used in cell therapy for regeneration of the damaged tissue after cellularization of the artificial tissue. Cell transplants are protected from immunological response within the construction of the closed fibril formation loaded with extracellular matrix sourced materials (20).

Encapsulation technology might provide a highly hydrophilic environment and higher water holding capacity in a 3-dimensional construct. Cells inside polymeric microbeads might be more viable and have long-term functioning (21). Natural polymers are more applicable for cell encapsulation study because of their different properties such as highly soft, more porous structure, low protein adsorption after transplantation, and providing a low interface between the fluids compared to synthetic polymers (22). Natural polymer-based microbeads are commonly used techniques in cell therapy. It has different properties such as easy interaction with the injection side, high biocompatibility inside the patient body, good inflammation response, and high regeneration capacity inside the damaged tissue. Natural polymers were grouped into two main categories. The first group of natural polymers is polysaccharides.

2.2.2.1 Polysaccharides

Polysaccharides are the type of carbohydrate located inside the extracellular matrix structure and have fundamental roles in biological processes in nature. Polysaccharides are consisting of sugar rings which are linked by glycosidic bonds. Glycosidic bonds might be easily degradable with glycoside hydrolase enzyme. They have a positive charge at their ammonium group (NH^{3+}) and negatively charged at their carboxylic groups (COO^{-}) and sulfate group (SO^{-3}). Interaction between the charged group and self-assembly of the polysaccharides chain gives their original shape. Polysaccharides were used in different technologies such as cell encapsulation technologies and tissue engineering applications (23). Polysaccharides might be isolated from different sources in nature such as sea moss, plant cells (alginate), animal sources. Naturally sourced polymers such as pectin, chitosan, agar, carrageenan, and alginate. Natural polymers might be classified their charged state such negatively charged alginate and positively charged chitosan.

Negatively charged alginate is a type of natural polymer used in pharmaceutical, textile, food, and biotechnological industries (24), (25). It has a linear polysaccharide structure and a 1,4-glycosidic bonding structure between the α-l-guluronic acid (G) and β-d-mannuronic acid side (M). Sequence and ratio MG blocks characterize alteration of alginate in nature especially upon the organism (26). The affinity of the alginate to the multivalent cations (Mg^{2+}, Ca^{2+}, Sr^{2+}, Ba^{2+}) enhances with increasing of α-l-guluronic acid (G) content because of the ionic interaction of multivalent cations with guluronic acid blocks. This process is described as an “egg-box” model. Alginate has unique gel properties, physical and chemical stability, crosslinking structure, biocompatibility, low toxicity, easy sterilization, low cost, and soft gelatinating process (27). However, the chemical and physical properties of alginate might be changed by many parameters such as ionic strength of the medium, gelling ions concentration, pH of the solution. Deprotonation of the carboxylic acid group might occur at a certain value of the pH. Deprotonation of a carboxylic group enhances the dissolving rate of the alginate in the solution. On the other hand, alginic acid is not completely soluble in any solvent such as water. A sodium-alginate solution is a

soluble form of alginate in waters. The solubility of the sodium alginate might be changed with increasing of the pH. Sodium-alginate might be precipitated and formed as an alginic acid via increasing the pH value. Precipitation of the sodium-alginate depends on the homopolymeric blocks and molecular weight of the polymer (28). 3D network of the alginate might be formed by the simple procedure of ionic bonding. Multivalent cations diffuse inside the alginate solution and these ions might be released by pH variation of the microenvironment (29). For that reason, more complex polymeric materials were designed to control the mechanical and swelling properties of the materials (30), (31). Additionally, alginate has limited stability *in vivo* conditions (ion exchange in physiological conditions). Different crosslinking agents were used to construct covalent crosslinks such as glutaraldehyde (32) hexamethylene diisocyanate (33). Oxidation of the hydroxyl groups at C-2 and C-3 might modify alginate. Oxidation with periodates construct to the formation of dialdehyde at each oxidized monomer unit. This form of alginate derivatives has more labeling capacity with an increased degradability and these derivatives can easily attach to substituents or reductive agents by the reductive amination process. The reductive amination process between the dialdehyde and alkyl amine is performed via reduction agents such as sodium borohydride ($NaBH_4$) and cyanoborohydride ($NaCNBH_4$). In this method, long alkyl chains might be introduced to alginate derivatives and new alginate derivatives which have various physical and chemical properties might be obtained. One of the studies showed that the alginates have higher biocompatibility and pore dimensions when it is grafted with low molecular weight polyethylene glycol (PEG) (34). Hydroxyl sites of alginate might modify with various groups such as acetyl, phosphor, sulfate. Acetylation of the alginate constitutes a more flexible polymer structure and a higher swelling ratio of the polymer (35). On the other hand, the phosphorylation ratio of the alginate polymer gives information about the rate of the resistance to degradation of the alginate. The sulfated form of alginate has unique high blood compatibility and anticoagulant activity (36).

Alginate might be chemically modified with a simple method such as esterification of the carboxylic groups. Esterification reaction of carboxylic groups might be performed by several alcohols and alkyl halides in presence of the catalyze

(37). One of the groups synthesizes that fatty alcohol (octanol, dodecanol, or hexadecanol) grafted amphiphilic alginate esters. The other study shows that esterification of the sodium alginate with vinyl sulfone-terminated multi-arm PEG (PEG-VS) might be used for microencapsulation of the cells (38). Sodium alginate-cysteine conjugate might be synthesized on thiolate residues and used in controlled drug release studies (39). Additionally, amidation of the alginate with amine molecules constructs the hydrophilic derivatives of the alginate (40). The other strategy for crosslinking of the alginate hydrogels might be performed with photo-irradiation such as exposure to ultraviolet (UV) light (41).

Positively charged chitosan is produced by the deacetylation process of the chitin. Chitosan is a composition of the alternating monomers which are 2-acetamido-2-deoxy--β-D-glucopyranose (GlcNAc; A) and 2-amino-2-deoxy- β-D-glucopyranose (GlcNAc; D) (42). The deacetylation process of the chitin might be made up of chitin deacetylase or alkaline conditions. Acetamido-groups of chitins are deacetylated in acid conditions, the β-glycosidic linkage is hydrolysis in this condition, and degradation of the polysaccharides has occurred. The second condition of deacetylation of the acetamide group is alkaline (15-20 M NaOH at 100-120 °C). No hydrolyzing of β-glycosidic linkage is obtained in this procedure. Deacetylation of the sequence has occurred on a different side of the GlcNAc sequence (43). Various studies illustrate that the deacetylation degree (DA) of the amino groups which are highly electronegative change polarity, pH, water-soluble behavior, ionic strength of the chitin of the alginate. Chitosan positively is charged via proton taken up and behave as hydrophilic polycations. Positively charged chitosan which can easily interact with transition and post-transition ions might be used for the removal of heavy and reactive metals from the wastewater (44). The water solubility of chitosan depends on its ionic concentration of it. An excess amount of HCl might construct chlorhydrate formation of the chitosan (45). Hydroxyl groups on C-3 and C-6 of chitosan is also reacted with a various reagent such as sulfhydryl. Phosphorylation of the chitosan by reacting of phosphorylating agent onto amino groups of chitosan increases the chelating properties and water solubility of chitosan (46), (47). The water solubility of the chitosan might be enhanced with quaternization of primary amine of deacetylated

glucosamine. Paracellular permeability of the chitosan might be obtained at a positively charged state. However, chitosan has positively charged at pH values lower than 6.5. For that reason, the different studies developed alginate derivative (mono N-carboxymethyl chitosan (MCC), and trimethyl chitosan (TMC)) to overcome this limitation alkaline pH values present in the small intestine (48), (49). The various crosslinking agent which are glutaraldehyde, oxalic acid, formaldehyde, glyoxal, and genipin might be used to improve physical (thermal stability, swelling ratio), chemical, and mechanical properties (mechanical strength). Chitosan derivatives via metallic ions, tripolyphosphate (TPP), sulfate, β-glycerophosphate molecules. The main criterion of the chemical and mechanical stability of the chitosan is pH. Low mechanical and chemical stability was observed via ionic crosslinking of the alginate because of the high pH-sensitive swelling (50) pH Graft copolymer might be synthesized with γ-radiation and UV-light. pH-sensitive chitosan with good swelling properties might be fabricated with ^{60}C-γ-radiation (51). Moreover, chitosan which is cationic functions might be interacting with different opposite charged polymers such as alginates and proteins. For that reason, chitosan has a large scale of potential application side (cell encapsulation, tissue engineering, and drug delivery system).

The degradation rate of the polysaccharide might be controlled with different physiological (enzymatic activities, redox potential, pH, and glucose concentration) and external stimuli (temperature, light, magnetic field, and mechanical forces) systems. Some polymeric structure is strongly dependent on alteration of the pH value. Alginate has a stable structure at pH values ranging from 5 and 10. Proton catalyzed hydrolysis has occurred when the pH value is lower than 5. Degradation of alginate at a pH value of more than 10 has occurred via β-alkoxy-elimination.

Hydrolysis of glycosidic bonds was described with 3 different mechanisms. The first mechanism is the protonation of the glycosidic oxygen. The second one is the oxonium ion. The last mechanism is explained with the addition of the water molecules to carbonium oxonium ion (52). Additionally, carbonate and phosphate ions might catalyze the β-alkoxy-elimination. Esterification of the alginate might perform with electron attracting effect on carbonyl group in C6. This process is followed by the

removal of the H-5. Degradation of alginate has also occurred *values* around neutrality. This process which is class ORC reactions (Oxidative Reductive Depolymerization) is varied with amounts of phenolic compounds (53).

Chitosan degradation might have occurred with acid hydrolysis. N-acetyl linkage and O-glycosidic linkage are catalyzed by acid. The rate of N-acetylation in dilute acid is equal to the rate of hydrolysis of glycosidic linkages. Hydrolysis of glycosidic linkage is controlled by the acetyl group in the structure of the alginate positively charged group which is close to the glycosidic linkages. At a lower pH value, acid hydrolyze β-glycosidic linkages which are cleaved at A-A and A-D sides. On the other hand, at higher *pH value* alkaline hydrolyze the chitosan, and degradation is occurred (54). A previous study showed that simple covalent modification on chitosan prevents the degradation of the chitosan in the stomach at low pH. Chitosan might be targeted to the small intestine side (55).

Enzymatic degradation of the polymer has occurred in various organisms via upregulation of enzymes at the target side. An enzyme-based approach for the targeted delivery system was applied to the different target sides. Alginate might be naturally degraded with alginate lysates or alginate polymerase. Alginate lyases use the β-elimination mechanism and each of them has unique properties. The first mechanism of the β-elimination is to remove the negative charge on the carboxyl anion. The second mechanism is that the general base catalyzes the proton abstraction on C5. The last mechanism is the elimination of the 4-O-glycosidic bonds. Elimination of 4-O-glycosidic bonds is done with transferring of the electron from the carboxyl group and formation of the double bond between the C4 and C5 (56). Enzymatic degradation of chitosan is performed at hydrolyzing of the glucosamine-N-acetyl-glucosamine, N-acetyl-glucosamine-N-acetyl-glucosamine, glucosamine-glucosamine linkage. Chitosan might be degraded by lysozyme and bacterial enzymes in the colon (57). Degradation of the chitosan not only lysosome activity but also DA. Lysosomal degradation of the chitosan is followed by degradation of chitosan into oligomers. Oligomer form of chitosan is degraded to monomers by NAGase (58). The DA of the chitosan gives chance to use chitosan in tissue engineering applications.

2.2.2.2 Proteins

Proteins are the types of polymers that made up blocks of amino acids. Proteins are a component of the extracellular matrix. Different approaches were used to mimic extracellular with various components such as fibrous proteins, adhesive proteins, proteoglycans, and glycosaminoglycans (59–61).

Collagens (around 30 types) have been identified with different roles and different target areas (59,60). Collagen is most abundant and a component of proteins inside the extracellular matrix (ECM). Type 1 collagen is predominantly in skin, tendon, and bone tissue. Collagen in cartilage is mostly type 2 collagen. Type 3 collage is inside the structure of the blood vessel. The other type of collagen is Type 4 which separates epithelial tissue from mesodermal tissue. Primary structure polymer indicates that collagens could be extracted from tissue because of the interchain connection between the amino acid sequences. Each type of collagen has a unique structure. The structure of collagen contains three α-chains. The sequence of α-chains is a repeating sequence $(Gly\text{-}X\text{-}Y)_n$. X and Y correspond to proline and hydroxyproline. The α-chains of collagen construct left-handed helices, and then left-handed helices turned and create right-handed triple helix. The formation of the triple helix model constitutes fibrils and fibers formations (62–64). Collagen might be isolated from bovine skin, fish, sea plants, and tendons (62,65). It causes a low inflammatory host response. It also has high biocompatibility and biodegradability properties. The extraction cost of the collagen is very high, for that reason, it has poor availability at different application sides. Collagen could be applicable with other polymers to obtain good biocompatibility and mechanical properties for clinical therapy.

Gelatin is produced from collagen Type I which is obtained from bovine or porcine. Gelatin might obtain with two different methods. One of them is the thermal treatment of collagen. Heat treatment to collagen breaks down the hydrogen bond of it. The formation of the collagen triple helix structure converts into gelatin. The other method to fabricate gelatin is the hydrolysis of collagen. Two types of gelatins might be obtained according to pH conditions. The formation of the gelatin Type A is

obtained in an acidic environment. Gelatin type B is produced in an alkaline solution. Each of the production methods alters the properties of the gelatin. Collagens contain a large amount of RGD (Arg-Glyc-Asp) sequence which have a direct role on cell adhesion and proliferation. Gelatin contains a similar amino acid sequence to an amino acid sequence of collagen, but gelatin could not induce antigenicity inside the body. The antigenicity property of the collagen might be obtained because of the presence of aromatic amino acids such as tryptophan, phenylalanine, and tyrosine (66–68). Gelatin has superior properties for tissue engineering applications. However, it could be directly used in tissue engineering applications because of the poor mechanical strength, high viscosity, fast enzymatic degradations.

Elastin mostly takes place in vascular and connective tissue because of its elasticity. Elastin provides the RGD sequence for cellular growth. Additionally, elastin is composed of a repeated amino acid sequence which is VPGVP (valine, proline, and glycine). Elastin is not applicable because of the contamination during the purification processing. The presence of the elastin might cause the immune response inside the body. Development of a synthetic version of the elastic is the alternative way because of this limitation of the elastin such as (synthetic tropoelastin, elastin-like polypeptides (ELP_s)).

Fibronectin has a crucial role in the construction of the extracellular matrix. Fibronectin is found not only in cells but also in plasma. They have almost the same two subunits. These subunits are composed of three repeating modules (Types I–III). Fibronectins enhance cell adhesion by binding of $\alpha5\beta1$ integrin of the cell membrane.

Laminins are cross-shaped glycoproteins. It contains a trimetric structure composed of α, β, and γ chains. Interaction between these proteins constructs space for adhesion of the molecules in various tissue types (59,69). Glycoproteins are important for cell migration, spreading, adhesion, and proliferation. Additionally, it takes an important role in the construction of many tissues especially during embryogenesis (61,69,70).

Silk proteins (SLP_s) have hydrophilic and hydrophobic blocks in their structure (71). The hydrophobic part of protein composes of the repeated sequence of sort amino acids (glycine, and alanine). Hydrophilic polymer of the proteins contains a non-repetitive sequence which is charged chains amino acid residues. SLP_s is highly bio-compatible polymer for an efficient therapeutic approach in cell therapy. Additionally, it is used as a genetic engineering tool for the efficient delivery of cells.

Growth factors are regulatory molecules that take part in cell signaling to manage cellular activity. GF_s can induce signaling in the endocrine, paracrine, and autocrine when it reacts at a suitable concentration. For that reason, GF_s take a part in various important processes such as cell migration, growth, proliferation, and differentiation. Their short half-life, low stability inside the body limits their physiological applications side. Various biomaterials and different approaches were used to preserve growth factor stability and sustained release in a target area. Commonly used GF_s are bone morphogenetic proteins (BMP_s), insulin-like growth factor-1 (IGF-1), platelet-derived growth factor (PDGF), vascular endothelial growth factor (VEGF), basic physiological growth factor (FGF-2), and transforming growth factor- β (TGF- β).

Decellularized extracellular matrix (dECM) is another biological source that contains various types of polymeric and biologic biomolecules. Extraction of the decellularized matrix from cellular components might be performed with different methods such as chemical (detergent, or enzymes) and physical (washing steps). Decellularized matrix must preserve its original structure and contain biologically active molecules such as GF_s. The extracellular matrix contains not only the heterogeneous mixture of the proteins (laminin, fibronectin, and GF_s) but also carbohydrates and proteoglycans (72,73). ECM might be damaged during the decellularization of the extracellular matrix from cell debris.

2.3 Stem Cell Encapsulation Technologies

There are many technologies were used for cell encapsulation technology. The main principle of this method is capturing the cells inside the liquid core (74). The

extrusion method which is the suspension of the liquid polymer and cells is the most applicable method for cell encapsulation strategy. Beads are formed via extrusion of the liquid mixture (polymer and cells) into the hardening solution which protects the bead formation. Various encapsulation strategies were used the obtain a more applicable size for cell therapy and the uniform shape of the beads.

2.3.1 Microgel encapsulation technologies

The main principle of the microgel encapsulation technique is the extrusion of a liquid mixture from nozzle tips. Droplets are formed at the discharge point of the nozzle in the system. Mechanism of the droplet formation changed with the interaction of the gravitational, surface tension, impulse, and frictional forces (75), (76). Classification of the extrusion techniques is simple dripping, electrostatic extrusion, coaxial airflow, vibrating jet/nozzle, jet cutting, and spinning disk atomization. Droplets might be solidified with different strategies either physical (cooling or heating) or chemical process (gelation). The main advantages of the extrusion techniques are that they are not affected by temperature and other solvents. Additionally, a highly viscous polymer solution might be used for encapsulation of the materials.

One of the methods for *drop generation by gravity* might be performed with gravity. Liquid sample extruded until the edge of the nozzle and gravity force is enough to overcome the surface tension until the drop is released from the edge of the nozzle. In this system size of the microbeads diameter depends on the size of the orifice diameters (77). The main disadvantages of this technique are the fabrication of low quantities and the large diameter of the droplets (>2mm).

Electrostatically assisted spraying is one of the methods to construct small-sized microbeads. The principle of spraying is based on pulling the biomaterials from the needle top into the gelling path. The voltage is applied between the needle and the electroconductive solution (hardening solution). This method is also known as electrostatic extrusion. The electric force is applied to the droplets to fall off the needle

tips and droplets fall off with their weight. Microbeads are constructed when the droplets fall into the hardening solution. The electric voltage (0-30 kVa) of the system used in this system does not damage cells and proteins. Moreover, this system allows the production of very small and uniform-sized particles.

The other techniques for the fabrication of the droplet are *coaxial airflow-induced dripping*. In this technique, a stream of compressed air is used for pulling the liquid droplet from the nozzle. Uniform size and shape droplets might be produced in this technique, but the main disadvantage of this technique is the low production rate of the droplets.

An aerodynamically assisted jetting system contains a controllable pressure chamber. In this system, an aerodynamic flow field is generated with a pressure gradient between the input and exit orifice. This aerodynamic flow field fabricates small-sized droplets from the needle throughout the exit orifice. The diameter of the small-sized droplet is 20 micrometers. The other techniques for microbeads fabrication are *Laminar Jet Breakup, Vibrating Jet / Nozzle Technique, Jet Cutting Technique, Rotating (Spinning) Disk Atomization.*

2.3.2 Macroencapsulation technologies

Various encapsulation strategies (macro and micro size) were used for the encapsulation of mammalian cells for different clinical usage (21). Capsules used in cell therapy acts as a barrier between transplanted cells and immunological response. Retrievable and scalable macro capsules were designed to obtain long-term viability and functioning of the cell inside the patient body. Macro capsules might localize at a specific location and provide the immune isolation of the cells. The size of the macro capsule is not counterbalanced organ size and function. The large retrievable macro capsule used in the experiment is 100.000 times lower than organ size (78), (79), (80). However, retrievable macro capsule devices might apply to some therapeutic approaches such as diabetes.

Studies on transplantation of islet cells loaded retrievable macro capsule showed that macro capsule might be long-term used for diabetes patients in clinical applications (Gabr et al., 2018), (82), (83). On the other hand, various cell types and genetically modified cells might load in the retrievable macro capsule to regulate protein or growth factor levels in protein deficiency disease for regenerative therapy (Saenz Del Burgo et al., 2018a). Additionally, co encapsulation of the two different cells might improve the efficiency of the therapeutic approach. In islet transplantation study, the immunosuppressive potential of mesenchymal stem cells (MSC_s) via increasing nitric oxide production and secreting higher levels of immunomodulatory cytokines enhance the efficiency of the islet transplantation (84). Moreover, pericapsular fibrotic overgrowth (PFO) might be decreased with mesenchymal stem cells which have a role in tissue repairing of the damaged tissue, promoting angiogenesis, and reducing inflammation.

2.4 Macroencapsulation for 3D in vitro Cell Culture

Cell therapy on tissue regeneration with patient-derived tissue or cell sources paves the way for new therapeutic opportunities for patients. Mesenchymal stem cell-based therapy is applied in various types of diseases and degenerative tissue such as tendons (85), intervertebral disk (86), bone (87), and articular cartilage (88). Various cell types such as beta cells were used for the regulation of hormone and growth factor levels for the treatment of patients. Clinically islet (Beta cell) transplantation is an alternative way to exogenous insulin independence for prolonged periods. The main limitations of islet transplantation are the lack of organ donors, inconsistent islet yield, and multiple organ donors per patient (89). The other severe limitation of the islet transplantation points out to the host immune rejection from recipient immune cells. These recipient immune cells and host immune rejection eliminate the long-term functionality and survival of the transplanted cells (90). However, decreasing the survival rate of delivered cells inside the patient body directly correlated with a decrease in the efficiency of cell transplantation therapy. So, immunosuppressive drugs have emerged as alternative tools for obtaining effective cell therapy but some immunosuppressive such as glucocorticoids had significant islet toxicity (89).

Immunological problems in cell therapy resulted in the development of new therapeutic strategies for the long-term survival of transplanted cells. Encapsulation of the cells via biocompatible and semi- permeable macro-capsules is an attractive way for tissue regeneration. So, implantable, and retrievable macro-capsules for cell therapy seem to provide outstanding advantages to improve the therapeutic efficiency, especially in genetically engineered cell transplantation ranging from the elimination of frequent administrations of cells to the isolation of delivered cells from immunogenic attacks (91).

Polymeric capsule-based strategies have yielded promising results in various disease models without the need for immunosuppressing agents (92). The cell-encapsulation strategy has emerged as a powerful tool for protecting cells from immunoreactions, hence allowing the nutrient transfer to maintain cell survival and function inside (93). Encapsulation strategies as macro and micro size were applied to mammalian cells for different clinical usage (21). Capsules have the potential to possess a special role as a barrier between transplanted cells and immune responses inside the body. Implantable and scalable macro- capsules were designed to obtain long-term viability and functioning of the delivered cell inside the patient body (21). On the other side, large-sized macro-capsules which are 100.000 times smaller than a regular organ size might demonstrate limited organ function (78–80). Still, studies on transplantation of islet cells loaded retrievable macro-sized capsule design showed that macro-capsule might provide long-term usage for diabetes in clinical applications (81–83).

Retrievable macro-capsule constructs have been utilized as attractive scaffolds for the delivery of various cell types and genetically modified cells to regulate protein or growth factor levels in protein deficiency diseases (84). Especially, an immunosuppressive feature of mesenchymal stem cells (MSCs) was shown to be enhanced in terms of the efficiency of the islet transplantation via increasing nitric oxide production and secreting higher levels of immunomodulatory cytokines (84). Based on these findings, the potential of MSCs for repairing damaged tissue, promoting angiogenesis, and reducing inflammation might be revealed to a greater

extent for patient-specific cellular therapies. In this study, we have designed a semi-permeable 3D macro-capsule for the proper delivery of MSCs, which can be evaluated as a container for the encapsulation of cells with high cell viability. Although several biomaterial-based encapsulation techniques have been previously established for cell transplantation, this design provides a container-based reservoir of encapsulated cells with a more effective, cheaper, reproducible, and achievable strategy for further cellular therapies. A biocompatible and biodegradable PCL polymer was preferred for 3D printing of this macro-capsule, for which the level of porosity was analyzed by measuring the amounts of transported biomarkers throughout such as consumed glucose and produced lactic acid. MSCs with high viability up to 72 hours might contribute to the development of effective approaches for biomaterial-based cellular therapy.

2.5 Microencapsulation for 3D in vitro Cell Culture

Stem cells might be delivered to the donor via intravenous infusion and transplantation. There is some limitation for transplantation of the stem cells to the patient such as immunoreaction, mechanical damage while injection, and entrapment of the cells in the lungs. Cell viability, proliferation, differentiation, and cryoprotection inside the encapsulate are important parameters for the efficiency of cell therapy after transplantation inside the patient body. Cultivation environment of the cells regulates the differentiation of the stem cells and proliferation of the cells (94) (95). Proliferation of the cells inside the capsule structure might be increased by mimicking of the tissue-specific architecture and physiological conditions. Various strategies were used to mimic tissue-specific architecture such as encapsulation of the cells with polymers. The concentration and types of the polymer such as alginate change the proliferation of the encapsulated stem cells(95). Moreover, alginate might provide long-term usage of alginate in cell culture applications for cell growth, proliferation, and biomolecule transportation such as diffusion inside the microbeads to the environment. Production of the alginic acid based on acid extraction from alginic tissue, and then extracts were neutralized with alkaline, lastly neutralized extract was precipitated by addition of calcium chloride or mineral acid.

One of the main challenges of the alginate *in vivo* experiment is that alginate is not enzymatically degradable inside the body. Gelation of alginate structure is degraded by immune reaction and *in vivo* conditions inside the body. Cells inside the alginate microbeads might be released via chelating of the Ca^{2+} molecules and breaking of the crosslinks between the chains. Moreover, the stability of calcium ions inside alginate gel is degraded by cell proliferation and cellular waste (lactate, phosphate, and citrate) inside the microbeads *in vitro* conditions. Alginate degradation inside the body is controlled by different strategies such as alginate lyase enzyme treatment (Leslie et al., 2013). A recent study on the fabrication of mesenchymal stem cell-loaded microbeads is showed that mesenchymal stem cells inside the microbeads were remain alive during a 3-week *in vitro* cell culture environment and for 3 months *in vivo* condition (97). Another study illustrates that high G rate alginate which has rigid structure compared to low G rate alginate eliminates the releasing of the stem cells from the microbeads and preserves viability from up to 14 days (98). Additionally, Arg-Gly-Asp-Try (GRGDY)-modified alginate (RGD-modified alginate) provide 80% viability after 15 days incubation periods. RGD modification on alginate proves that mesenchymal stem cell attachment and elongation on the polymeric structure (99). Extracellular matrix proteins were used in microencapsulation to mimic the microenvironment and long-term survival and proliferation of the cells inside the microcapsule.

Gelatin is the one of the extracellular matrix proteins used in encapsulation of the mesenchymal stem cells. It produced from collagen type 1 by various strategies such as thermal treatment and hydrolysis. Production method of the gelatin from collagen alter not only structure but also properties of the gelation. Alteration of the pH during the production of the gelation change the formulation of the gelatin such as gelatin type A (acidic environment) and gelatin type B (alkaline solution). Large amount of the RGD (Arg-Glyc-Asp) sequence inside the collagen provide unique properties for cell adhesion and proliferation. However, collagen possess aromatic ring groups induce antigenicity inside the body. Production of the collagen from gelatin decrease the aromatic ring groups inside the collagen structure and antigenicity inside the body.

Stem cell differentiation inside the microbeads might be altered by various conditions such as cultivation environment and polymer type. It was shown that mesenchymal stem cells (MSCs) inside the alginate-based capsule are differentiated into insulin production cells via cultivation of the differentiation medium (95). Additionally, concentration of the polymer changes the porosity of the microbeads formation. According to research, average matrix pore size change from 10.9 µm to 3.4 µm according to alginate concentration (0.5% to 2% (w/v)). The pore size of the microbeads also controls the diffusion of the macromolecules and metabolic activity of the cells during the cultivation period. On the other hand, porosity of the microbeads is regulated by the size of the microbeads. Cell concentration inside the microbeads is positively correlated with the size of the microbeads. The number of cells in the microbeads regulates the differentiation because of the cell-cell interaction (100,101). Human mesenchymal stem cells (hMSCs) which are encapsulated in PEG and poly (ethylene glycol)-diacrylate (PEGDA) hydrogels differentiated into chondrocytes (102,103). Another example of the osteogenic differentiation of the stem cells in-vitro and in-vivo achieved by co encapsulation of the murine Anti-BMP2 monoclonal antibodies (mAbs) into alginate microcapsule (104).

Blend formation of the gelatin and alginate mixture might apply as an injectable gel and microbeads formation. Viability of the cells inside the formulation might positively correlated with gelatin content in blend formation. On the other hand, mechanical properties of the gel formulation increase with alginate content blend formation. For to increase mechanical properties of the alginate-gelatin mixture, research used the ferric ions to increase the mechanical properties of the alginate gelatin mixture. In this research, they showed that ferric acid constructs the ionic coordination between the carboxylic group of alginate and gelatin (105). This bonding formation increase the mechanical stability of the gelling structure and stability of the mixture provide the increasing of the gelatin capacity inside the blend formation. Moreover, gelatin content inside the mixture positively correlated with cell viability inside the gel (105).

Encapsulation of the stem cells might maintain the viability of the cells after cryopreservation of the stem cell and during the storage period. Semipermeable alginate hydrogels which is cross-linked by strontium enhance cell viability and proliferation rate of the cells such as human mesenchymal stem cell (hMSC) and mouse embryonic stem cells (mESCs) (106). Moreover, mESCs which is loaded arginine-glycine-aspartic acid-serine (RGDS)-coupled calcium alginate in 10% (v/v) dimethyl sulfoxide (DMSO) have higher stem cell marker, higher cell survival rate, and better cell healthy compared with suspension one. Cell loaded alginate-gelatin (AlGel) microbeads gives promising result to angiogenesis of endothelial cell (107), maturation of human myelomonocytic cells line U937 (108), preservation of the stemness feature of cardiomyoblasts (109), and cytoprotectiveness and cytofunctionality effect inside the microbeads (110).

2.5.1 Cell loaded microcapsule for regeneration studies

Cells loaded microbeads were investigated in vitro condition to apply on various diseases such as bone, cartilage, cardiovascular, brain, diabetes, skin, liver, and cancer.

Bone tissue might be regenerated with an injection of the stem cell which might minimize invasive surgeries. Bioactive calcium phosphate cement (CPC) is alternative strategy to construct bone and provide a good scaffolding capacity. Osteoblast cell attachment and expression capacity is much higher level due to mimicking of bone mineral structure. Bioactive calcium phosphate cement (CPC) has low mechanical properties and cannot tolerate stress-bearing. Porogens and absorbable fibers were used to increase the mechanical properties of CPC (111). On the other hand, the injection of alginate microbead to the target area which is the alginate-chitosan-CPC (CPC-AC-cell) construct has a great potential to regenerate complex-shaped bone defects (112). Injectable cell-loaded microbeads which have osteogenicity, osteoconductivity, and osteoinductivity properties have a great potential to repair tissue damage, especially bone tissue. In this structure, osteogenicity and osteoinductivity are regulated by the content of MSCs, and osteoconductivity is constructed by collagen meshwork (113).

Cartilage has a limited healing capacity which makes regeneration of cartilage tissue research an attractive topic today. Strategy on encapsulation of the cells into the chondro-conductive matrix might be used in cartilage regeneration and repair. Cell encapsulation is important for the localization of the transplanted cell into the target side (114). Microencapsulation of the mesenchymal stem cell (MSCs) inside the self-assemble collagen microbeads could provide excellent cell delivery devices for tissue regeneration (115). The chondrogenic cell might be produced with different sources such as embryonic stem cells or human embryonic stem cells. Embryonic stem cells have limited chondrogenic differentiation capacity and tumorigenicity risk because of the cellular heterogeneity of the different cell populations. Chondrogenic cells might be isolated from human embryonic stem cells which are differentiated depends on selective medium condition such as TGFβ1, FGF2, and PDGF.

Cardiovascular diseases are caused by loosing of cardiac cells in patients who need organ transplantation or cell transplantation to their bodies. Cell therapy is seeming an attractive therapeutic approach for regenerative therapy in the hearth. Various cell types such as embryonic stem cells (ESCs) are used to differentiate them into cardiomyocyte-like cells. The first limitation of ESCs differentiation is the multicellular aggregate formation or embryoid bodies (EBs) in vitro conditions (116,117). Encapsulation of the ESCs via poly-L-lysine (PLL)-coated alginate might solve aggregation with the liquefaction of the cores. Single ESCs cells are placed within each bead and with a specific size. Moreover, ESCs cells in PLL-coated alginate microbeads might be cultured in serum-free conditions or serum supplement medium, and the large number of the ESCs might be produced in scalable stritted-suspension bioreactors (118). Encapsulation of the cardiac stem cells (CSC) eliminates the mechanical clearance and increases the acute retention of the CSCs. Various polymers such as agarose-fibronectin or fibrinogen are applicable for microencapsulation of the human CSCs. Agarose-fibronectin or fibrinogen microbeads maintain CSC viability even under hypoxic stress conditions. The other advantage of the transplantation of the encapsulated CSCs cell compared with transplantation of the cell suspension in the production of a large amount of the pro-angiogenic/cardioprotective cytokines and production of the pro-angiogenic/cardioprotective cytokine increase the vascular

regeneration (119). Mouse ESCs and cardiomyocytes loaded injectable nano matrix gels containing Arg-Gly-Asp-Ser (PA-RGDS) are also used to regenerate hearth myocardial infractions. The injectable construct of mESC-CMs with PA-RGDS enhances cardiomyocyte functioning and long-term functioning at the target site of the tissue for 12 weeks (120).

Brain injury might cause unexpected disease due to the disability or death. The brain is not able to regenerate defect brain tissue. Restoration of the brain tissue might be achieved with stem cell transplantation (121). Human wharton's jelly mesenchymal stem cells (hUCMSCs) loaded gelatin-laminin (GL) 3D bioactive scaffold were implanted to the injured site. This strategy prevents the release of the hUCMSCs to the environment and degradation of the transplanted cells from the host's immune response and neuroinflammation (122). Application of mesenchymal stem cell-loaded alginate on traumatic brain injury decreases the neural cytoskeletal and cortical glial cell abnormalities and hippocampal neural cell loss. Additionally, mesenchymal stem cells might regulate the expression of specific peptides such as GLP-1 for the prevention of the accumulation of amyloid-beta (Abeta) peptides which cause Alzheimer's disease (AD) (123,124).

Diabetes is caused by damaged pancreatic islet cells (β-cells). β-cells in diabetes patients could not secrete insulin hormone inside the tissue. Exogenous insulin injection to the patient body is a strategy to balance insulin hormone levels inside the patient body. Lack of organ donors, inconsistent islet yield, and multiple organ donors per patient are the main challenges of islet transplantation (89). Allogenic islet transplantation creates host immune rejection which degrades cells and decreases the long-term functionality, survival, and efficiency of the cell therapy inside the tissue (90). Encapsulation of the islet cells might decrease the immunological response to the islet cell and increase the therapeutic efficiency of the cell. Mesenchymal stem cells which are derived from mouse bone marrow or human umbilical cord blood might be differentiated into insulin-producing cells. Encapsulation of insulin-producing cells via alginate prevents immune degradation of the cells while decreasing the blood glucose levels and increasing body weight. Additionaly, co encapsulation of the islet

cells with mesenchymal stem cells is another strategy to mimic the islet microenvironment. In this strategy, MSCs have an immunomodulatory property inside the tissue. Immunomodulation of the MSCs increases the functioning of the islet and survival of the islet cell graft (125).

Skin tissue construct for regeneration study contain tissue-engineered dermis (TED) and this dermis structure consists of the collagen-chitosan scaffold. The main limitation of this construct does not contain any vascular structure in it. It has been demonstrated that microencapsulation of the VEGF gene-modified hUCMSC-derived fibroblast cells increases the vascularization structure in collagen-chitosan laser drilling acellular dermal matrix composite scaffold after transplantation into skin defect wounds in pigs (126).

Liver fibrosis might be reduced by mesenchymal stem cell (MSCs) therapy. This mechanism is related to MSCs secreted some anti-fibrotic and anti-inflammatory effects in liver fibrosis. One of the studies illustrates that encapsulated mesenchymal stem cells with alginate polyethylene glycol secrete some soluble molecule to reduce liver fibrosis. These molecules are anti-apoptotic (IL-6, IGFBP-2) and anti-inflammatory (IL-1Ra) cytokines and matrix metalloproteinase 9. Secretion of these factors decreases the expression of the alpha-smooth muscle actin (α-SMA) which is the regulatory factor of live fibrosis (127).

In a cancer patient, stem cells that have a migration potential to the target area have been used as a carrier to therapeutic approach. Encapsulation of the stem cells provides a physical barrier to eliminate extrinsic factors and increase therapeutic efficiency (128). The researcher showed that ICORVIR17 and mesenchymal stem cells loaded synthetic extracellular matrix is the best options for reduction of the tumor regrowth compared with direct injection of the ICORVIR17 to the tumor area (129).

The different diseases are caused by the dysfunction of the different cell types. The complexity of the tissue-specific architecture limits the control cellular process in vitro. There are many regulatory elements and signaling pathways that have a role in

the cellular process in vitro. This problem also seems in drug development studies for the treatment of various diseases. Cell transplantation to the patient is a more attractive strategy to regenerate tissue. Transplanted cells might produce specific proteins and hormones at specific sides. Transplanted cells might be isolated from the patient's own body (autologous cells) or donor (allogeneic cells). Stem cells are capable to differentiate into specific cells by regulation of environmental factors (128). The other classification of stem cells is the source of the cells which are embryonic stem cells (ESCs) or adult stem cells (ASCs) (130).

2.5.1.1 The effect of AlGel encapsulation and BET on osteogenic differentiation

Cell-loaded alginate gelatin microsphere gives promising results for enhancement of mechanical properties of microbeads, maturation of the osteoblast cell, and regeneration of the bone fractions. AlGel crosslinked microcapsule (ADA-GEL) leads to tunable stiffness and stability properties compared to alginate hydrogel (131). nHA inside the AlGel microcapsule increases the mechanical property of the microsphere, cellular proliferation, and osteogenesis of the cells. The effect of mechanical property on osteogenic differentiation inside the AlGel microcapsule might be associated with mitogen-activated protein kinase activation downstream of the RhoA-Rho associated protein kinase (ROCK) signaling pathway (132), (133). Additionally, stiffer AlGel microcapsule increases the mineral deposition and osteogenesis potential. On the other hand, metabolites such as ATP are important for the cellular differentiation of mesenchymal stem cells (134). Respiration of the cell and oxidative stress inside the microbeads might be regulated via blend formulation of the alginate microbeads. Gelatin inside the alginate microbeads enhance the aerobic respiration of the human adipose-derived mesenchymal stem cells (135).

Differentiation of mesenchymal stem cells into osteocytes, adipocytes, and chondrocytes *in vitro* is regulated by environmental factors such as the interaction of the biomaterials and stem cells and supplements inside the osteogenic medium (fetal bovine serum, ascorbic acid, beta-glycerophosphate, dexamethasone, etc.). Biomaterial's interaction with stem cells activates various signaling pathways such as

TGF-β/BMPs, Notch receptor, Wnt/β-catenin, Hedgehog, and MAPK (136). Activation of signaling pathways via biomaterials promotes cell adhesion, proliferation, and osteogenic differentiation of mesenchymal stem cells. Cell adhesion of mesenchymal stem cells to biomaterial also activates intracellular pathways such as mitogen-activated protein kinase (MAPK) signaling pathways (137). In the MAPK signaling pathway, the maturation of the stem cells is initiated with adhesion of the cells, and followed by proliferation, and completed by differentiation of the stem cells (138). Maturation process is followed by activation of ERK pathways (7-11 days), activation of the JNK pathways and p38 which regulate the late stages of cell differentiation and apoptosis. Maturation process is ended with calcium depositions and ECM synthesis (collagen) (13-17 days).

Betulin (BET) is a type of triterpenoid and extracted from betule bark which have been used for the treatment of micro-fracture and dislocated bone in traditional medicine (139). BET has various pharmacological properties such as anti-tumor activity, anti-inflammatory activity, anti-viral activity, antibacterial activity, and osteogenic activity (140,141). Anti-tumor effect of betulinic acid is demonstrated on various types of cell lines such as melanoma, neuroblastoma, medulloblastoma, glioblastoma, head & neck cancer, ovarian carcinoma, cervix carcinoma, lung carcinoma leukemia (142). BET effect on cancer cells might correlate with the induction of apoptosis via loss of mitochondrial membrane potential. The osteogenic potential of BET showed by various signaling cascades especially the activity of JNK and ERK (143). A recent study showed that BET activates JNK, ERK1/2, and mTOR kinase-dependent signaling pathway and enhance osteogenesis of human fetal osteoblast cell line (hFOB 1.19) (144).

3 MATERIALS AND METHODS

3.1 Material Preparation

Alginate (low viscosity, A1112, Sigma-Aldrich) solution was dissolved with %4 concentration in saline (Polypharma/ Polyfleks) solution and stirring at RT during overnight.

Gelatine (Gelatin from bovine skin, Type B, Sigma Aldrich) solutions were prepared with %1, %2, %10, and %20 concentration (by weight) in saline (Polypharma/ Polyfleks). Gelatine solutions (% 0, 5, 10, 20, 40 ratio by volume) were added into total alginate solution and by this way, gelatin/alginate mixtures (AlGel) were prepared.

Calcium chloride ($CaCl_2$) (75 mM) was used as a crosslinking solution. Incubation of nozzles (0.35 mm) inside sodium citrate solution (85 mM) prevent clogging of the system. Sterilization of encapsulation systems performed with ethanol (%70) and then treated with UV (2 hour) inside the cell culture hood before the cell culture experiment.

3.2 Macrocapsule Production

Designed macro-capsule were 3 dimensionally (3D) drawn in Autodesk Fusion 360 program. Drawn with assigned dimensions as 2x5x10 mm, macro-capsules were printed by using Axolotl Bioprinter Dual Print Head System (Axolotbio, Turkey) which was loaded with polycaprolactone (PCL) (Mwt: 80 kDa). The highly permeable membrane through the capsule structure was expected to allow the transportation of nutrients and GFs inside the capsule to the environment. The permeability of the porous membrane was optimized with various printing options (feed rate: 25%, 70 psi, first layer height: 2, extruder temperature: 120 °C, working stage: 55 °C, printing path: random). Printing options of programs (REPETIER-HOST and SLIC3R) change capsule structure and permeability of the porous membrane. Lastly, the macro-capsule is visually controlled to the presence of leakage on the closed form of the macro-

capsule. Then, the permeability of the macro-capsule is tested via the transportation of human serum albumin (HSA) protein and trypan blue dye from inside to capsule to outside during the day.

3.3 Macrocapsule Permeability Study

Obtained macro-capsules were checked for their permeability abilities by using Trypan blue dye as an indicator. Trypan blue dye (50μL) was injected into the macro-capsule. The injection zone was filled with melted polycaprolactone. Trypan blue release from microcapsule was analyzed after 1 day of incubation time.

Human serum albumin (50 μL/ 10000 μg) (20% HSA, Octapharma, Switzerland) was used to test protein transportation between inside to capsule to outside during the day. Injection of HSA inside the capsule was sealed with melted PCL. Protein-loaded macro- capsule was periodically transferred to fresh test tubes containing an equal volume of fresh PBS solution in each period at RT (0, 0.5, 1, 3, 6,12, and 24 hours). Releasing of HSA content to the environment each time at RT was determined and quantified by using a calorimetric measurement BCA assay kit (BCA assay, Takara, Shiga, Japan) according to the manufacturing procedure.

Macro-capsule was coated with 3.5 nm of gold- palladium and visualized with SEM (Thermo Fisher Scientific QuattroS, ABD). The imaging process was done under a low vacuum with as EDS detector at 5 kV.

3.4 Macroencapsulation in Cell Culture

Green fluorescence particle (GFP) tagged human umbilical cord mesenchymal stem cells (Acıbadem Labcell, Turkey) inside MSC nutrient- free medium (Biological Industries, Sartorius, Israel) were incubated at 37 °C with 5% CO_2. Medium exchange is performed every 48 hours until the 80% confluency of the flask was reached. Then, cells were trypsinized, centrifuged at 300 RCF for 10 minutes, and then collected in ringer lactate solution (containing 0.5% HSA by volume). Cell number and cell

viability were counted with a cell counter device (TC20 Automated Cell Counter, BioRad, ABD)

Sterilization of macro-capsules was performed with serial washing with 10mM PBS and 4% (v/v) ethanol solution. UV sterilization procedure for 2 hours was applied after the antibiotic treatment (2% Penicillin-streptomycin) to the macro–capsules, which were later on directly and indirectly contacted to MSC cells for the measurement of their cytotoxicity effects. Prior to the experiment, cells were GFP-tagged so that cytotoxicity assessment of the cells was performed by comparing the GFP intensity signals (Image J program).

This process was comparably for both cells in cryoprecipitate (Kızılay, Turkey) solution and non-cryoprecipitate solution encapsulated into the macro-capsules for 15 days of incubation time.

This process was conducted comparably for both cells in cryoprecipitate (Kızılay, Turkey) solution and non-cryoprecipitate solution encapsulated into the macro-capsules for 15 days of incubation time. Each group of cells (250.000 cells in 50µL media) was injected into the macro-capsules, and the area of the injection site was sealed with previously melted PCL polymer. Afterward, these macro- capsules were incubated in MSCs nutrient-free medium for 15 days at 37 °C and 5% CO_2. At different time points (1, 3, 5, 7, and 15 days), the culture medium was renewed and collected media was evaluated for the measurement of glucose consumption level and lactic acid production level. The cultivation medium was analyzed via the ADVIA® 1800 Clinical Chemistry System (Siemens, Germany) (145).

3.5 Microbead Production

System were sterilized with ethanol (%70) and UV treatment before the operation of the system (Nisco Encapsulator VAR V1 LIN-0043, Nisco Engineering AG, Zurich, Switzerland). Research-grade alginate (UV sterilized) sterilized with UV and was loaded on 50 mL syringe. Syringe pump set up 5 mL/hour flow rate. Then loading of

the system (cables and tip) with alginate solution was performed. The electrode inside the system was dipped inside the $CaCl_2$ (75 mM) crosslinking solution. Voltage of the system was adjusted after dripping of alginate solution. Optimum electrostatic force (6 kVa) is applied for alginate microbead fabrication (L. Wang et al., 2013). After 30 minutes running of the system, the voltage and syringe pump were closed. Different concentration of the microbeads group (5000, 2500, 1250, 500, and 250 (1^{st} replicate), 2000, 1000, 500, and 250 (2^{nd} replicate), 2240, 1120, 560, and 280 (3^{th} replicate)) were incubated in MsC nutrient medium. The fresh medium was exchanged with waste medium before the measurement of the microbeads diameter. The number of microbeads for each group of the experiment is also calculated.

Research-grade alginate (UV sterilized) and gelatin (UV sterilized) solutions were loaded into system and system set to a flow rate of 5 mL/hour. Then system was run with alginate-gelatin solution (AlGel). AlGel microbeads were fabricated with 6 kVa electrostatic force (L. Wang et al., 2013).

3.6 Visualization of Microbeads

Culture medium was exchanged before the visualization of the microbeads with a microscope (Zeiss Axio Vert.A1 inverted microscope) for advanced routine and the diameter of the microbead was measured with Zeiss Program (Carl Zeiss Microscope). The diameter value of each group was graphed using Microsoft Excel Program.

3.7 Microbead in Different Condition

Morphological structure and also size of microbead is controlled at various environmental condition (Medium solution (Nutrient Free Medium (Biological Industries), Phosphate Buffer Solution (PBS, Gibco), Acetate solution)). Microbeads were visualized at day 1 and 5 with a fluorescence microscope (Zeiss Axio Vert.A1 inverted microscope) and the diameter of the microbeads was measured with Zeiss Program (Carl Zeiss Microscope). The diameter value of each group was graphed using Microsoft Excel Program.

3.8 Cell Culture Experiment

Fibroblast cells (L929, ATCC, NCTC clone 929) were cultured in DMEM (Dulbecco's Modified Eagle Medium) with %10 Fetal Bovine Serum (FBS) and %1 Penicillin Streptomycin (PSA). L929 cells were thawed according to the manufacturing procedure, and cells (60,000 cells/cm^2) were seeded in cell culture dishes. Cells were incubated at 37 ^oC and 5% CO_2. Medium exchange were performed each 48 hours. Cells were trypsinized at %80 confluency and centrifuged at 300 RCF 10 min. Cells were collected in ringer lactate solution (%0.5 Human Serum Albumin Solution). Cell numbers were calculated with a cell counter device (BioRad).

Adipose isolated stem cells were cultured in MSC nutrient-free medium (Biological Industries) with 1% PSA. After thawing of the MSC, cells (15,000 cells/cm^2) were seeded in a cell culture dishes. During the incubation of the cells, the medium were replaced with fresh medium every 48 hours. When cells were reached %80 confluency of the flask, cells were trypsinized and centrifuged 300 RCF for 10 minutes. Cell numbers were calculated with a cell counter device (BioRad).

The human osteoblast cell line (hFOB 1.19, ATCC, CRL-11372) were cultured in Dulbecco's Modified Eagle's Medium (DMEM) (Phenol Red Free, Gibco, New York, USA) supplement with 10% fetal bovine serum (FBS, Gibco), 1% peniciline-streptomycine (PSA, Gibco) at a temperature of 37 ^oC and humidified 5% CO_2 atmosphere. After thawing of the human fetal osteoblast cells, cells (40,000 cells/cm^2) were seeded in a cell culture flask. The medium was replaced with fresh medium every 48 hours. When cells were reached %80 confluency of the flask, cells were trypsinized and centrifuged at 300 RCF 10 min. Cell numbers were calculated with a cell counter device (BioRad).

3.8.1 Microencapsulation of cells

Fibroblast cells (L929), mesenchymal stem cells (MSCs), and human fetal osteoblast cells (hFOB 1.19) were trypsinized from petri dishes and counted with a

cell counter (BioRad cell counter). L929 (20 million cells), MSCs (10 million cells), and hFOB 1.19 (20 million cells) were obtained after trypsinization of the cells. Cells were diluted into 4 million cells/mL (L929) (48 cells in 1 microbeads) and 2 million cells (MSC) (24 cells in 1 microbeads), a with alginate put into the syringe. 4 million cells/mL (hFOB 1.19) (48 cells in 1 microbeads) with alginate-gelatin polymer and put into the syringe.

Then the system was run for each group of cell-alginate or cell-alginate-gelatin (AlGel) mixture. Microbeads were fabricated by applying of desired electrostatic force (6 kVa) which is an optimum for microbead production (L. Wang et al., 2013). The voltage and syringe pump were closed after 30 minutes of the running of the solution. Cell loaded alginate and AlGel microbeads were fabricated with 6 kVa electrostatic force (L. Wang et al., 2013).

Cell-loaded microbeads were collected inside the 50 mL falcon tube. Microbeads were two times washed with saline solution. Various concentrations of the cell loaded microbeads were transferred in a medium solution and cultured at 37 ^{o}C and 5% CO_2.

Microbeads were visualized with microscope after adding of fresh medium and the measurement of the microbeads diameter with zeiss program (Carl Zeiss Microscope). The diameter value of each group was graphed using Microsoft Excel Program.

After fabrication process, hFOB 1.19 cell-loaded AlGel microbeads (1000 microbeads/mL) were cultivated in DMEM containing %10 FBS and were visualized with a fluorescence microscope after adding fresh medium on days 2, 4, 6, 8, 10, and 12. A total of 3 microbeads were selected for each group, the measurement of microbeads diameter was performed with zeiss program (Carl Zeiss Microscope, Oberkochen, Germany). The graph of microbead diameter was drawn using Microsoft Excel Program.

3.8.2 Analysis of GFP secretion from MSCs

Medium exchange was performed each 48 hours and then, MSCs loaded microbeads were visualized with fluorosens microscope (Zeiss Axio Vert.A1 inverted microscope for advanced routine). The measurement of GFP signal was performed using the ImageJ program. Graph of microbeads GFP intensity values were graphed with Microsoft Excel program.

3.8.3 Glucose consumption and lactic acid production of the cells

After microencapsulation, metabolic activity of the cells was analyzed for 12 days. Glucose and lactic acid level in medium were measured during the incubation time. Results were given information about the energy metabolism of the cells. Cell medium was collected 12 days period and analyzed with the ADVIA® 1800 Clinical Chemistry System (145).

3.8.4 Cell viability in culture medium

Cell culture medium was collected on day 12 and attached cells to the flask surface were collected after trypsinization process. Cell numbers were calculated with a cell counter device (BioRad). Cell viability and cell number was calculated with trypan blue staining protocol.

3.8.5 Total mRNA and protein level in culture medium

Cell medium was collected on day 12. The amount of total mRNA in the medium was measured by nanodrop (Thermo Scientific Nanodrop One). Measurement of total mRNA concentration was graphed with the Microsoft Excel program.

The total protein amount in the medium was analyzed with a BCA assay kit according to product manuel (Takara). Total protein concentration in the medium was

measured with a microplate reader at a 562 nm spectrophotometer. Total protein concentration was graphed with the Microsoft Excel program.

3.8.6 SDS-PAGE experiment

Cell medium was collected on day 12. Alteration of the protein distribution inside the medium was investigated via sodium dodecyl sulphate (SDS) PAGE electrophoresis. The protein concentration of the medium was measured by BCA assay (TAKARA) according to the product manual. An equal amount of the protein mixtures were loaded into SDS page. During the run of the sample, 90V was applied during the 30 minutes and 120V was applied during the 90 minutes. SDS-Page is stained with Coomassie Brilliant Blue Dye. Gels pictures were observed with hemiDoc Imaging System BioRad. Band intensities were measured with ImageLab Program and graphed using Microsoft Excel Program.

3.8.7 Cell proliferation and metabolic activity

Effect of BET on hFOB 1.19 cells proliferation were investigated with MTS Assay Kit (Abcam, ab197010, Cambridge, UK). hFOB 1.19 cells (5×10^3 cell/well) were seeded on 96 well plate. After 24 hours, cells were treated with different concentration of the BET (0, 0.01, 0.1, 0.5, 1, 5 μM) in DMEM containing %1 FBS without addition of osteogenic supplements (Mizerska- Kowalska vd., 2019). After 96 hours, hFOB 1.19 cell proliferation were examined with MTS assay kit according to manufacturer's instruction.

Effect of BET on hFOB 1.19 cell proliferation inside the microbeads were investigated with MTS Assay Kit (Abcam, ab197010, Cambridge, UK). After fabrication of hFOB 1.19 cell- loaded AlGel microbeads, hFOB 1.19 cell-loaded AlGel microbeads were treated with various concentration of BET (0, 0.01, 0.1, 0.5, 1, 5 μM) in DMEM containing 1% FBS, 1% PSA, 10 mM of β-GlyP (Sigma) and 50 μg/mL of AA (Sigma). On days 12, hFOB 1.19 cells loaded microbeads were collected and viability of the hFOB 1.19 cells examined with MTS assay kit according to

manufacturer's instruction. Measurement of hFOB 1.19 cells viability inside microbeads were performed in triplicate wells. Viability level in control well was considered as 100% and the compared with among groups. Viability values (%) were graphed using Microsoft Excel Program.

3.8.8 Live and dead assay

Viability of hFOB 1.19 cell-loaded AlGel microbeads which is cultured with various concentration of the BET (0, 0.01, 0.1, 0.5, 1, 5 μM) in DMEM containing 1% FBS, 1% peniciline-streptomycine (PSA), 10 mM of β-GlyP and 50 μg/mL of AA were measured using Live and Dead cell assay (ab115347, Cambridge, UK).

hFOB 1.19 cell loaded microbeads which is culture in 0 μM BET were collected at each time point on days 2, 4, 6, 8, 10, and 12 and hFOB 1.19 cell loaded microbeads which is treated with different concentration of the BET (0, 0.01, 0.1, 0.5, 1, 5 μM) were collected on days 6 and 12. Each group of microbeads were suspended (1:1 ratio) with 10x live and dead stains. Samples were incubated with live and dead stains for 10 minutes at room temperature. Stained hFOB 1.19 cell loaded microbeads were photographed with a fluorescence microscope (EVOS^{TM} M5000 Cell Imaging System, ThermoFisher, Bothell, WA, USA). Red and green cell inside the microbeads in three microbeads from each sample were selected to count viable cell number. Viable cell numbers in microbeads were graphed using Microsoft Excel Program.

3.8.9 ConA-AF488 and DAPI staining

Collected cells at each time point of the experiment were washed with phosphate buffer saline (10 mM PBS) solution 3 times. Cell-loaded microbeads were firstly stained with 20 μg/mL concentration of the Concavalin AlexaFluor488 (ConA-AF488) solution and incubated for 1 hour. After the incubation period, cells were washed with PBS solution for 3 times and then stained with 10 μg/mL DAPI solution for 6 minutes. After the incubation period, cells were washed with 10 mM PBS

solution for 3 times. Stained microbeads were pictured with a microscope (Zeiss Axio Vert.A1 FL inverted microscope).

hFOB 1.19 cell loaded microbeads which is cultured in various concentration of the BET (0, 0.01, 0.1, 0.5, 1, 5 μM) in DMEM containing 1% FBS, 1% peniciline-streptomycine (PSA), 10 mM of β-GlyP and 50 μg/mL of AA were collected on days 0 and 12 and washed with 10 mM PBS solution 3 times. Each group of microbeads were suspended with 20 μg/mL concentration of the ConA-AF488 solution and incubated for 1 hour. After the incubation period, microbeads were washed with 10 mM PBS solution for 3 times and then stained with 10 μg/mL DAPI solution for 6 minutes. After washing steps, hFOB 1.19 cell loaded microbeads were visualized with a fluorescence microscope (EVOS^{TM} M5000 Cell Imaging System, ThermoFisher, Bothell, WA, USA). A total of 3 microbeads were selected to count signal intensity of ConA-AF488 solution and DAPI for each group. Graph of intensity values were drawn using Microsoft Excel Program.

3.8.10 Assay of osteopontin production

ELISA method was applied to measure osteopontin (OPN) concentration in the cell culture media of hFOB 1.19 cell and hFOB 1.19 cell loaded microbeads. hFOB 1.19 cells were seeded in 96 well plate at a density of 30 x10^3 cell/well. After 24 hours, cells were treated with different concentration of the BET (0, 0.01, 0.1, 0.5, 1, 5 μM) in DMEM containing %1 FBS, 1% PSA, 10 mM of β- GlyP and 50 μg/mL of AA for 12 days and cultured medium of samples were collected on days 12.

After production of hFOB 1.19 cell loaded microbeads, hFOB 1.19 cell loaded microbeads were incubated with various concentration of BET (0, 0.01, 0.1, 0.5, 1, and 5 μM) in DMEM containing %1 FBS, 1% PSA, 10 mM of β-GlyP and 50 μg/mL of AA for 12 days and cultured medium of samples were collected on days 12.

Collected medium samples were centrifuged and stored at -80 ^{o}C before use in osteopontin level measurement using a Abcam human osteopontin elisa kit (Abcam,

Boston, USA) according to manufacturer's procedure. Osteopontin level in control well was considered as 100% and compared among each group. Osteopontin level in a sample (%) were graphed using Microsoft Excel Program.

3.8.11 Alizarin Red S staining

Mineralization degree of the extracellular matrix of hFOB 1.19 cell and hFOB 1.19 cell loaded microbeads were evaluated using Alizarin Red S (Merck, Darmstadt, Germany) staining. Before the staining, hFOB 1.19 cell and hFOB 1.19 cell loaded microbeads were incubated with various concentration of BET (0, 0.01, 0.1, 0.5, 1, and 5 μM) in osteogenic medium for 12 days. After treatment with BET, hFOB 1.19 cells washed 2 times with PBS and fixed with 4% formalin solution. hFOB 1.19 cells washed 2 times with ddH_2O, stained with Alizarin Red S for 1 hour, and lastly washed 2 times with ddH_2O. Stained cells were visualized with a fluorescence microscope (EVOS^{TM} M5000 Cell Imaging System, ThermoFisher, Bothell, WA, USA).

After treatment with BET, hFOB 1.19 cell loaded microbeads were collected and washed with ddH_2O solution for 2 times. Microbeads were stained with Alizarin red (Merck, Darmstadt, Germany) (2%) and incubated during the 30 minutes. Stained microbeads were washed with ddH_2O for 2 times and visualized with a fluorescence microscope (EVOS^{TM} M5000 Cell Imaging System, ThermoFisher, Bothell, WA, USA).

Extraction of the alizarin red dye from stained microbeads with 10% cetylpyridinium chloride (Sigma, C0732) in 10 mM sodium phosphate (pH=7) for 1 hours via rotation of the plate at RT. After incubation period, 200 μL extracted sample were transferred into 96 well plate. Extracted sample were serially diluted for quantification of the matrix calcium deposition. Absorbance of the samples at 562 nm was measured by microplate reader (FLUOstar Omega, BMG Labtech, Almendgrün, Ortenberg, Baden-württemberg, Germany). All measurement of mineralization degree of samples were performed in triplicate wells. Mineralization degree in control well was considered as 100% and the compared with among groups.

3.8.12 Alkaline phosphatase (ALP) activity

hFOB 1.19 cell loaded microbeads were incubated with various concentration of BET (0, 0.01, 0.1, 0.5, 1, and 5 μM) in osteogenic medium for 12 days. After treatment with BET, hFOB 1.19 cell loaded microbeads were collected and washed with PBS solution for 2 times. hFOB 1.19 cell loaded microbeads were incubated with BCIP/NBT plus suppress solution (34070, ThermoFisher) for 60 minutes. ALP positive microbeads were washed with PBS for 2 times and visualized with a fluorescence microscope (EVOS^{TM} M5000 Cell Imaging System, ThermoFisher, Bothell, WA, USA).

3.8.13 Statistical analyses

Statistical analyses were performed using Microsoft Excel software (Redmond, WA, USA). Obtained results were analyzed by running a student's *t*-test from the averaged data obtained from 3 independent experiments with a *p*-value < 0.05. Levels of significance were shown at *: $p<0.05$, **: $p<0.01$, and ***: $p<0.001$.

4 RESULTS

4.1 Macrocapsule Fabrication

A 3D macro-capsule design was constructed via Autodesk Fusion 360 program and verified with the Repetier-host program (Figures 1 A, and B). This designed capsule was printed by using Axolotl Bioprinter Dual Print Head System (Figure 1C) with extrusion (pneumatic) based bioprinting, where a synthetic polyester polymer, PCL, was first melted at the syringe upon heating up to 120 °C, and then it was printed on the plate at room temperature with 0.25 mm nozzle. The permeability of the obtained macro-capsule was tested with 0.5% Trypan blue dye. It was observed that the aqueous part of trypan blue solution (prepared in 10mM PBS) was released into the environment, but the blue-colored dye stayed inside the capsule after 1 day of incubation at room temperature. Compared with small molecular weight dye molecules, the permeability of the printed macro-capsules was also studied with HSA, as a model for high molecular weight, but the globular biological protein-based sample. As a time-dependent manner, almost all HSA injected into the macro-capsule's inner cavity was demonstrated to be released within 6 hours and 98% of total HSA protein was measured to be released from the macro-capsule in 24 hours of incubation (Figure 1D). Lastly, the sealed site of the leakage form for the porous capsule after the injection of the solution of interest inside was imaged after the completion of the release study under SEM microscopy. The injection site of the macro-capsule was successfully sealed with PCL and the injection site of the macro-capsule was stable after releasing the protein out as shown in Figure 1E. Moreover, a closed and hollow form of the PCL-based macro-capsule was used for cell culture experiments as a control group (Figure 1).

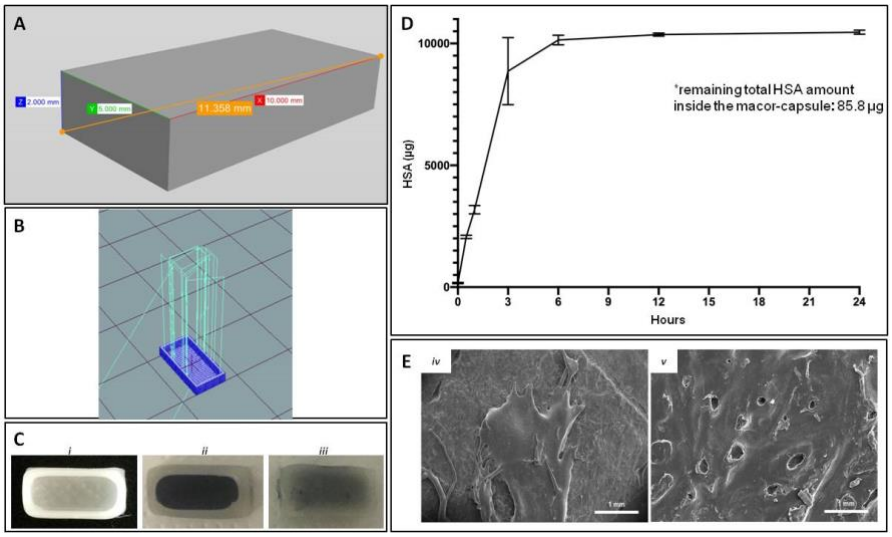

Figure 1. (A) Dimensions of designed macro-capsule with Autodesk Fusion 360 program, (B) printing path for 3D Bio-printer, (C) closed form of macro-capsule (*i*) trypan blue loaded macro-capsule (*ii*) closed form of trypan blue loaded macro-capsule (*iii*), (D) HSA release profile upon its diffusion from the macro-capsule, (E) SEM images of the macro-capsule before (*iv*) and after (*v*) HSA permeability tests.

4.2 Cytotoxicity of Macrocapsule

After sterilization of the macro-capsules, their cytotoxicity behavior was evaluated on GFP-tagged MSCs. Two different methods were applied to the macro-capsules for their interaction with cells. In the former one, macro-capsules were directly put on top of the seeded cells in a petri dish. On the other hand, the indirect contact method included the incubation of cells with a media where macro-capsules were previously incubated for 72 hours at 37 $^{\circ}$C and 5% CO_2. After incubation of cells for 24, 48, and 72 hours, cells were visualized under fluorescent microscopy for their morphology as well as their GFP expressions as an indication of cytotoxicity level. Figure 2A compares the adhered cells on petri dishes with the non-treated MSCs as a negative control group. Significant cytotoxicity levels were not observed for MSCs investigated for their indirect interaction with the prepared macro-capsules. However, a slight decrease in the cell viability was detectable for the ones subjected to the direct contact method depending on the incubation time. This behavior was also confirmed by the measurement of the GFP fluorescent signal of processed images by the Image J program (Figure 2B). This difference in obtained cytotoxicity results may be

attributed to the elimination of nutrient uptake by macrocapsule as incubation time gets prolonged. Additionally, it was observed that MSCs were detached from petri dishes upon their being scratched due to direct contact with the outer surface of the macro-capsule. However, cell attachment and proliferation were not observed under the macro-capsule contact surface.

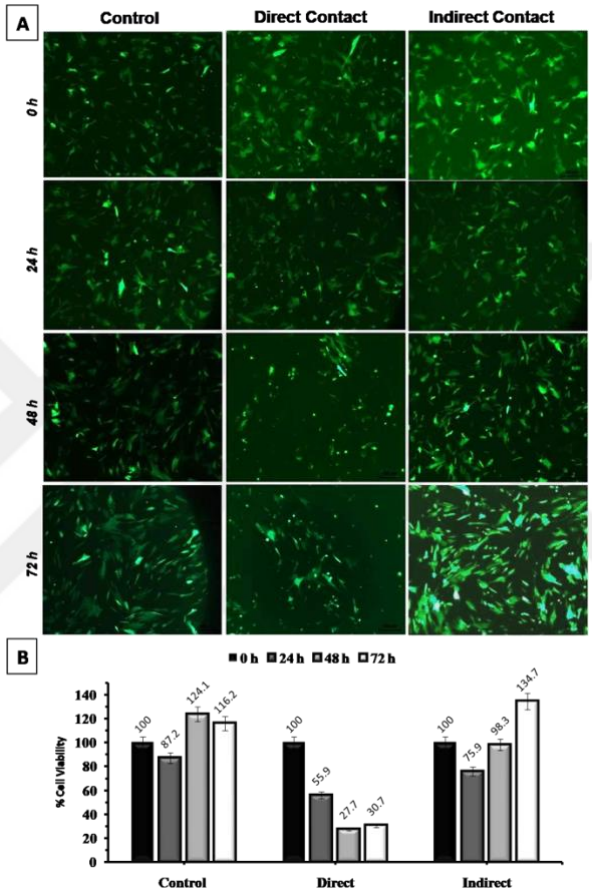

Figure 2. Fluorescent microscopy images of GFP tagged MSCs at different times upon incubation with the macro-capsule (A), a comparative graph for corresponding GFP signal intensities calculated by Image J (B).

For a better understanding of the metabolic activities of living cells in the incubation media, two key biological molecules were analyzed quantitatively. The first one is glucose molecule, which is an essential element, especially for cell proliferation, whereas the other one is lactic acid produced by cells as a metabolic waste molecule during cultivation. Determination of amounts of glucose and lactic acid with respect to incubation time is a well-accepted method for monitoring cellular metabolic

activities. The glucose and lactic acid levels inside the culture medium of cells encapsulated inside the macro-capsule were presented in Figure 3 (A and B, respectively) for 15 days of the incubation period. Samples collected from the incubation solution were analyzed by ADVIA® 1800 Clinical Chemistry System and compared with the results obtained from the 2D cell culture experiment as a control. Alterations in the glucose and lactic acid levels were observed in both 2D cell culture conditions and cells in macrocapsules. Results indicate that the prepared macro-capsules bear a porous architecture allowing the passage of molecules associated with metabolic activity while ensuring the viability of encapsulated living cells inside 3 (A and B, respectively).

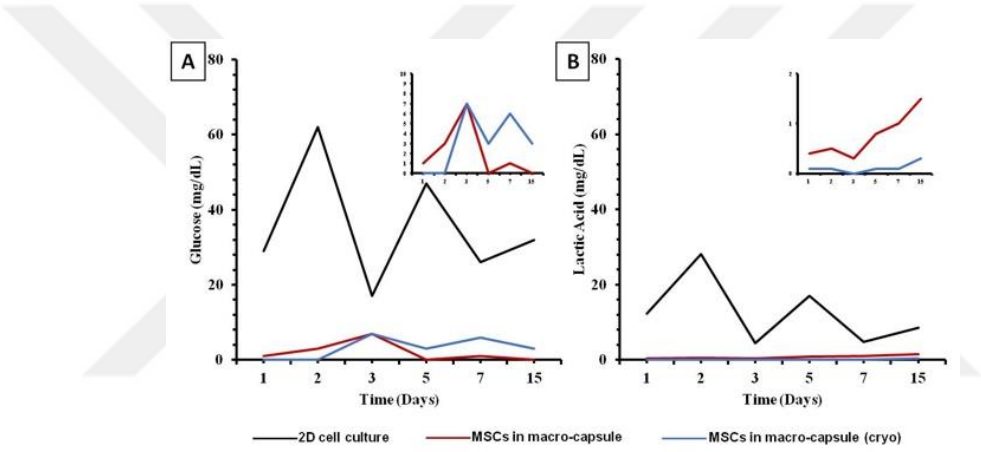

Figure 3. Glucose consumption (A) and lactic acid production (B) profiles of MSCs encapsulated in the macro-capsule.

4.3 Microbead Fabrication

After production of alginate microbeads, microbeads were cultured in MSC Nutrient Free Medium (Biological Industries) during 14 days in medium (Figure 4 A).

In this study 41.600 microbeads were produced in 30 minutes. Diameter changes among the group (5000 microbeads/well, 2500 microbeads/well, 1250 microbeads/well, 500 microbeads/well, 250 microbeads/well) for 12 days were recorded microscope. Diameter results were graphed using Microsoft excel. The

diameter of the microbeads is increased from 190 to 280 µm day by day among the groups of the experiment (Figure 4.B, and C).

The number of microbeads was counted at each time point of the first replication of the experiment. Slightly different results were observed not only between each group of the experiment but also each time points and then we optimize the dilution of the microbeads.

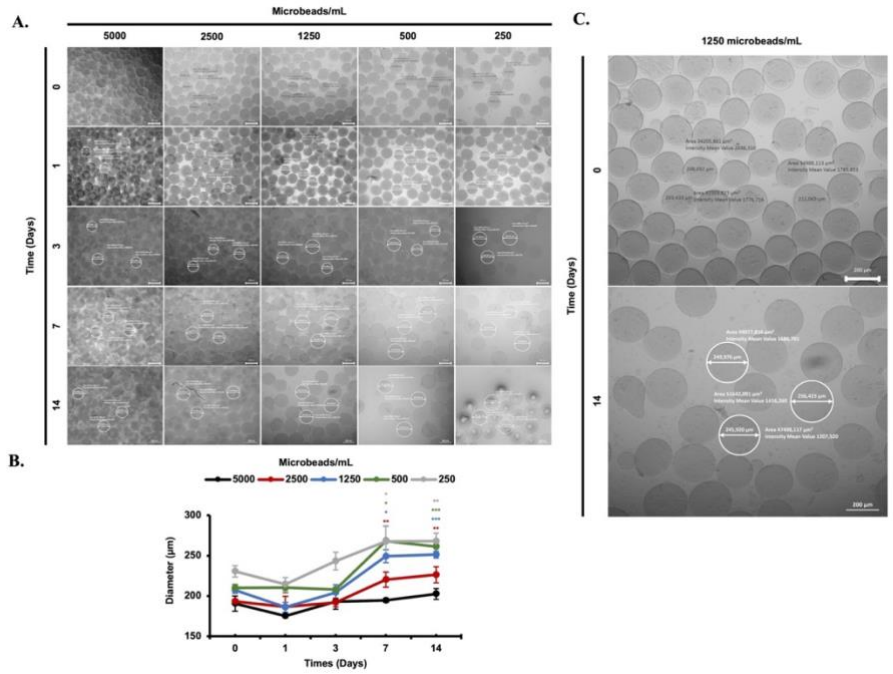

Figure 4. Diameter changes among groups of the samples are pictured during 14 days of incubation under the microscope (5×, scale bar: 200 µm) (A). Diameter changes amoung groups of an experiment are graphed (B). Diameter changes of 1250 microbeads/mL between day 0 and day 12 are shown (C).

4.4 Stability of Empty Microbeads in Different Conditions.

The morphologic structure of the microbeads was tested in different incubation conditions (100 mM pH:5.5 Acetate Solution, Medium, PBS, and saline @ 37 °C). The morphology of the microbeads were compared between among groups of the experiment (Figure 5). Salt formation around the microbeads was observed at day1

(Figure 5. C) and salt formulation can be removed via medium and saline wash of the microbeads (Figure 5. F).

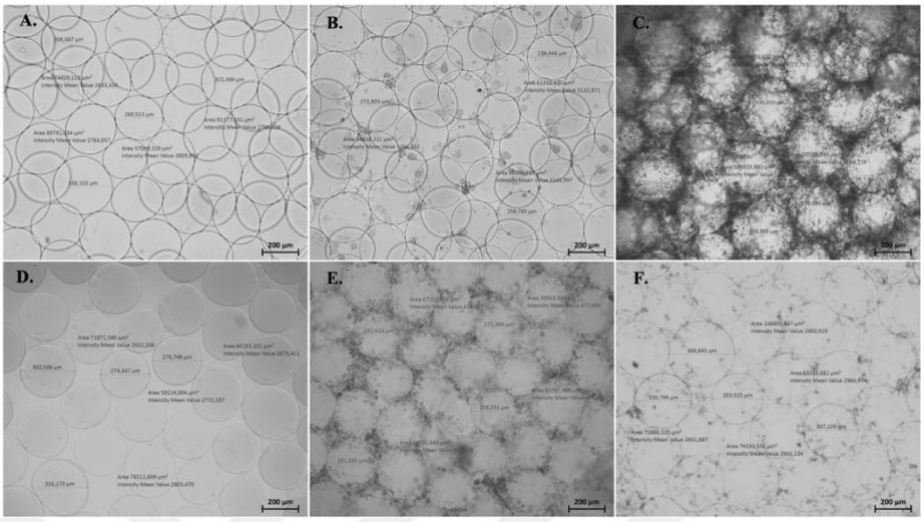

Figure 5. Morphological structure and size of empty microbeads at 37 ºC in different incubation conditions. Acetate solution day 1 (A), Medium condition day 1 (B), Phosphate buffer saline (PBS) condition day 1 (C), Acetate solution day 5 (D), Medium incubation after day 5 (E), PBS incubation after day 5 (F).

4.5 Morphological Evaluation of Cell-Loaded Microbeads

Cell (L929, MsC, and hFOB 1.19) stability and proliferation were tracked with various concentration of the microbeads (Figure 6 and Figure 7). The diameter of cell-loaded microbeads was recorded (visualized) with microscope. Diameter changes among the group of the experiment were compared to investigate the cell viability and proliferation during 12 days of the experiment (Figure 6. B and Figure 7. B).

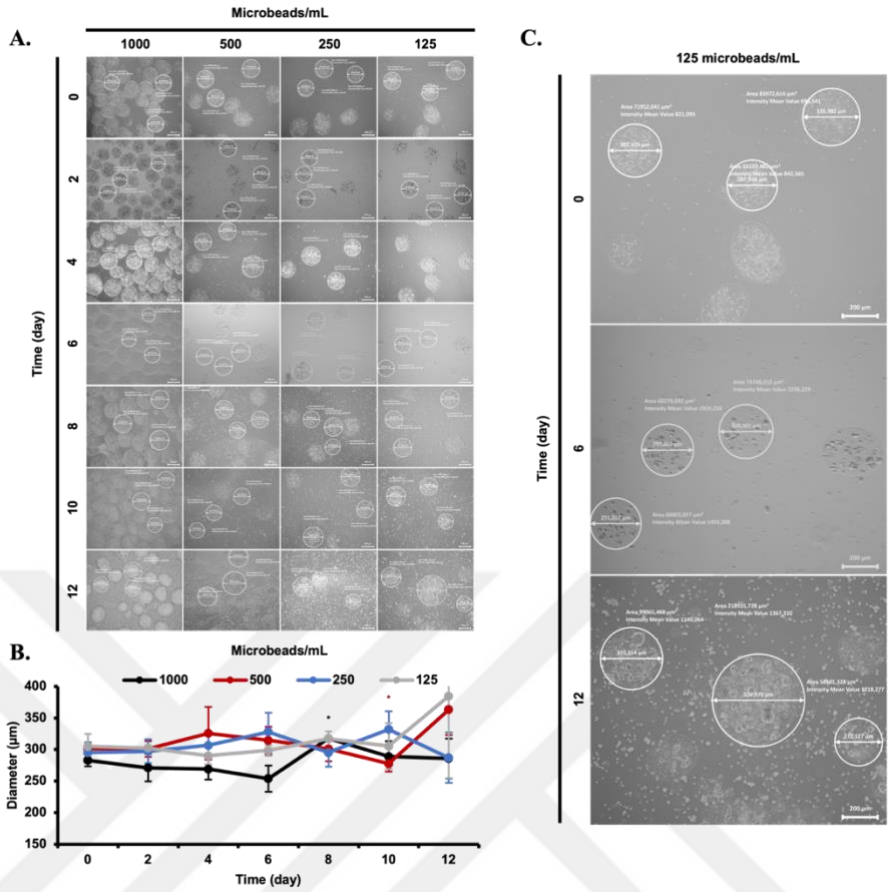

Figure 6. L929 loaded alginate microbeads under the microscope (5×, scale bar: 200 µm) (A). Diameter change of L929 loaded beads during 12 days was graphed (B). Diameter change of 125 microbeads/mL on days 0, 6, and 12 for are shown (C).

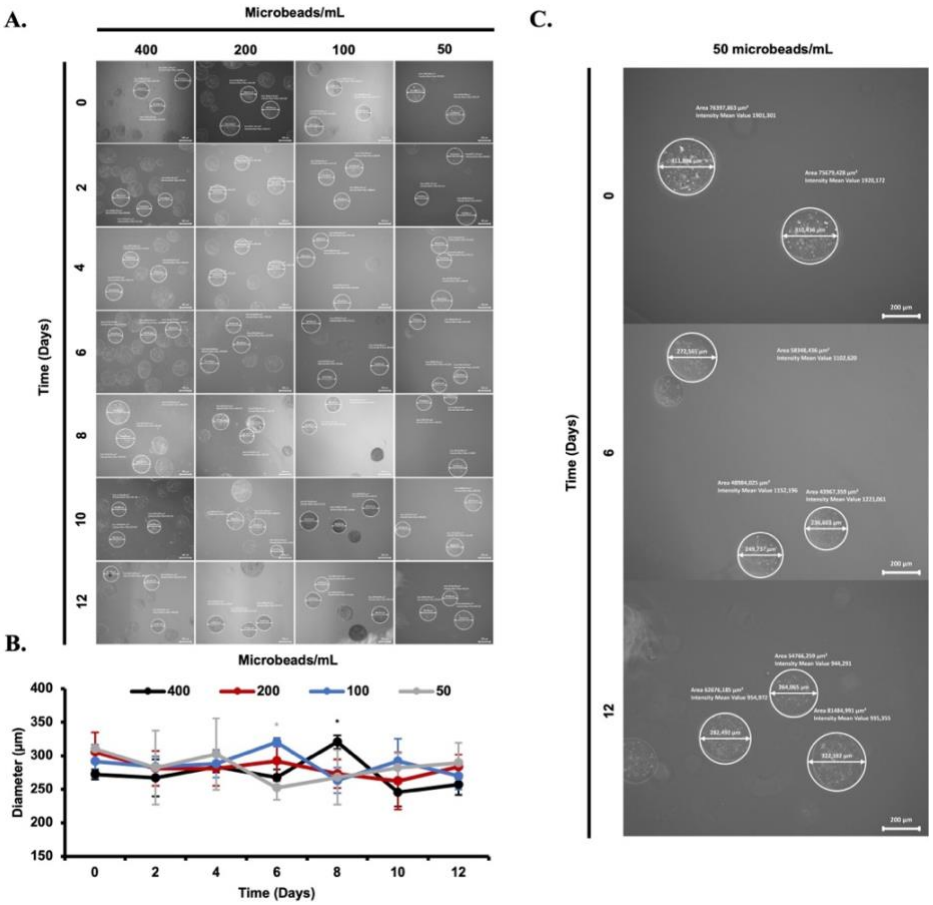

Figure 7. MSCs loaded microbeads during 12 days under fluorescence microscope (A). Graph of MSCs loaded beads diameter change during 12 days period (B). Diameter changes between days 0, 6, and 12 of 50 microbeads/mL are shown (C) (5×, scale bar: 200 µm).

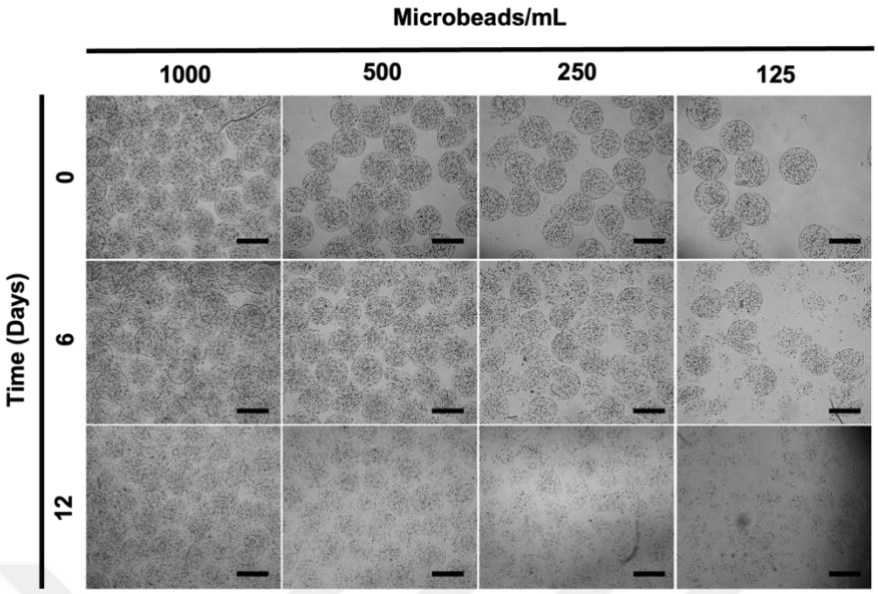

Figure 8. Stability of cell microencapsulated in AlGel. Visualization of hFOB 1.19 cell stability inside the AlGel microbeads and hFOB 1.19 cell line released from microbeads under the microscope (scale bar: 200 μm).

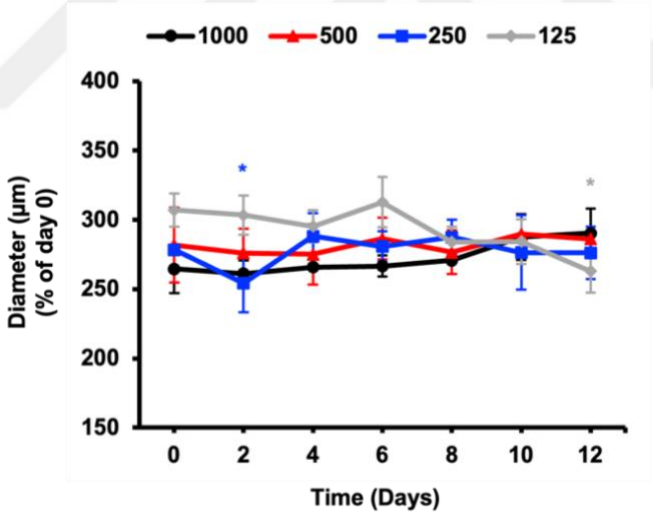

Figure 9. Diameter of hFOB 1.19 loaded AlGel microbeads in DMEM medium for 12 days period.

4.6 GFP Secretion from MSCs Loaded Microbeads

Green fluorescent protein (GFP) signal of MSCs was recorded by fluorosens microscope (Zeiss Axio Vert.A1 inverted microscope) for 12 days (Figure 10).

Fluorosens intensity of cell-loaded microbeads was observed during 12 days. Alteration of the GFP intensity was observed at each group of microbeads day by day until 12. day. GFP intensity from the microbeads was measured in the ImageJ program (Figure 10.B).

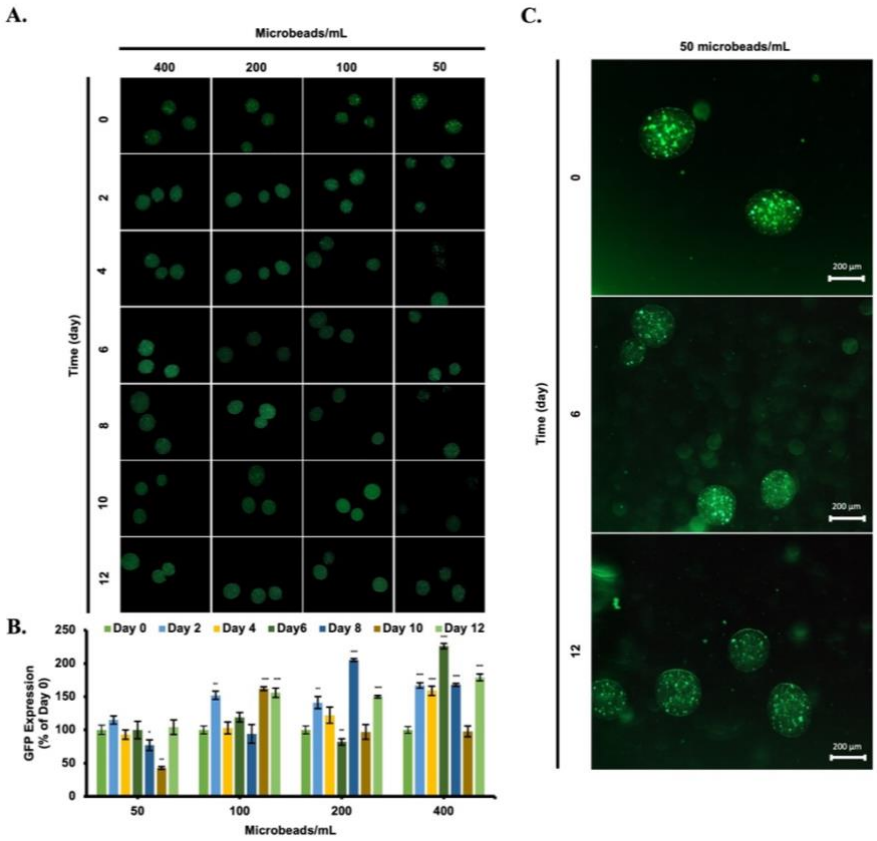

Figure 10. Picture of GFP secretion by MSCs loaded microbeads under microscope (5×, scale bar: 200 µm) (A). Graph of GFP intensity MSCs loaded (B). Picture of GFP secretion by MSCs loaded 50 microbeads/mL on day 0, 6, and 12 (C).

4.7 Glucose Consumption and Lactic Acid Production

Metabolite level in the cell culture medium show cell proliferation and growth. Both cell lines (L929 and MSCs) continuously proliferated in the microbeads according to glucose consumption level both cell lines (Figure 11. A, and C). While glucose level in culture medium is sharply decreased, lactic acid level in culture medium consistently is increased in 2 days incubation time (Figure 11. B, and D). A

consistent plot between glucose and lactic acid level in culture medium was observed following incubation periods.

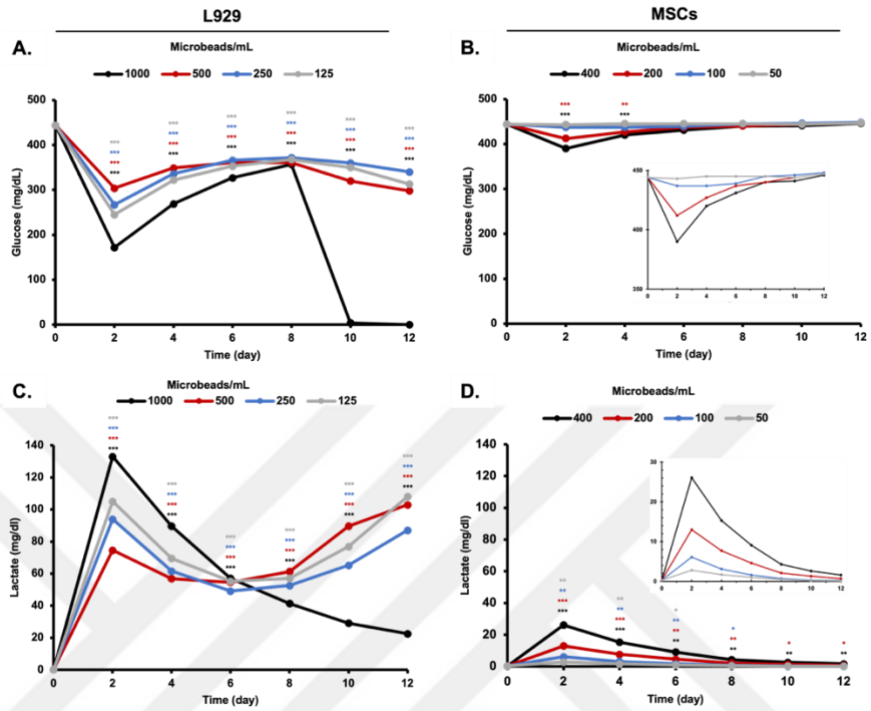

Figure 11. Glucose and lactic acid level inside L929 and MSCs cell medium. (A) Glucose level of L929 cell medium, (B) lactic acid of L929 cell medium, (C) glucose of inside MSCs cell medium, and (D) lactic acid of MSCs cell medium.

4.8 L929 and MSCs Cell Viability Inside the Alginate Microbeads.

Trypan blue dye was used labeling of both cell lines. Total cell numbers of both cells inside the medium and petri dish were calculated using cell counter device. Percentage of the cell viability (L929 cell lines) was decreased with decreasing of the microbeads numbers in media (500, 250, 125 microbeads number in following orders percentage of the L929 cell viability %67.5, %54, %60). Cell viability was stable with decreasing of the microbeads numbers in culture media (400, 200, 100, 50 microbeads number in following orders percentage of the MSCs cell viability % 42.5, % 45.5, % 46.5, %66) (Figure 12. B).

Both cell number (L929, and MSCs) inside the medium was decreased with decreasing of the microbeads numbers. The concentration of the cells in alginate solution was 4 million cells/mL and 2 million cells/mL. Cell numbers of the L929 and MSCs cell-loaded microbeads were 48 L929 and 24 MSCs cells per microbeads. Total cell numbers in the microbeads are also consistently increased among each group (Figure 12.A).

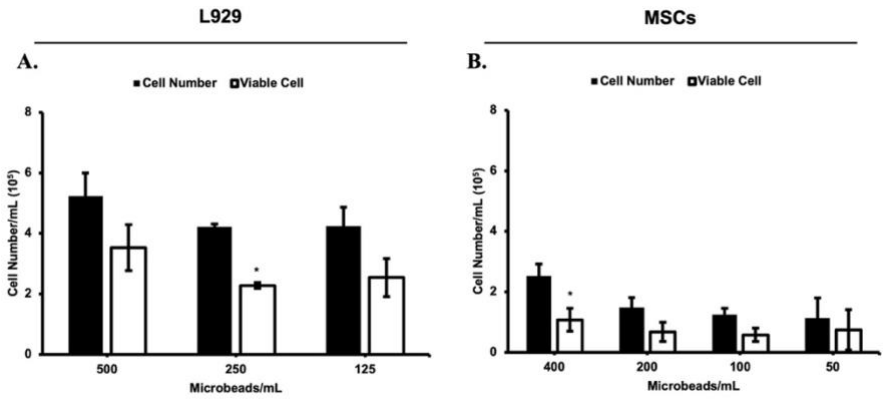

Figure 12. Cell viability of released L929 (A) and MSCs (B) cell lines from microbeads at day 12.

4.9 Total mRNA and Protein Concentration in Culture Medium

Total mRNA concentration inside the culture medium is essential for the cell cycle inside the culture medium. Alteration of the mRNA level was observed between each group of experiments. mRNA concentration of L929 culture medium is not significantly changed. The concentration of the mRNA level of MSC is decreased during the incubation time. Significant differences between day 2 and day 12 are not observed in the mRNA path on the graph compared with the protein path on the graph.

Quantification of the total protein concentration by BCA protein assay was performed for in a biological assay. Total protein concentration was evaluated on day 12 and alteration of the total protein contents in the cultured medium of L929 and MSCs cell lines were compared with glucose and lactic acid level in culture medium

(Figure 13). The total protein amount inside the medium is gradually increased with increasing in the number of microbeads.

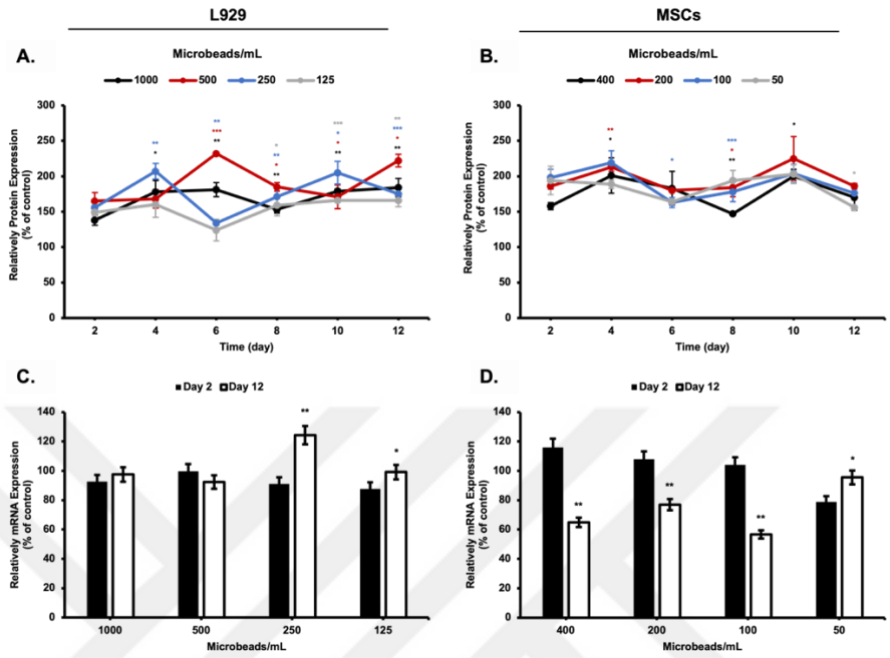

Figure 13. Concentration of protein in culture medium solution of L929 (A) and MSCs (B). Concentration of mRNA in culture medium solutions of L929 cell line (C) and MSCs (D).

4.10 Protein Profile of the Culture Medium

Protein concentration inside the culture medium of L929 and MSCs cell-loaded alginate microbeads was previously measured with BCA assay according to the manufacturing procedure. Alterations of the protein concentration were compared between each day and groups of experiments. We couldn't obtain correlated data between each group experiment with the BCA experiment. For that reason, we performed an SDS-PAGE experiment to illustrate the alteration of the protein profile. We observed different protein profiles during the incubation period but expressed protein was seen to aggregate inside the medium during the incubation period (Figures 14. A and B). We have also investigated the protein profile of the medium of L929 cell-loaded AlGel microbeads (%1 (v/v) of %2 (w/v) gelatin solution). Distinctive bands were observed between each group during the incubation periods.

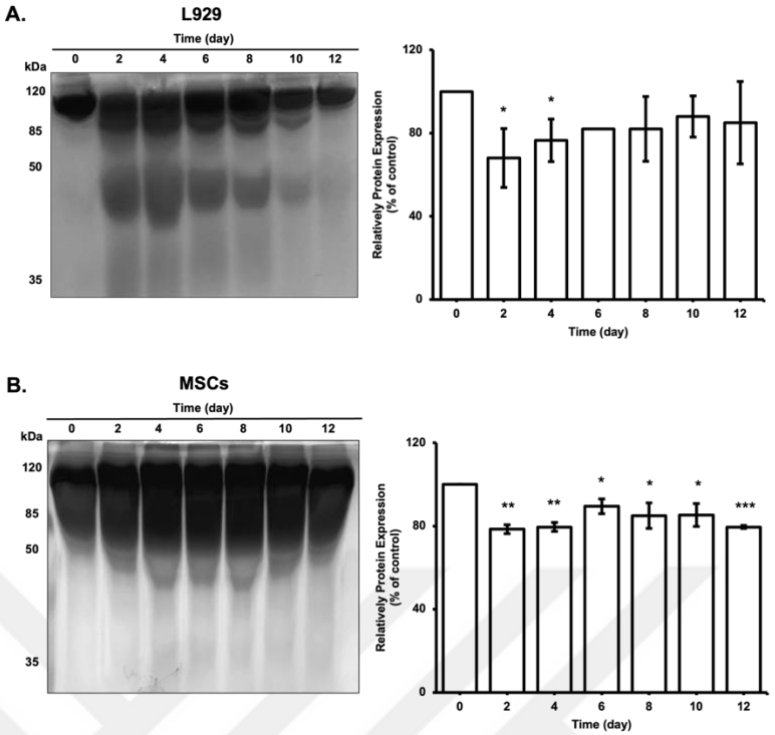

Figure 14. SDS PAGE picture of protein distribution taken from cell culture medium of L929 (A) and MSCs (B) day12.

4.11 Influence of Gelatin Volume on AlGel Microbeads Morphology

After production of AlGel microbeads with the encapsulator device and AlGel microbeads were incubated for 12 days in cell medium. Gelatin solutions were added to the alginate solution with various volume ratios. The addition of the gelatin solution to the alginate solution changes the spherical form of alginate. There is no intact and spherical microbeads formed by the addition of gelatin solution with more than %2 (v/v) ratio. According to the result, increasing the volume of gelatin inside the total polymer solution decreases the stability and sphere shape of the obtained AlGel microbeads. For that reason, %2 volume ratio of %1 (w/v) gelatin is the best option for preparing the AlGel microbeads. Then, we tested the effect of gelatin concentration by weight on alginate-based microbeads formation. By realizing that %2 volume ratio of %1 (w/v) gelatin and %1 volume ratio of %2 (w/v) gelatin solutions contain same amount of gelatin polymer as 2mg, we did not observe any significant difference in terms of shape between these two conditions (Figure 15). Thus, a concentrated form

of gelatin (%1 volume ratio of %2 (w/v) gelatin) was preferred to fabricate the cell-loaded AlGel microbeads. Then we tested a more concentrated gelatin solution (%10-20 gelatin by weight) to fabricate the alginate-gelatin microbeads. We observed the same morphological distribution with increasing gelatin volume inside the total polymer mixture but there is no significant effect observed in terms of microbead morphology due to more gelatin content inside the mixture (Figure 17). We used %2 volume ratio of %20 (w/v) gelatin solution for the cell culture experiment to investigate cell proliferation.

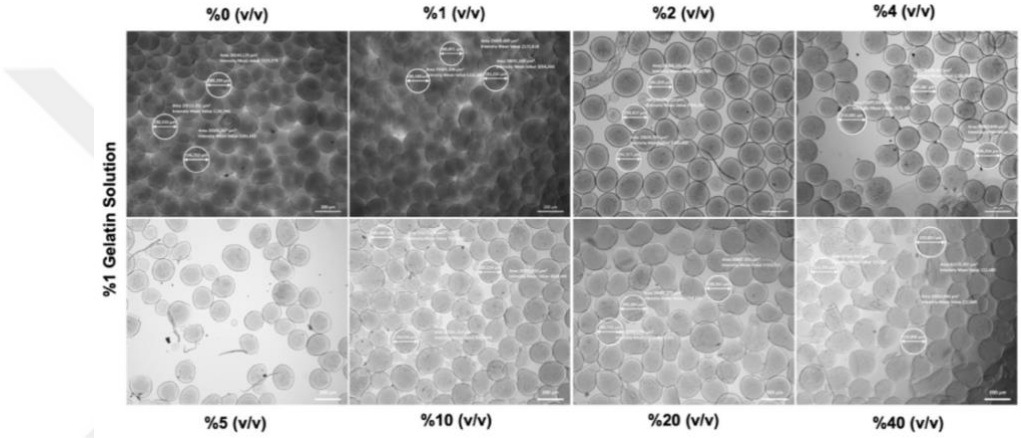

Figure 15. Morphology changes for AlGel microbeads upon the increase of the gelatin content.

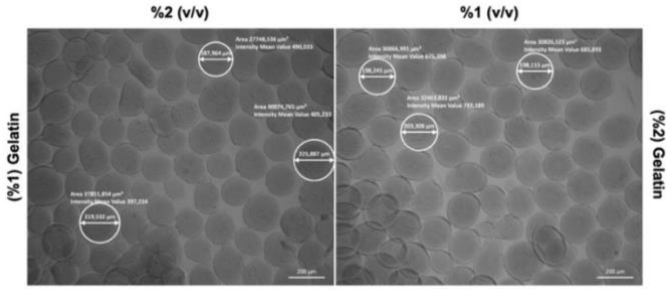

Figure 16. Effect of gelatin concentrations (%1 and %2 gelatin solution) on microbeads formation.

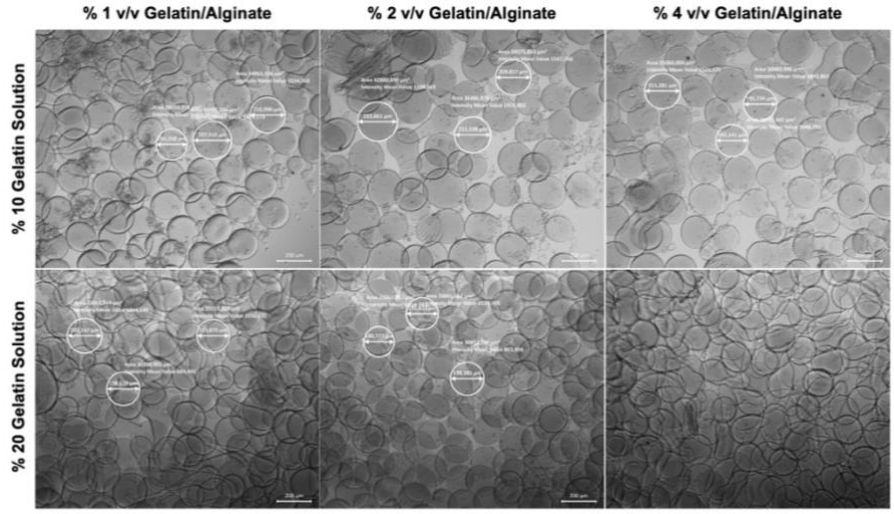

Figure 17. Effect of different volumes of gelatin (%10 and %20 gelatin solution by weight) on microbeads formation.

4.12 L929 Cells in Various AlGel Microbeads

L929 cells were tested inside alginate-gelatin (%1 volume ratio of %2 (w/v) gelatin solution) microbeads. The proliferation of the cells inside the microbead is observed by increasing the cell density inside. There is no cell release observed during the cultivation period. The proliferation of L929 cells was at a lower rate when it is compared with the previous experiment, but it preserves spherical shape during the cultivation time and no significant diameter change was observed during the cultivation period (Figure 18).

L929 cell-loaded AlGel microbeads were labeled with Alexa fluor 488 and DAPI dye for the fluorescence-dependent visualization of cell membrane and nuclei, respectively. After thawing of the cell-loaded AlGel microbeads, spherical shape is disrupted as it is clearly seen in Figure 19. There is disruption observed during the incubation period of the L929 cell-loaded AlGel microbeads. Disruption of the microbeads membrane might be caused by the release of calcium ions and subsequent alginate polymer dissociation during the incubation period of the microbeads. It was promising to notice that deformation of the micro structure was not observed until day 6 after the thawing cycle. Microbead preserved their microbead shape because of

enough alginate and calcium content inside the polymeric shell of microbead. The signal intensity of the cells decreased day by day, but the diameter of the signal intensity increased with time probably because of the cell proliferation.

We have also performed the encapsulation of L929 cells by using an alginate-gelatin solution mixture with (%2 volume ratio of %20 (w/v) gelatin) to see the effect of gelatin content on cell proliferation. After construction of L929 cells-loaded AlGel microbeads, we observed high cell proliferation, cell release to the environment, and increasing acidity inside the medium at 1000 microbead/mL concentration. Acidity conditions inside the medium seem to cause burst release of the microbead, more salt content inside the medium, and increasing in medium turbidity. We observed a high turbidity level and large salt content inside the medium on day 4 of incubation. After the washing step of the medium, we observed highly proliferated cell content inside the culture dish (Figure 20). We also observed high cell concentration inside the microbead after staining the microbead with Alexafluor 488 and DAPI dyes. Then we performed the same experiment and conditions by decreasing the microbead (500 µicrosphere/mL) number in the medium (Figure 21). The same acidity was not observed inside the medium during over 12 days of incubation period. Moreover, we observed that released cells were attached to polystyrene cell culture flask on day 12. It indicates that cells remained viable inside the AlGel microbead during 12 days of incubation. We also detect attachment and differentiation of cells inside the microbead during the incubation periods after Alexafluor 488 staining. Moreover, disruption on the microbeads membrane was not observed at each time point of the incubation period.

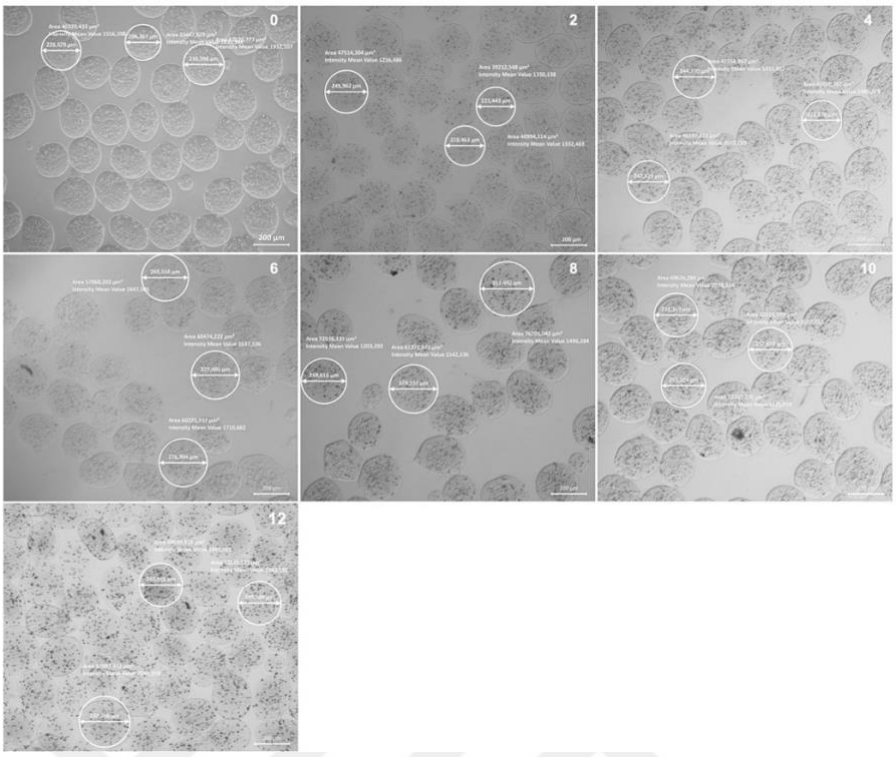

Figure 18. Visualization of L929 cell-loaded AlGel microbeads (%2 (w/v) | %1 (v/v) ratio gelatin).

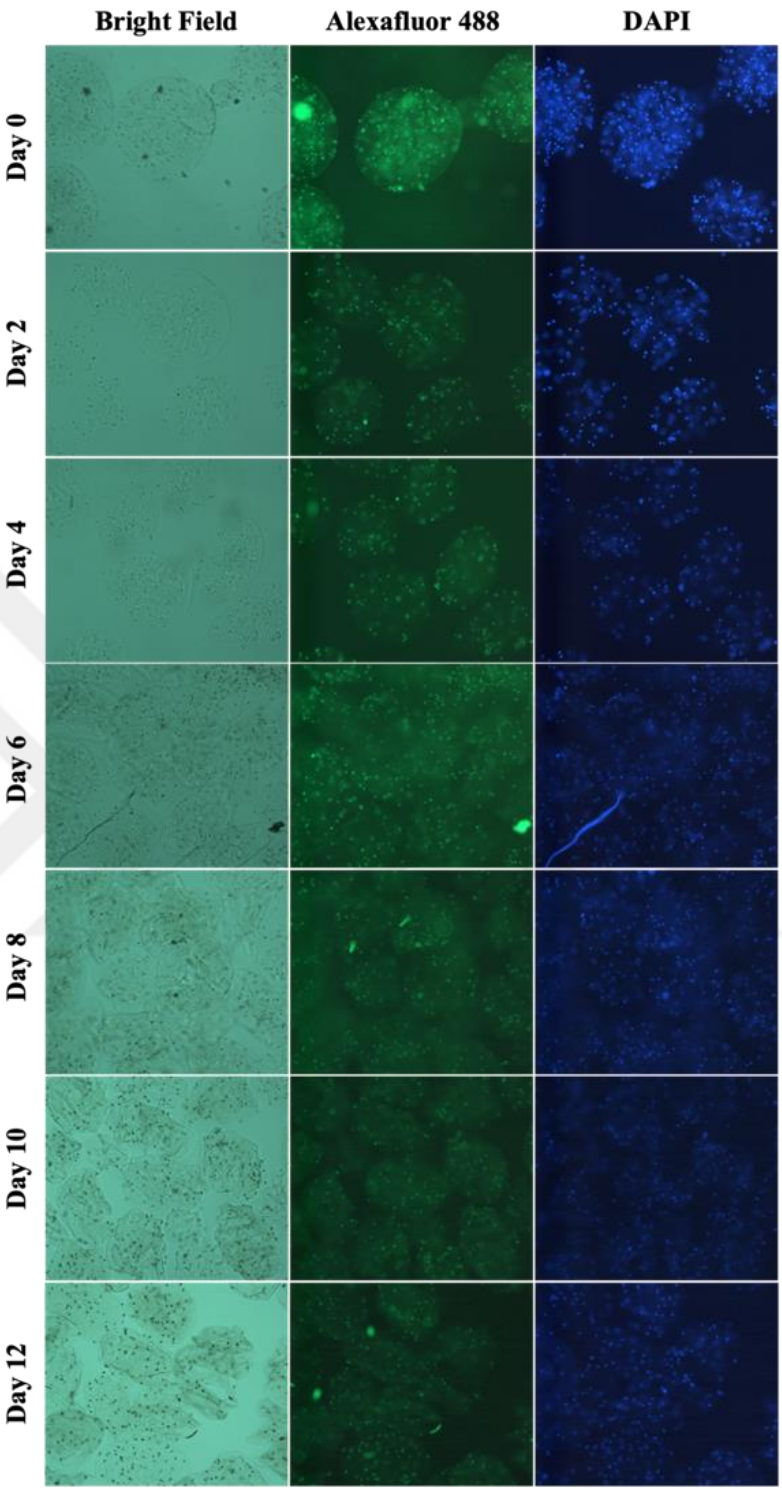

Figure 19. Visualization of ConA-AF488 and DAPI labeled L929 cell-loaded AlGel microbeads (%2 (w/v) | %1 (v/v) ratio gelatin).

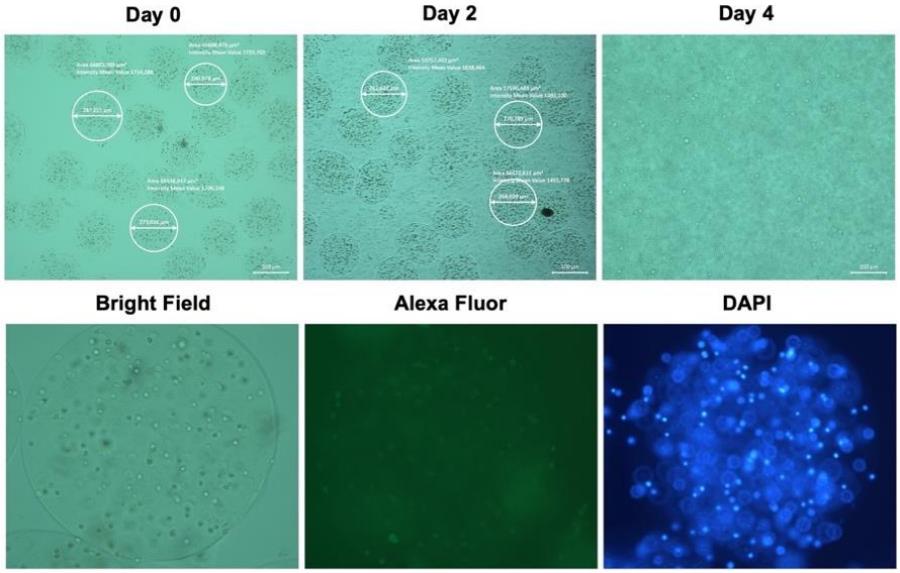

Figure 20. Visualization of ConA-AF488 and DAPI labelled L929 cell-loaded AlGel microbeads (%20 (w/v) | %2 (v/v) ratio gelatin).

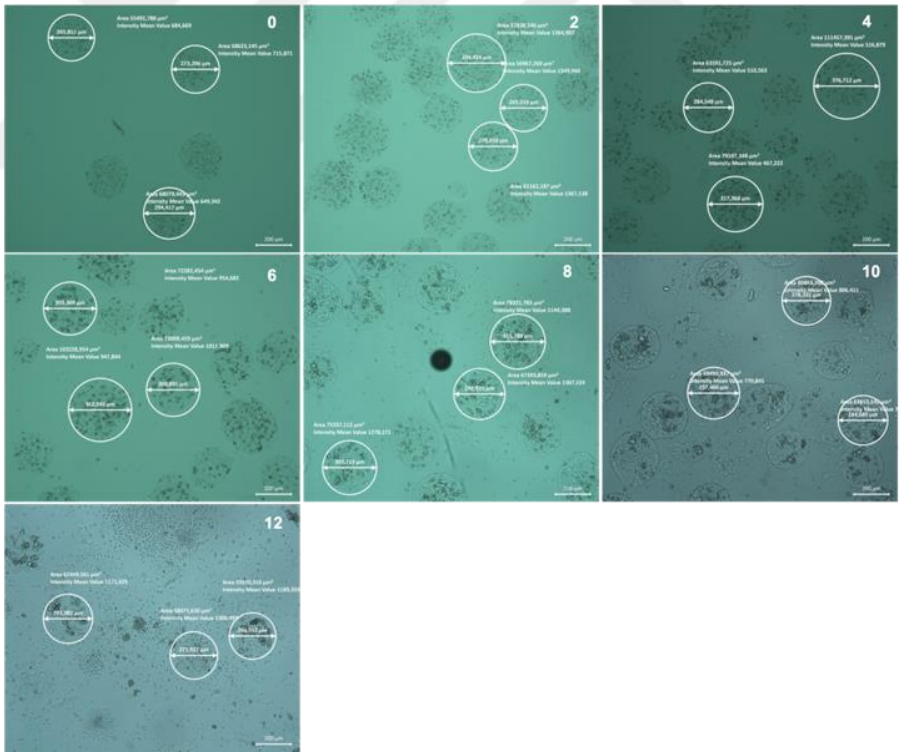

Figure 21. Visualization of L929 cell-loaded AlGel microbeads (%20 (w/v) | %2 (v/v) ratio gelatin).

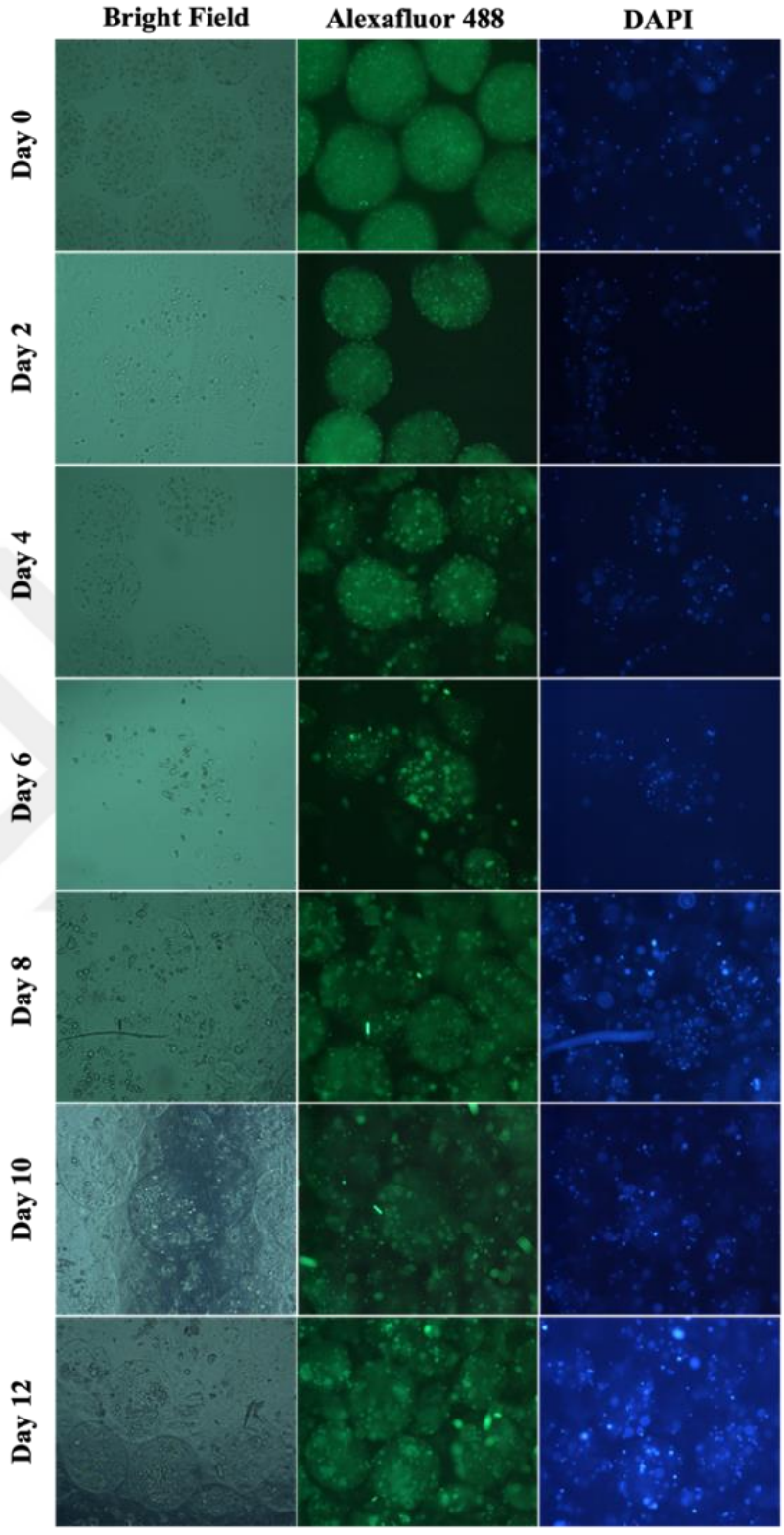

Figure 22. Visualization of ConA-AF488 and DAPI labeled L929 cell loaded alginate-gelatin (%20 (w/v) | %2 (v/v) ratio gelatin) microbeads.

4.13 Effect of BET on Metabolic Activity of hFOB 1.19 Cells

Effect of the BET on metabolic activity of hFOB 1.19 cell lines were tested with various concentration of the BET by MTS assay. Mitochondrial respiration of the cells, cell viability, growth rate of cells and cellular energy capacity (indirectly) evaluated by MTS assay (CHACON et al., 1997). In this experiment, even though cytotoxicity effect of BET on hFOB 1.19 cell lines was observed at 5 µM of BET on day 6, 5 µM of BET did not suppress to metabolic activity of hFOB 1.19 cell line inside the microbeads on day 12. According to results, while statistically significant decrease of mitochondrial activity of the cells were observed at 0.5, 1, and 5 µM BET on day 6, there is no statistically significant decrease observed effect of BET on mitochondrial activity of the cells loaded AlGel microbeads on day 12 (Figure 23). Thus, AlGel microbeads behave as a barrier for reduction to susceptibility of hFOB 1.19 to BET.

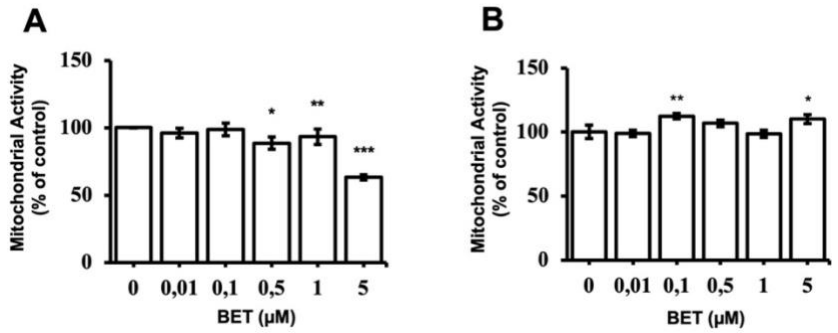

Figure 23. Effect of BET on mitochondrial activity of hFOB 1.19 cell in 2D cell culture (A) on day 6 and hFOB 1.19 cells in AlGel (B) on day 12 were investigated in growth medium (%1 FBS) supplement with various concentration BET.

4.14 Effect of BET and AlGel Microbeads on Cell Viability

Living and dead cell inside the microbeads was pictured for 12 days period by Live and Dead Cell Assay (ab115347, Abcam). While percentage of viable cells is gradually decreased ranging from 93% on day 0 to 57% on day 12, statistically significant decrease of viability was firstly observed on day 4 (Figure 24. C). Number of dead cells inside the bigger aggregates is enhanced day by day inside the AlGel

microbeads. However, cytotoxic effect of BET on cells viability did not detect among groups on day 6 and 12 (Figure 24. B, D and E).

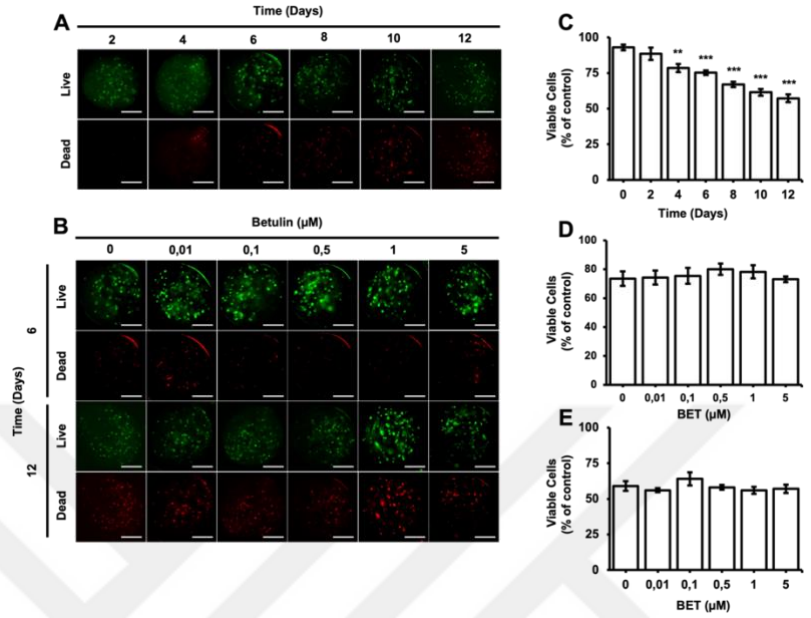

Figure 24. Viability of hFOB 1.19 cells in AlGel. Fluorescence image of live/dead staining for hFOB 1.19 cells in AlGel on days 2, 4, 6, 8, 10, and 12 (scale bar: 100 μm) (A). Percent viable cells in AlGel on days 2, 4, 6, 8, 10, and 12 (C). Fluorescence image of live/dead staining for hFOB 1.19 cells in AlGel incubated with various concentration of BET (0-5 μM) on days 6 and 12 (scale bar: 100 μm) (B). Percent viable cells in AlGel incubated with different concentration BET (0-5 μM) on days 6 (D) and 12 (E).

4.15 Alteration of High-Mannose-Type Glycans (HM_s) Level in Microbeads

Concanavalin-A which is a type of lectin has a strong binding affinity to mannose than other sugars. ConA-AF488 might be used for the evaluation of cell-cell communication by enabling the measurement of the level and localization of the high mannose type N-glycans (HMs) which have a different role in a cell such as transportation of proteins from the golgi apparatus to the various part of the cells (Koyama et al., 2018). According to intensity of high-mannose-type glycans inside the microbeads, cell-cell and cell-AlGel microbeads communication elevated during the incubation of the microbeads (Figure 25. B and C). However, there is no significant effect obtained on intensity of HM inside the microbeads upon treatment with BET

concentration of 0.1, 0.5 and 1 μM on day 12. Statistically slight effect on HM inside the microbeads upon treatment with BET concentration of 0.01 and 5 μM was illustrated according to measurement of relatively ConA-AF488 intensity (Figure 25. A and D).

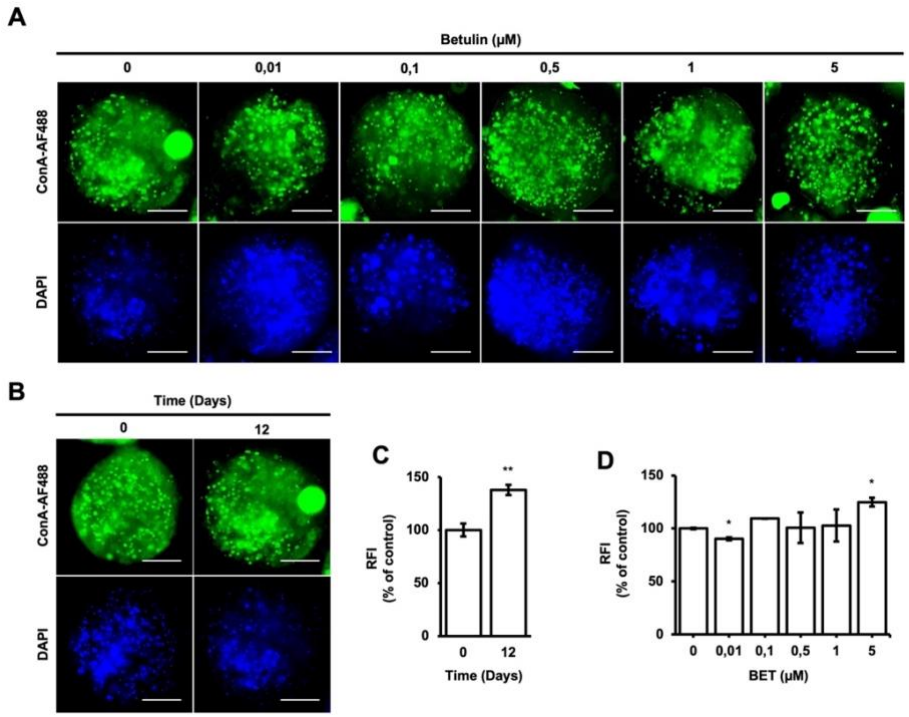

Figure 25. Localization of HMs in hFOB 1.19 cells microencapsulated in AlGel. Fluorescence image of conA-AF488 and DAPI labeled hFOB 1.19 cells microencapsulated in AlGel incubated with different concentration of BET (0-5 μM) on day 12 (scale bar: 100 μm) (A). hFOB 1.19 cells in AlGel on days 0 and 12 (scale bar: 100 μm) (B). Relatively ConA-AF488 intensity of hFOB 1.19 cells in AlGel on days 0 and 12 (C). Relatively ConA-AF488 intensity of hFOB 1.19 cells in AlGel incubated with different concentration of BET (0-5 μM) on day 12 (D).

4.16 Influence of BET on Expression of Osteogenic Markers

Expression of osteogenic markers of encapsulated and non-encapsulated hFOB 1.19 cells is evaluated with measurement of the osteopontin (OPN) expression and glycosaminoglycan (GAGs). Production of osteopontin by osteoblast cells is a marker of differentiation process at terminal stage. Expression of the OPN protein in encapsulated cells increased upon treatment with BET concentration of 0.1 and 0.5 on day 12. There is no statistically significant increment detected on expression of the

OPN protein in non-encapsulated cells. Similarly, secretion of glycosaminoglycans (GAG) from encapsulated cells elevated upon treatment with BET concentration of 0.1 and 0.5.

Moreover, osteogenic differentiation of the hFOB 1.19 cells construct the noodle formation which is detected by alizarin red staining at the end of the 12 days. Microscopic picture of hFOB 1.19 cells shows more noodle formation upon treatment with various BET concentration on day 12 (Figure 26. A). Mineralization level of hFOB 1.19 cells was quantitively analyzed to evaluate calcium content after encapsulation and treatment with BET (Figure 26. D and E). Alizarin Red staining indicate that BET treatment induces osteogenic differentiation of hFOB 1.19 cells. Additionally, induction of the osteogenic differentiation of hFOB 1.19 cells by BET treatment is much higher level on encapsulated hFOB 1.19 cells when compared to non-encapsulated hFOB 1.19 cells (Figure 26. D and E). On the other hand, ALP activity of encapsulated hFOB 1.19 assessed to indicate osteogenic differentiation of hFOB 1.19 cells the after-BET treatment. Dark color spots of ALP positive microbeads inside the picture illustrate that better ALP activity and early bone formation developed upon treatment with BET (Figure 27. B).

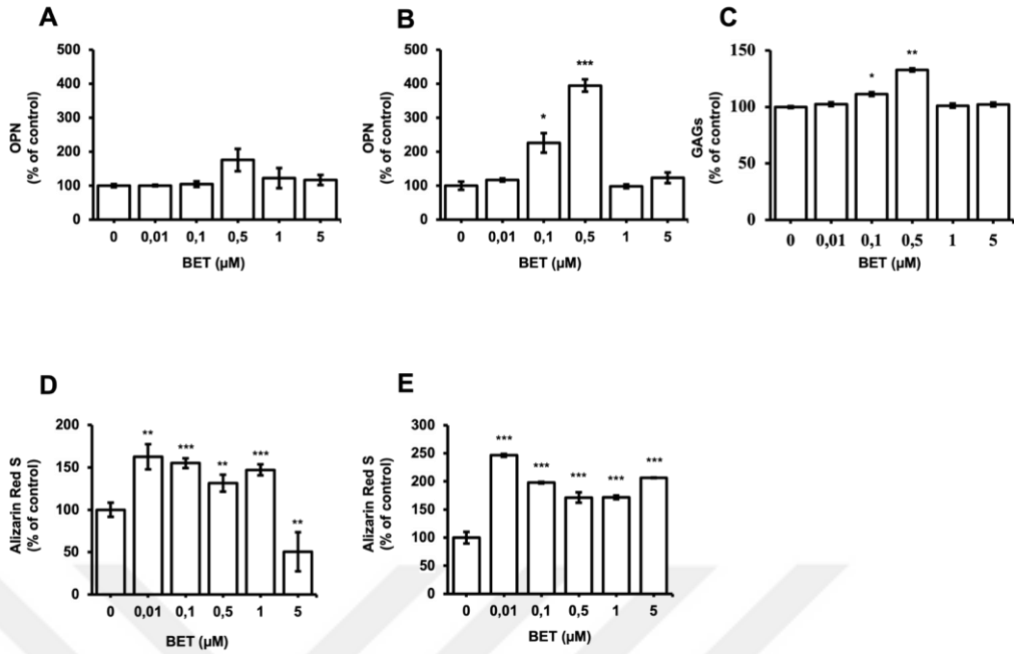

Figure 26. Expression of the osteo-inductive markers from hFOB 1.19 cells after treatment with various concentration of BET (0-5 μM). The amount of OPN in the culture media from the hFOB 1.19 cells (A). hFOB 1.19 cells in AlGel (B) incubated with different concentration of BET (0-5 μM) on day 12. The amount of GAG in the culture media from the hFOB 1.19 cells in AlGel (C) incubated with various concentration of BET (0-5 μM) on day 12. The amount of calcium deposited in the extracellular matrix from the hFOB 1.19 cells (D) and hFOB 1.19 cells in AlGel (E) incubated with various concentration of BET (0-5 μM) on day 12.

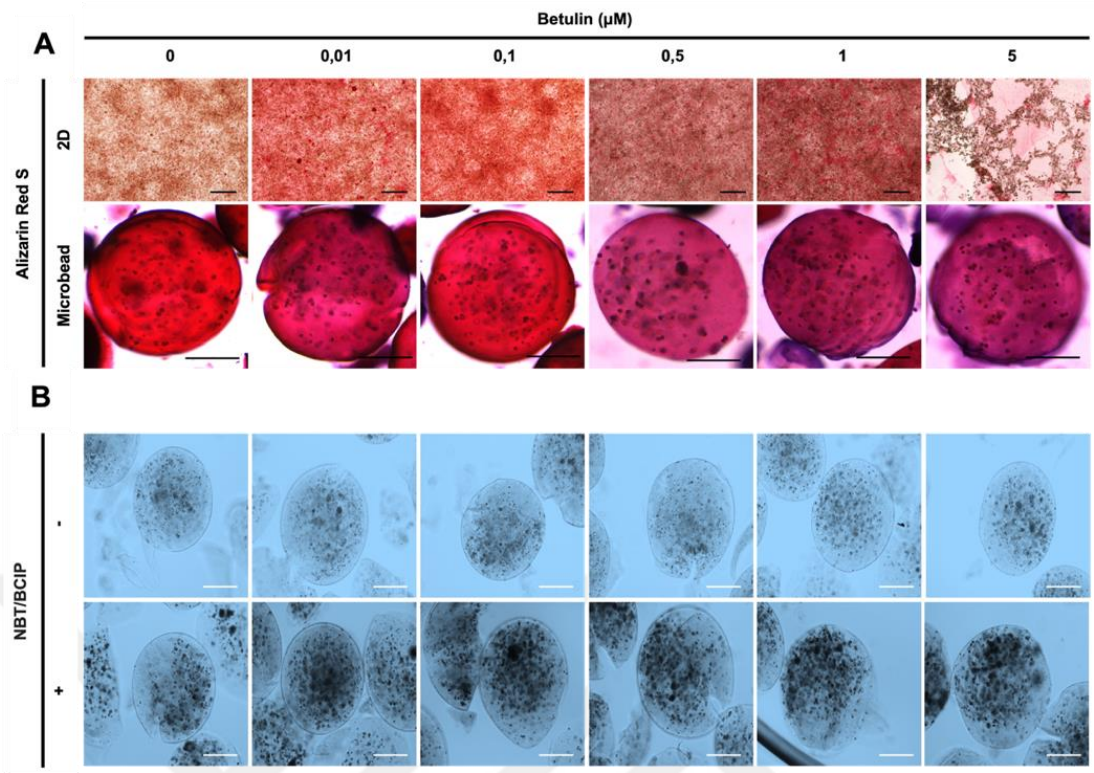

Figure 27. Effect of BET on mineralization and ALP activity of hFOB 1.19. Images showing calcium deposition of non-encapsulated (scale bar: 200 μm) and encapsulated (scale bar: 100 μm) hFOB 1.19 cells upon treatment with BET after 12 days of incubation using alizarin red S (A). ALP enzyme activity of hFOB 1.19 cells (100 μm) in AlGel microbeads after 12 days of incubation using NBT/BCIP (B).

5 DISCUSSION

In this study, various cell lines were encapsulated via electrostatically assisted spraying methods. After construction of the cell-loaded microbeads, cells were analyzed with a fluorescence microscope and their metabolic activity in the microbeads was examined with measurement of the glucose consumption, and lactic acid production. The aim of the experiment is the development of the cell-loaded alginate microbeads and the investigation of cell activity in microbeads construct. Our results showed that cell-loaded microbeads were successfully constructed with alginate and alginate-gelatin polymers and the microbeads were preserve their structure during 12 days of periods. Mesenchymal stem cells were currently used for regeneration of the various tissue types (146), (147). The previous study showed that alginate microbeads are stable *in vitro* condition during 12 days of periods and 2 weeks *in vivo* study. In this study, we hypothesis that mesenchymal stem cells inside the microbeads might be viable, functional and they can continue metabolic activity during 12 days of period.

Mesenchymal stem cells (MSCs) therapy has emerged as a highly effective method for the regeneration of damaged tissue and balancing the hormone level inside the body (85–88,148). Proper isolation of the immune cells might provide ameliorated cell therapy to the patient. Encapsulation of MSCs might be an advantageous strategy for improving the cell survival rate and enhancing cell functioning post transplantation. So, in first chapter of this study aims to construct a polymer-based macro-capsule for the accommodation of cells in an isolated platform once implanted inside the body, which seems to contribute to the increased metabolic activity of the transplanted cell population. A synthetic, yet biodegradable and biocompatible polymer, PCL was utilized for the fabrication of the designed macro-capsule, and it was 3D bio-printed in fiber structure to have permeability ability for the exchange of nutrients reaching the cells inside and removal of waste products out. Obtained results point out that 3D printed PCL-based macro-capsule has enough permeability for the release of HSA, which might enable the proper transfer of albumin proteins inside out for the macro-capsule.

The designed macro-capsule with dimensions of 2x5x10 mm was a small macro-capsule when it's compared to the previously published macro-capsule versions (145). That is why an injection of a small amount of material with a small-sized syringe needle (insulin syringe, 31 G) creates a big gap in it. The closed form of the macro-capsule might be boomed by gas pressure inside the macro-capsule during the injection of cell solution inside. In addition, the printed form of the macro-capsule contains only a two-layer height which is thin enough for possessing a good permeability property possible. After injection of the cell solution into the macro-capsule, the injection gap was filled with a melted form of PCL to prevent immediate cell release once the macro-capsule was dipped into the incubation solution (149). The burst release profile is a major indication for showing the leakage formation of the macro-capsule. Leakage assessment of capsule with HSA protein with a molecular weight of 66.5 kDa (Figure 1C) indicates that protein molecules can pass through the permeable surface of macro-capsule (150).

Although PCL is commonly used in polyester and synthetic polymer for the construction of scaffolds in tissue engineering applications, the major challenge is its cytotoxicity problem emerging from the formation of foreign body response (fibrotic response) when it is in direct contact with the cellular environment(151,152). Our results show that there is no significant adverse effect of the 'indirect contact' method on the viability of MSCs for 72 hours of incubation time. Direct contact of the macro-capsule to cells has resulted in a slight decrease in a cell. These results suggest that the PCL-based macro-capsule platform might outstand as a convenient carrier of the transplantation of MSCs into the body without decreasing the cell viability significantly after the implantation of the cell-loaded macro-capsule.

The metabolic activity of the encapsulated cells which is intended to be used in protein therapy applications (in the near future) is important to monitor for the secretion of the intended protein at the target site in the body. So, the secretion and release of the metabolic products from inside to outside of the macro-capsule are crucially important for understanding its potential as a biomaterial for the regeneration of the target tissue or balancing of the protein level in the target area. Nutrient and

oxygen transition during the cultivation of MSCs has a tremendous effect on cell viability and metabolic activity. In our study, the metabolic activity of encapsulated cells was analyzed by measuring the glucose level and lactic acid level inside the medium (153). Alterations in the glucose and lactic acid levels were monitored during the cell incubation process, where the glucose amount in the medium was measured to decrease by almost 10% by time in a newly refreshed media, compared to 2D cell culture conditions. On the other hand, the produced lactic acid was not seen in the medium at the beginning of the incubation process as expected, whereas demonstrated to emerge in the outer media and was detected to be increased in amount by approximately 8% compared to its 2D version at the end of 15 days of the incubation period.

The diameter of the alginate microbeads was analyzed in a previous study (154). Previous project showed that the diameter of the microbeads was observed around the 400-micrometer (154). In our study, the diameter of the microbeads was observed around the 200-micrometer. The structure of anionic polymer contains net negative charged group. Environmental pH effect on the hydrophilicity of the carboxyl groups inside the anionic polymer. Ionizable carboxylic groups are turned into negatively charged carboxylate ions in high pH conditions (155). Alginate microbeads swell day by day because of the presence of the chelators, monovalent ions, and non-crosslinking divalent cations like Mg^{2+} (156,157). Moreover, the higher concentration of the $CaCl_2$ content in microbeads causes releasing of the calcium from microbeads and increase of the diameter of the microbeads.

The morphology of the microbeads is controlled in various environmental conditions. Salt contents were observed after a 1-day incubation with phosphate buffer solution and salt content in PBS condition was removed with a saline wash. Moreover, the same salt content was also observed in the medium condition on day 5. Calcium ions in microbeads diffuse into the medium and PBS solution and these ions form a calcium salt inside the medium and PBS. Effect of the acetate conditions to H-bonding in alginate polymer eliminate to salt content formation inside the solution (158).

The other finding indicates that cell lines were not only proliferated around the sphere but also attached and proliferated inside the microbeads. L929 cell lines among groups of the experiment were proliferated inside the microbeads for 7 days and some of them were released to the petri dish because of the swelling of the microbeads (figure 6). Moreover, a non-uniformly sized cell-loaded alginate microbeads was observed in the cell culture experiment compared with the unloaded microbeads (159). The non-uniformly distribution of microbeads was caused by cell proliferation inside the microbeads. Cell concentration differences between the MSCs and L929 in alginate solution were also affected by cell proliferation inside the microbeads (160). Although MSC stays stable until 12 days of periods, cell release and debris were seem in 400 microbeads/mL at day 12 (figure 6). The viability of the mesenchymal stem cell was controlled with an expression of GFP. Non-uniformly GFP signal intensity was measured day by day for MSC samples (97). GFP signal intensity inside of each microbeads might be changed because of the nonuniform cell distribution in microbeads (figure 10). Additionally, fluctuating of the GFP signal intensity is related to the cell release and proliferation during the culturing of the cell-loaded microbeads.

Glucose is a carbohydrate which is important for metabolic activity and growth of cell inside the microbeads (153). Lactic acid is the metabolic product of the cellular respiration process. Glucose and lactic acid level inside the culture medium indicate cellular proliferation and metabolic activity *in vitro* conditions. Glucose level inside the media significantly decreases after culturing the cells at day 2 in both cell lines (L929 and MSCs). The same curved line was observed for both glucose and lactic acid level for 12 days periods. Moreover, glucose and lactic acid level inside the media were gradually observed in L929 cell lines like 2D cell culture (160). However, glucose consumption is significantly increased, and lactic acid production is significantly decreased in 1000 microbeads/mL groups. This result is observed because of the salt formation inside the cell culture medium (figure 11). This amount of the microbeads might be the maximum microbeads number for culturing of the L929 cell lines.

Protein distribution inside the culture medium significantly affects to cell cycle during cultivation. Especially, content of culture media effect to metabolic activity of the cell and regulates the double-time and cellular growth of the cell (160) (161). Alteration of the protein content during the incubation of the cell induces expression and regulation of other proteins. Protein paths show that protein inside the medium was increased, but glucose and lactic acid level inside the medium show an approximately linear curve. These results shows L929 cells in microbeads were doubled during the incubation time and their protein expression level was increased day by day, but the same path was not observed during the incubation of the mesenchymal stem cell incubation (figure 11).

Cell-loaded alginate microbeads has a great potential to applicate on regenerative therapy. Cell viability is a key point for the therapeutic efficiency of cell therapy. In this research, released cells from the microbeads were remain viable on day 12 of periods among groups of the experiment (Figure 6 and 7). Different cell numbers at 12 days were obtained between each group of experiments (L929 and MSC_s). The difference between each group has consisted of initial cell numbers both L929 and MSC_s. These results show that both L929 and MSC_s were proliferated and doubled during the 12 days of the periods. Moreover, spheroids formation of the L929 cells line was observed on day 12. Spheroid's formation of the L929 cell lines indicates that L929 cells were proliferated inside microbeads. The viability of the released cells among the group of the experiment was similar (figure 12).

On the other hand, cell loaded alginate-gelatin microbeads give a promising result for cell viability and proliferation. Positively correlation between the gelatin content and cell viability is also demonstrated with various cell type (107), (110), (109), (108). For that purpose, L929 cell-loaded AlGel microbeads are constructed with electrostatically assisted spraying method. Morphology of obtained AlGel microbeads was analyzed and uniform group of AlGel detected with bright field microscopy. The L929 cells inside the AlGel microbeads was evaluated via DAPI and Concanavalin-A Alexaflour 488 staining. Protein distribution in SDS-Page was also investigated to demonstrate alteration of protein content during the incubation time. Our results

showed that cells in AlGel microbeads preserve cellular structure and can release secreted proteins to the culture medium. Previous literature studies showed that the AlGel microbead provides more intact microbead formation compared to the alginate form (110). In this study, we aim to provide more biomimetic culture conditions for L929 which potentially ensure more protein secretion and high cell proliferation during the 12 days of incubation time, which would be an enough time for cellular therapies in general.

Fish gelatin has a similar property to human gelatin and limited biomechanical properties for tissue engineering applications. Limited biomechanical properties of gelatin restrict to fabrication of the scaffold structure to assist cellular attachment, proliferation, and adhesion. Blending gelatin with alginate increases the viscosity of the solution and ensure the mechanical and biological properties for tissue engineering application (162). Boonyagul and coworkers illustrated that a 1:1 ratio of 6% gelatin and %11 alginate bioink mixture might be used as a skin tissue graft (163). In that research, they showed the viscosity and mechanical stability of the bioink directly correlated with the concentration of the alginate polymer in the blend solution. The other research group investigated the ionic coordination between the COO^- of alginate, ferric acid, and gelatin. They showed that a low amount of alginate content in alginate and gelatin mixture causes the release of ferric ions and the disappearance/dissociation of the hydrogels. They also showed that the viability and proliferation of the cells were enhanced by increasing the gelatin ratio in the alginate–gelatin mixture. Gelatin inside the solution might assist RGD (Arg-Gly-Asp) residues to better cell adhesion (105). They also showed that %82.5 of cells after 1 day of implantation and %32.8 of them after 3 days of implantation seem to be stable inside injectable hydrogels, and there is no significant difference observed in osteogenic differentiation. Compared to these results, what we have observed for our cell-loaded Al-Gel microbeads point out that increasing the gelatin concentration inside the polymer blend results in non-uniform microbeads formation (figure 15).

Gelatin is the denaturation type of collagen type 1 which is the main component of the extracellular matrix, which means that alginate-gelatin (AlGel) microbeads

contain the RGD-rich proteins for enhanced cell adhesion, differentiation, and proliferation compared to the alginate only microbeads (164). Cell loaded AlGel microbeads were previously prepared with various cell types such as a human endothelial cell (HUVEC), rat cardio myoblast, and U937 (110), (109), (165) (107). In this research, they have not fabricated injectable size of the microbead and there is no compression about the content of gelatin effect on microbead formation, long-term morphological changes of the microbeads, and cell stability inside the microbeads. In our study, we evaluate the effect of gelatin content on cell stability inside the microbeads formation and compare it to the previous cell-loaded alginate microbeads study. Our findings show that the volume of the gelatin inside the AlGel microbeads disrupts microbeads formation to a certain degree. Additionally, there is no significant morphological change observed with increasing the gelatin content inside the alginate microbeads. The release Ca^{+2} ions from L929 cell-loaded AlGel microbeads might have been occurred via diffusion from inside of the microbeads to the environment. This situation results in a decrease in the alginate content inside the microbeads, an increase in the size of alginate porosity, and subsequent swelling of the microbeads. This process increases the diffusion rate of medium, oxygen, and other nutrients inside the microbeads, and later cells release outside from the microbeads. Luckly, we have not observed any cell release and change in microbeads diameter during the incubation period of L929 cell-loaded AlGel (%1 (v/v) | %2 (w/v) gelatin) microbeads (figure 18). This situation might have occurred with a large number of microbeads incubation or the limited cell proliferation inside the AlGel microbeads. Increasing the gelatin (%2 (v/v) | %20 (w/v) gelatin) content inside the alginate microbeads have a directly correlated effect on not only the proliferation rate of L929 cells but also rise the acidity of the medium during the cultivation period. So, increasing the acidity inside the medium results in the destabilization of the microbeads form and the release of polymer chains into the medium on day 4 (figure 20). This process was also consistent with L929 cell-loaded alginate microbeads.

In order to visualize encapsulated cells in the microbeads, fluorescent dyes were utilized to stain the nuclei and cell membrane of cells inside the microbeads. One of them is concanavalin-A conjugated Alexafluor488 (ConA-AF488). Con-A is a type of

lectin which specifically binds to various molecules such as sugars, glycoproteins, and glycolipids. Especially, concanavalin has a strong binding affinity to mannose than other sugars (166). ConA-AF488 specifically binds to alpha-mannopyranosy and alpha-glucopyranosy. ConA-AF488 is also used to visualize cytoplasm and cell surface. One of the literature studies illustrates that conA-AF488 might be used for the evaluation of cell-cell communication by enabling the measurement of the level and localization of the high mannose type N-glycans (HMs) which have a different role in a cell such as transportation of proteins from the golgi apparatus to the various part of the cells. The relationship between the intracellular localization of HMs and the intensity of the ConA-AF488 signal indicates the cell-cell communication (CCC) level between the cells. They illustrated that cellular shape and cell-to-cell communication of cancer cells might be regulated with golgi monoxides inhibitors and n-glycans. Moreover, they disclosed that n-glycan accumulation inside the cells causes a more spherical form of the cancer cell. They also observed increasing in the cell length and attachment of the cells via regulation of the golgi monoxides inhibitor concentration (167). ConA-AF488 is also used for the detection of the cellular state inside the tissue (168). For our results, we observed that L929 cells preserved their cellular shape inside the AlGel microbeads during the 12 days of incubation period (Figure 19). Structural integrity of microbeads from day 6 to day 12 was disrupted after the freeze-thaw cycle of the microbeads. Disrupted forms of L929 cell-loaded alginate microbeads might be an indication for the release of Ca^{+2} ions and the following dissociations of alginate polymer along the incubation periods. This release profile might be an outstanding reason for the observed decrease in the microbeads stability over time. Furthermore, this dissociation of microbeads integrity results in cell release from the microbeads into the surrounding medium, which was easily detected by light microscopy visualization. That is why cell number inside the microbeads was decreased day by day and the intensities of ConA-AF488 and DAPI staining originating from the inside part of microbeads were diminished gradually over incubation time.

Regarding the microbead numbers with which further characterizations were performed, the acidity inside the cultivation medium was seen as the key limitation. Increased acidity inside the medium mostly probably happens due to either a large

number of cells inside the microbeads or a large number of microbeads inside the medium. The increased acidity of the alginate microbeads resulted in salt formation inside the cultivation medium (Figure 20). This salt formation is constructed by releasing a large amount of sodium from alginate into the environment and their binding to chloride ions with an ionic interaction. pH value is also decreased with the increase of cellular waste inside the microbeads environment. A low pH value inside the alginate microbeads increases the hydrogen concentration inside the microbeads. Deprotonation of the carboxylic acid groups of alginate polymers might enhance the dissolving of the polymer chains, as well. Consequently, a large amount of cellular waste accumulated inside the microbeads seems to regulate not only the pH value of the environment but also affects structural integrity of microbeads.

Cellular differentiation, cell to cell communication, and cell to environment communication might be detected via the interaction of the high mannose type N-glycans (HMs) around the cells (167). For that purpose, ConA-AF488 and DAPI labeled cells were monitored inside the microbeads. The conA-AF488 intensity shows us that the cellular interaction profile is not only detected inside of the cells but also observed outside the cells. The profile of ConA-AF488 intensity is consistent with the bright field image of the microbeads. Moreover, the sphere formation of the cells inside the AlGel microbeads shields and lowers the detection of DAPI intensity (Figure 22). In future, nuclear shape change of cells inside the microbeads might tracked via embedding the microbeads inside the paraffin and then, staining of the with hematoxylin and eosin dye which indicate cellular formation, extracellular structure, and nuclear formation during the incubation period. Additionally, the embedding of the microbead prevents disruption of the microbead structural integrity by eliminating the washing steps which were performed after ConA-AF488 and DAPI staining.

The protein profile of culture media was investigated to demonstrate alteration of protein content during the incubation period. For that purpose, the culture medium of the cell-loaded AlGel microbeads was collected during the incubation period. Differently expressed same protein profiles were observed at each time point of cell culture incubation. However, the aggregation of proteins inside the culture medium

results in a degradation profile on SDS-PAGE (Figure 14). The degradation profile on SDS-PAGE and aggregates were not eliminated by applying the previously reported method (169). A significant band observed in the SDS page might represent bovine serum albumin protein which is around 66,5 kDa (figure 14). Similar protein profiles in a cell culture medium were observed in a previous literature study (170). Similarly, low abundant proteins inside the culture medium could not be detected because of the low protein expression. For overcoming this limitation, we increase the microbeads number inside the cell culture, and the intensity of the low abundant proteins inside the cell culture was increased directly. Detected proteins were mostly higher than the bovine serum albumin. The previous literature study shows that cell derived extracellular matrix is higher than 75 kDa (171). The proteins we observe on the SDS gel might be cell-sourced extracellular matrix proteins that have a role in the construction of the extracellular matrix structure.

AlGel microbeads seem to have a great potential for construction of cell-loaded microbeads for cell therapy. Their stability clearly has a positive impact on cell viability and cell-cell interaction inside the structural integrity of microbeads. Protein release from encapsulated cells indicates that this approach might be utilized for protein therapy for the regeneration of the degenerative tissues, as well. According to these results, cells inside the AlGel microbeads remain viable during the 12 days of incubation period. Cellular differentiation was preserved during 12 days and spheroid formation was also observed inside the microbeads.

Alginate based microbeads are commonly used in therapeutic delivery research and cell culture study (Jacobs-Tulleneers-Thevissen et al., 2013). Previous studies showed that alginate-based microbeads provide excellent cellular ECM and 3D microenvironment to construct modular tissue by building blocks (Nabavinia et al., 2019). Bringing biopolymers of alginate and gelatin together enhance performance, and quality of microscaffolds and simulate signaling cascades related to ossification, osteogenic differentiation, and proliferation of the cells. Combinations of biopolymers by addition of gelatin to alginate microbeads makes microbeads more applicable for proliferation and differentiation of osteoblast cells (Nabavinia et al., 2019). On the

other hand, some triterpenoids such as betulin derivatives improve osteogenic differentiation of some murine cells in osteogenic condition in vitro (Yogeeswari & Sriram, 2010). Moreover, porcine chondrocyte inside the betulin treated scaffolds induce expression of anabolic genes, catabolic genes, and differentiation factors. Although, osteogenic activity of betulin (BET) on murine osteoblast models is confirmed in vitro, there is limited number of studies examined the effect of BET and 3D microenvironments on osteoblast cell models for in vitro research. In this study, osteogenic differentiation of hFOB 1.19 cell lines inside the combinations of biopolymers of alginate and gelatin microbeads is examined upon treatment with BET.

Gel strength of calcium crosslinked alginate decrease over the incubation time in vitro condition. Degradation of microbeads by ion exchange mechanism change to size, shape, porosity, and stability of crosslinked alginate. Decreasing of crosslinking density in calcium crosslinked alginate over the time result the disintegration of alginate, weak hydrogel formation, increasing pore size (Shoichet et al., 1996). Increasing pore size of microbead accelerate inward diffusion of ions from outside of the microbeads and then swelling in alginate microbeads by them (Leslie et al., 2013). However, microbead presence or absence of the cells shows slightly different degradation over the time. Rate of microbead degradation presence of the cells gradually increase as the microbeads concentration decrease while there are no statistically significant changes observed in microbead diameter over the 12-days period. Microbead degradation presence of the osteoblast cells might be associated with native enzymatic activity of mammalian cells or calcium uptake by osteoblast-like cells from the environment (Modi et al., 2019).

In this report, antiproliferative activity of the betulinic acid investigated on encapsulated and non-encapsulated normal osteoblast cell line hFOB 1.19 model. Effect of betulin on cell proliferation, osteoblast differentiation, osteoclastogenesis have described in vitro research studies. There are various reports showing alteration in antiproliferative activity of BET depending upon cell type. For example, while 1-20 μM of BET treatment on cell viability of murine pre-osteoblast cell line MC3T3-E1 do not significantly decrease cell viability (Lo et al., 2010), proliferation of human

osteoblast cell (hFOB 1.19) and neoplastic osteoblast-like cell (Saos-2) were inhibited by BET at concentration of 1 μM and 5 μM (Mizerska-Kowalska et al., 2019). On the other hand, 10 and 20 μM BetA treatment on fifth day promotes the proliferation of human periodontal ligament stem cells (hPDLSCs) (Li et al., 2021). Cytotoxicity effect of BET on hFOB 1.19 used in this report as previous reports are, BET exerted no cytotoxity on encapsulated hFOB 1.19. Microencapsulation of hFOB 1.19 limit to BET effect on metabolic activity of encapsulated hFOB 1.19 cells and provide the long-term functionality and survival of the cultured cells (Leslie et al., 2020; Sun et al., 1996). Thus, these results suggest that encapsulation strategy is powerful way to maintain metabolic activity and functioning of cultured cells upon treatment with BET concentration of 5μM.

Viability of the transplanted cells post injection is crucial for efficiency of injectable cell-based therapies at injured side. Direct injection of stem cells presents the syringe needle flow force which disrupt the cell membrane and decrease the viability of transplanted cells ranging from 1% to 32% (Aguado et al., 2012). Cell viability rate post injection might be improved by encapsulation of cells by hydrogels which protect to cells from damaging effect of extensional forces by direct injection. In studies using alginate hydrogel as a scaffold for cell-based therapy, composition of alginate hydrogel not only modifies chemical and physical properties of hydrogel, but also effect to cellular response and efficiency of injectable cell-based therapies (Nabavinia et al., 2019). Many studies on relationship between the cellular response and hydrogel illustrated that gelatin content inside the alginate solution contains the RGD-rich proteins for enhanced cell viability compared to the alginate solution (Alipour et al., 2021; Azhar et al., 2014; Firouzi et al., 2020; Salinas & Anseth, 2008). However, in vitro studies showed that weakened structure of polymeric materials and proliferation of the cells inside hydrogels limit cell-material contact area and reduces viability of encapsulated cells during the cultivation (Aguado et al., 2012; Leslie et al., 2013). Previous studies support to our findings that shows decreasing of cell viability rate inside the alginate-gelatin microbeads from day 1 to day 12.

The formation of the cells such as spherical form and elongated form in the microbeads gives to information about the interaction between the cells and materials. According with previous research on cellular response to material, gelatin content inside the alginate mixture provides better cell adhesion properties because of the RGD (Arg-Gly-Asp) residue inside them (Anamizu & Tabata, 2019). Cell to cell and cell to material communication might be evaluated by enabling the measurement of the level and localization of the high mannose type N-glycans (HMs) which have a different role in a cell such as transportation of proteins from the golgi apparatus to the various part of the cells. Additionally, cellular shape and cell-to-cell communication of cells is regulated with level of n-glycans inside the cell, for example accumulation of n glycans give sphere formation to the cells (Koyama et al., 2020). Our findings support previous studies that show increasing of cell to cell and cell to material communication day by day inside the AlGel microbeads (Sarker et al., 2015).

Three stages responsible for the maturation of the mesenchymal stem cell into osteoblast cells followed by cell proliferation (condensation), secreting of extracellular matrix, terminal differentiation with matrix calcification, and new bone formation. Fraction healing process consist to maturation of osteoblast cells proceeding of serious of cascades reaction and expression of genes and markers. Level of expressed genes indicate progression stage of maturation on bone formation and bone defect healing. Activation of the signaling cascades by various agents such as betulinic acid induce differentiation of mesenchymal stem cells into mature osteoblast cells (Li et al., 2021; Lo et al., 2010; Mizerska-Kowalska et al., 2019; Senamontree et al., 2021). Betulin promotes to upregulation runt-related transcription factor 2 (RUNX2) which is responsible for expression of osteoblast marker genes such as alkaline phosphatase (ALP), osteocalcin (OCN), and osteopontin (OPN). Additionally, betulin has role on regulation to glucose and lipid metabolism, and beneficially effect on obesity via activation of UCP-1 (Poher et al., 2015). Moreover, one of the studies confirmed to opposite relationship between adipogenesis and osteogenesis via identification of mechanism on deacetylation of RUNX2 by Sirt-1 is known as a major regulatory of longevity and metabolic disorder. In supportive way, resveratrol activates Sirt-1 and block nicotinamide (NAM) which inhibit RUNX2 and stimulate to PPARγ for

adipogenesis (Shakibaei et al., 2012). Similarly, BA induce to differentiation of osteoblast murine cells (MC3T3-E1) instead of adipogenesis of adipocytes (3T3-L1) (Brusotti et al., 2017). Consistently, betulin acid treatment at 0.5 μM to hFOB 1.19 cells significantly enhance to expression of OPN which is late-stage differentiation marker. Moreover, increment degree of calcification and calcified nodule formation of osteoblast cells after betulin acid treatment support to previous findings on mineralization.

Alginate microbeads stimulate to expression of the osteogenic gene markers such as RUNX2 (Leslie et al., 2013). Alginate microbeads provides sufficient environment to the bone cells for osteogenesis, maturation of mesenchymal stem cells to osteoblast cells, stimulation of collagenous and non-collagenous protein expression in ECM of the bone (Qiu et al., 2022). Chemical composition of alginate microbeads alters to functionality of cells and efficiency of cellular therapy after the transplant process. For example, bolus of calcium ions on the surface of alginate microbeads interacts with surrounding phosphate ions and result to calcification minerals which is similar to hydroxyapatite (HA) (Lee et al., 2010). On the other hand, calcified microbeads were obtained *in vitro* via incubation of microbeads with dulbecco's modified eagle medium (DMEM) which provides accumulation of the PO_4^{-3} and Ca^{2+} ions and formation of the bone like HA coating on microbeads surface (Xu et al., 2022). HA coating materials *in vivo* absorb various adhesive proteins such as fibronectin from serum solution (Deligianni et al., 2000). Absorption of proteins from HA coated materials makes polymeric surface more suitable for migration, and adhesion of the osteoblast cells (García & Boettiger, 1999). Similarly, HA inside alginate microbeads provide better strength of gelatin binding to microbead and more efficient environment to osteoblastic cell proliferation and differentiation (Nabavinia et al., 2019). Moreover, HA content inside the microbead up-regulate osteoblast marker genes such as osteopontin (OPN), osteocalcin (OCN), and RUNX-2 (Alipour et al., 2021). Previous findings in line with our study which reported significant increase in the osteogenic markers such as ALP, OPN, and calcification inside the alginate- gelatin microbeads compared to 2D cell culture.

Tissue engineering studies provide more efficient cell therapeutics with sustaining functional ability of cell transplant for early regeneration of defect side. Cells require a supplement for differentiation and maturation of cell transplant to indicate desired effect on defect side. Previous research on osteoblast cell loaded alginate-gelatin microbeads and betulin give promising results for studies on treatment of bone defect and osteoporosis. This study confirms the other study that indicate combination of osteoblast cell loaded microbead and betulin might provide more effective osteoblastic cell proliferation and differentiation *in vitro*.

6 CONCLUSION

In the first chapter of this study, polymeric macro-capsule (2x5x10 mm) constructs were fabricated using a polyester-based PCL polymer by an FDM-based 3D bio-printing technology and then analyzed for their different features like their protein release profiles, impact on metabolic activity of encapsulated cells and *in vitro* cytotoxicity levels. A thin layer of porous macro-capsule was investigated for its permeability degree by release studies with different molecules such as trypan blue, and HSA. 98% of the protein was released from the permeable surface of the macrocapsule within 24 hours. Metabolic assessment and viability of cells inside the macro-capsule together with biomaterial toxicity was demonstrated that 3D printed porous macro-capsule platform might be a suitable carrier for patients' stem cell transplantation (91).

Secondly, we fabricate to alginate and alginate-gelatin cell loaded microbeads which provide stable and efficient delivery system and in vitro cell culture model. Analyzes of this system indicate that cell loaded microbeads is applicable in cell therapy according to its stability, biodegradability, and size. In this chapter, we optimize to fabrication of L929 and MSCs cell loaded alginate microbeads in vitro. Cellular state was controlled by various experiment such as glucose, lactic acid measurement, GFP intensity calculation and SDS page. Spheroid form of L929 and MSCs cell was observed inside microbeads and spheroids formation inform enhanced metabolic activity, cell viability, cellular functioning. Initially releasing of cell from microbeads to environment shows to degradation of the polymeric walls of microbeads during the time. Cellular proliferation from during to 12 day is also proved by increasing of the protein expression levels of L929 cells from 68% to 85%.

These findings clearly indicate that microencapsulation of living cells under optimized conditions has a strong impact on providing a powerful tool for ensuring the survival and metabolic activity of cells to be delivered to the injured or damaged tissue part for cellular therapy purposes.

Lastly, osteoblastic effect of betulin on osteoblast cells investigated in 2D environment and in alginate-gelatin microbeads. Our work suggests that combination of the cell encapsulation and treatment of supplements to osteoblast cells improve expression of osteogenic markers *in vitro* model. Based on our data, microbeads eliminate negative effect of BET on cell viability and metabolic activity of osteoblast cells at concentration of 1 μM and 5 μM BET. Furthermore, differentiation studies confirm that microbeads promote better osteopontin secretion and calcium deposition rather than 2D cell culture environment. The overall study reveals that combination osteoblast cell encapsulation with BET treatment speed up to mineralization and differentiation of the osteoblast cells.

7 REFERENCES

1. Ma G, Fang D, Liu Y, Zhu X, Nie J. Electrospun sodium alginate/poly(ethylene oxide) core-shell nanofibers scaffolds potential for tissue engineering applications. Carbohydr Polym. 2012;87(1):737–43.
2. Jeong B, Kim SW, Bae YH. Thermosensitive sol-gel reversible hydrogels. Vol. 64, Advanced Drug Delivery Reviews. 2012. p. 154–62.
3. Yoo HS, Park TG. Biodegradable polymeric micelles composed of doxorubicin conjugated PLGA-PEG block copolymer. Journal of Controlled Release. 2001;70(1–2):63–70.
4. Shubhra QTH, Tóth J, Gyenis J, Feczkó T. Poloxamers for surface modification of hydrophobic drug carriers and their effects on drug delivery. Polymer Reviews. 2014;54(1):112–38.
5. Zhu W, Chuah YJ, Wang DA. Bioadhesives for internal medical applications: A review. Vol. 74, Acta Biomaterialia. 2018. p. 1–16.
6. Ahn JS, Suh JM, Lee M, Jeong B. Slow eroding biodegradable multiblock poloxamer copolymers. Polym Int. 2005;54(5):842–7.
7. Yu L, Zhang Z, Zhang H, Ding J. Biodegradability and biocompatibility of thermoreversible hydrogels formed from mixing a sol and a precipitate of block copolymers in water. Biomacromolecules. 2010;11(8):2169–78.
8. Ward MA, Georgiou TK. Thermoresponsive polymers for biomedical applications. Polymers (Basel). 2011;3(3):1215–42.
9. Cheaburu CN, Ciocoiu ON, Staikos G, Vasile C. Thermoresponsive sodium alginate-g-poly(N-isopropylacrylamide) copolymers III. Solution properties. J Appl Polym Sci. 2013;127(5):118–26.
10. Gong C, Qi T, Wei X, Qu Y, Wu Q, Luo F, et al. Thermosensitive Polymeric Hydrogels As Drug Delivery Systems. Curr Med Chem. 2012;20(1):79–94.
11. Frandsen JL, Ghandehari H. Recombinant protein-based polymers for advanced drug delivery. Chem Soc Rev. 2012;41(7):2696–706.
12. Kavimandan NJ, Losi E, Peppas NA. Novel delivery system based on complexation hydrogels as delivery vehicles for insulin-transferrin conjugates. Biomaterials. 2006;27(20):3846–54.
13. Kleemann E, Neu M, Jekel N, Fink L, Schmehl T, Gessler T, et al. Nano-carriers for DNA delivery to the lung based upon a TAT-derived peptide covalently coupled to PEG-PEI. In: Journal of Controlled Release. 2005. p. 299–316.
14. Torchilin VP, Levchenko TS, Rammohan R, Volodina N, Papahadjopoulos-Sternberg B, D'Souza GGM. Cell transfection in vitro and in vivo with nontoxic TAT peptide-liposome-DNA complexes. Proc Natl Acad Sci U S A. 2003;100(4):1972–7.
15. Xia CQ, Wang J, Shen WC. Hypoglycemic effect of insulin-transferrin conjugate in streptozotocin-induced diabetic rats. Journal of Pharmacology and Experimental Therapeutics. 2000;295(2):594–600.

16. Widera A, Kim KJJ, Crandall ED, Shen WC. Transcytosis of GCSF-Transferrin across rat alveolar epithelial cell monolayers. Pharm Res. 2003;20(8):1231–8.
17. Dinerman AA, Cappello J, Ghandehari H, Hoag SW. Solute diffusion in genetically engineered silk-elastinlike protein polymer hydrogels. Journal of Controlled Release. 2002;82(2–3):277–87.
18. Dinerman AA, Cappello J, El-Sayed M, Hoag SW, Ghandehari H. Influence of Solute Charge and Hydrophobicity on Partitioning and Diffusion in a Genetically Engineered Silk-Elastin-Like Protein Polymer Hydrogel. Macromol Biosci. 2010;10(10):1235–47.
19. Asghari F, Samiei M, Adibkia K, Akbarzadeh A, Davaran S. Biodegradable and biocompatible polymers for tissue engineering application: a review. Vol. 45, Artificial Cells, Nanomedicine and Biotechnology. 2017. p. 185–92.
20. David G. Collagen-based 3D structures-versatile, efficient materials for biomedical applications. In: Biopolymer-Based Formulations: Biomedical and Food Applications. 2020. p. 881–906.
21. Evron Y, Colton CK, Ludwig B, Weir GC, Zimermann B, Maimon S, et al. Long-term viability and function of transplanted islets macroencapsulated at high density are achieved by enhanced oxygen supply. Sci Rep. 2018 Dec 1;8(1):6508–21.
22. Uludag H, De Vos P, Tresco PA. Technology of mammalian cell encapsulation. Adv Drug Deliv Rev. 2000;42(1–2):29–64.
23. Halib N, Perrone F, Cemazar M, Dapas B, Farra R, Abrami M, et al. Potential applications of nanocellulose-containing materials in the biomedical field. Vol. 10, Materials. 2017. p. 977–1007.
24. Shukla RK, Tiwari A. Carbohydrate molecules: An expanding horizon in drug delivery and biomedicine. Crit Rev Ther Drug Carrier Syst. 2011;28(3):255–92.
25. Wiederschain GYa. Polysaccharides. Structural diversity and functional versatility. Biochemistry (Moscow). 2007;72(6):1204–371.
26. Min KH, Sasaki SF, Kashiwabara Y, Umekawa M, Nisizawa K. Fine structure of SMG alginate fragment in the light of its degradation by alginate lyases of Pseudomonas sp. J Biochem. 1977;81(3):555–62.
27. Rowley JA, Madlambayan G, Mooney DJ. Alginate hydrogels as synthetic extracellular matrix materials. Biomaterials. 1999;20(1):45–53.
28. Grasselli M, Diaz LE, Cascone O. Beaded matrices from cross-linked alginate for affinity and ion exchange chromatography of proteins. Biotechnology Techniques. 1993;7(10):707–12.
29. Pawar SN, Edgar KJ. Alginate derivatization: A review of chemistry, properties and applications. Vol. 33, Biomaterials. 2012. p. 3279–305.
30. Hari PR, Chandy T, Sharma CP. Chitosan/calcium-alginate beads for oral delivery of insulin. J Appl Polym Sci. 1996;59(11):1659–808.
31. Mi FL, Sung HW, Shyu SS. Drug release from chitosan-alginate complex beads reinforced by a naturally occurring cross-linking agent. Carbohydr Polym. 2002;48(1):61–72.

32. Chan AW, Whitney RA, Neufeld RJ. Semisynthesis of a controlled stimuli-responsive alginate hydrogel. Biomacromolecules. 2009;10(3):609–16.
33. Bhattarai N, Zhang M. Controlled synthesis and structural stability of alginate-based nanofibers. Nanotechnology. 2007;18(45):455601–11.
34. Laurienzo P, Malinconico M, Motta A, Vicinanza A. Synthesis and characterization of a novel alginate-poly(ethylene glycol) graft copolymer. Carbohydr Polym. 2005;62(3):274–82.
35. Skjåk-Bræk G, Zanetti F, Paoletti S. Effect of acetylation on some solution and gelling properties of alginates. Carbohydr Res. 1989;185(1):131–8.
36. Freeman I, Kedem A, Cohen S. The effect of sulfation of alginate hydrogels on the specific binding and controlled release of heparin-binding proteins. Biomaterials. 2008;29(22):3260–8.
37. Sinquin A, Hubert P, Dellacherie E. Amphiphilic Derivatives of Alginate: Evidence for Intra- and Intermolecular Hydrophobic Associations in Aqueous Solution. Vol. 9, Langmuir. 1993. p. 3334–7.
38. Mahou R, Meier RRH, Bühler LH, Wandrey C. Alginate-poly(ethylene glycol) hybrid microspheres for primary cell microencapsulation. Materials. 2014;7(1):275–86.
39. Bernkop-Schnürch A, Kast CE, Richter MF. Improvement in the mucoadhesive properties of alginate by the covalent attachment of cysteine. Journal of Controlled Release. 2001;71(3):277–85.
40. Vallée F, Müller C, Durand A, Schimchowitsch S, Dellacherie E, Kelche C, et al. Synthesis and rheological properties of hydrogels based on amphiphilic alginate-amide derivatives. Carbohydr Res. 2009;344(2):223–8.
41. Coates EE, Riggin CN, Fisher JP. Photocrosslinked alginate with hyaluronic acid hydrogels as vehicles for mesenchymal stem cell encapsulation and chondrogenesis. J Biomed Mater Res A. 2013;101 A(7):1962–70.
42. Kumar MNVR, Muzzarelli RAA, Muzzarelli C, Sashiwa H, Domb AJ. Chitosan chemistry and pharmaceutical perspectives. Chem Rev. 2004;104(12):6017–84.
43. Zhao Y, Park RD, Muzzarelli RAA. Chitin deacetylases: Properties and applications. Vol. 8, Marine Drugs. 2010. p. 24–46.
44. An HK, Park BY, Kim DS. Crab shell for the removal of heavy metals from aqueous solution. Water Res. 2001;35(15):3551–6.
45. Chattopadhyay DP, Inamdar MS. Aqueous behaviour of chitosan. Int J Polym Sci. 2010;2010:1–7.
46. Jayakumar R, Reis RL, Mano JF. Chemistry and applications of phosphorylated chitin and chitosan. E-Polymers. 2006;6(1):1–16.
47. Jayakumar R, Nagahama H, Furuike T, Tamura H. Synthesis of phosphorylated chitosan by novel method and its characterization. Int J Biol Macromol. 2008;42(4):335–9.
48. Rúnarsson ÖV, Holappa J, Jónsdóttir S, Steinsson H, Másson M. N-selective “one pot” synthesis of highly N-substituted trimethyl chitosan (TMC). Carbohydr Polym. 2008;74(3):740–4.

49. Rosenthal R, Günzel D, Finger C, Krug SM, Richter JF, Schulzke JD, et al. The effect of chitosan on transcellular and paracellular mechanisms in the intestinal epithelial barrier. Biomaterials. 2012;33(9):2791–800.
50. Berger J, Reist M, Mayer JM, Felt O, Peppas NA, Gurny R. Structure and interactions in covalently and ionically crosslinked chitosan hydrogels for biomedical applications. Vol. 57, European Journal of Pharmaceutics and Biopharmaceutics. 2004. p. 19–34.
51. Cai H, Zhang ZP, Ping CS, Bing LH, Xiao XZ. Synthesis and characterization of thermo- and pH- sensitive hydrogels based on Chitosan-grafted N-isopropylacrylamide via γ-radiation. Radiation Physics and Chemistry. 2005;74(1):26–30.
52. Timell TE. THE ACID HYDROLYSIS OF GLYCOSIDES: I. GENERAL CONDITIONS AND THE EFFECT OF THE NATURE OF THE AGLYCONE. Can J Chem. 1964;42(6):1456–72.
53. Smidsrød O, Haug A, Lársen B. Oxidative-reductive depolymerization: a note on the comparison of degradation rates of different polymers by viscosity measurements. Carbohydr Res. 1967;5(4):482–5.
54. Menchicchi B, Fuenzalida JP, Bobbili KB, Hensel A, Swamy MJ, Goycoolea FM. Structure of Chitosan determines its interactions with mucin. Biomacromolecules. 2014;15(10):3550–8.
55. Chen S, Cao Y, Ferguson LR, Shu Q, Garg S. Evaluation of mucoadhesive coatings of chitosan and thiolated chitosan for the colonic delivery of microencapsulated probiotic bacteria. J Microencapsul. 2013;30(2):103–15.
56. Thiang Yian Wong, Preston LA, Schiller NL. Alginate lyase: Review of major sources and enzyme characteristics, structure-function analysis, biological roles, and applications. Vol. 54, Annual Review of Microbiology. 2000. p. 289–340.
57. Kean T, Thanou M. Biodegradation, biodistribution and toxicity of chitosan. Vol. 62, Advanced Drug Delivery Reviews. 2010. p. 3–11.
58. Lim SM, Song DK, Oh SH, Lee-Yoon DS, Bae EH, Lee JH. In vitro and in vivo degradation behavior of acetylated chitosan porous beads. J Biomater Sci Polym Ed. 2008;19(4):453–66.
59. Kular JK, Basu S, Sharma RI. The extracellular matrix: Structure, composition, age-related differences, tools for analysis and applications for tissue engineering. Vol. 5, Journal of Tissue Engineering. 2014. p. 1–17.
60. Bason C, Gallorini M, Berardi AC. The Extracellular Matrix, Growth Factors and Morphogens in Biomaterial Design and Tissue Engineering. In 2018. p. 1945–56.
61. Kusindarta DL, Wihadmadyatami H. The Role of Extracellular Matrix in Tissue Regeneration. In: Tissue Regeneration. 2018. p. 65–73.
62. Fidler AL, Boudko SP, Rokas A, Hudson BG. The triple helix of collagens - An ancient protein structure that enabled animal multicellularity and tissue evolution. Vol. 131, Journal of Cell Science. 2018. p. 1–15.
63. Dong C, Lv Y. Application of collagen scaffold in tissue engineering: Recent advances and new perspectives. Vol. 8, Polymers. 2016. p. 42–62.

64. Meyer M. Processing of collagen based biomaterials and the resulting materials properties. Biomed Eng Online. 2019;18(1):24–98.
65. Copes F, Pien N, Van Vlierberghe S, Boccafoschi F, Mantovani D. Collagen-based tissue engineering strategies for vascular medicine. Vol. 7, Frontiers in Bioengineering and Biotechnology. 2019. p. 1–15.
66. Wang X, Ao Q, Tian X, Fan J, Tong H, Hou W, et al. Gelatin-based hydrogels for organ 3D bioprinting. Vol. 9, Polymers. 2017. p. 401–24.
67. Gorgieva S, Kokol V. Collagen- vs. Gelatine-Based Biomaterials and Their Biocompatibility: Review and Perspectives. In: Biomaterials Applications for Nanomedicine. 2011. p. 17–52.
68. Bello AB, Kim D, Kim D, Park H, Lee SH. Engineering and functionalization of gelatin biomaterials: From cell culture to medical applications. Vol. 26, Tissue Engineering - Part B: Reviews. 2020. p. 164–80.
69. Hohenester E. Structural biology of laminins. Vol. 63, Essays in Biochemistry. 2019. p. 285–95.
70. Hosoyama K, Lazurko C, Muñoz M, McTiernan CD, Alarcon EI. Peptide-based functional biomaterials for soft-tissue repair. Front Bioeng Biotechnol. 2019;7(205):1–19.
71. Nyberg E, Holmes C, Witham T, Grayson WL. Growth factor-eluting technologies for bone tissue engineering. Drug Deliv Transl Res. 2016;6(2):184–94.
72. Bejleri D, Davis ME. Decellularized Extracellular Matrix Materials for Cardiac Repair and Regeneration. Vol. 8, Advanced Healthcare Materials. 2019. p. 1–53.
73. Seo Y, Jung Y, Kim SH. Decellularized heart ECM hydrogel using supercritical carbon dioxide for improved angiogenesis. Acta Biomater. 2018;67:270–81.
74. Hashemi M, Kalalinia F. Application of encapsulation technology in stem cell therapy. Vol. 143, Life Sciences. 2015. p. 139–46.
75. He Y. Application of flow-focusing to the break-up of an emulsion jet for the production of matrix-structured microparticles. Chem Eng Sci. 2008;63(9):2500–7.
76. Đorđević V, Balanč B, Belščak-Cvitanović A, Lević S, Trifković K, Kalušević A, et al. Trends in Encapsulation Technologies for Delivery of Food Bioactive Compounds. Vol. 7, Food Engineering Reviews. 2014. p. 452–90.
77. Chan ES, Lee BB, Ravindra P, Poncelet D. Prediction models for shape and size of ca-alginate macrobeads produced through extrusion-dripping method. J Colloid Interface Sci. 2009;338(1):63–72.
78. Weir GC, Bonner-Weir S. Scientific and political impediments to successful islet transplantation. Vol. 46, Diabetes. 1997. p. 1247–56.
79. Scharp DW, Marchetti P. Encapsulated islets for diabetes therapy: History, current progress, and critical issues requiring solution. Vols. 67–68, Advanced Drug Delivery Reviews. 2014. p. 35–73.

80. Jacobs-Tulleneers-Thevissen D, Chintinne M, Ling Z, Gillard P, Schoonjans L, Delvaux G, et al. Sustained function of alginate-encapsulated human islet cell implants in the peritoneal cavity of mice leading to a pilot study in a type 1 diabetic patient. Diabetologia. 2013;56(7):1605–14.
81. Gabr MM, Zakaria MM, Refaie AF, Ismail AM, Khater SM, Ashamallah SA, et al. Insulin-producing Cells from Adult Human Bone Marrow Mesenchymal Stromal Cells Could Control Chemically Induced Diabetes in Dogs: A Preliminary Study. Cell Transplant. 2018 Jun 1;27(6):937–47.
82. Tomei AA, Villa C, Ricordi C. Development of an encapsulated stem cell-based therapy for diabetes. Vol. 15, Expert Opinion on Biological Therapy. Taylor and Francis Ltd; 2015. p. 1321–36.
83. Skrzypek K, Groot Nibbelink M, Van Lente J, Buitinga M, Engelse MA, De Koning EJP, et al. Pancreatic islet macroencapsulation using microwell porous membranes. Sci Rep. 2017 Dec 1;7(1):1–12.
84. Vaithilingam V, Evans MDM, Lewy DM, Bean PA, Bal S, Tuch BE. Co-encapsulation and co-transplantation of mesenchymal stem cells reduces pericapsular fibrosis and improves encapsulated islet survival and function when allografted. Sci Rep. 2017 Dec 1;7(1):1–13.
85. Moshaverinia A, Xu X, Chen C, Ansari S, Zadeh HH, Snead ML, et al. Application of stem cells derived from the periodontal ligament orgingival tissue sources for tendon tissue regeneration. Biomaterials. 2014;35(9):2642–50.
86. Kook YM, Kang YM, Moon SH, Koh WG. Bi-compartmental 3D scaffolds for the co-culture of intervertebral disk cells and mesenchymal stem cells. Journal of Industrial and Engineering Chemistry. 2016;38:113–22.
87. Huebsch N, Lippens E, Lee K, Mehta M, Koshy ST, Darnell MC, et al. Matrix elasticity of void-forming hydrogels controls transplanted-stem-cell-mediated bone formation. Nat Mater. 2015;14(12):1269–77.
88. Park JS, Shim MS, Shim SH, Yang HN, Jeon SY, Woo DG, et al. Chondrogenic potential of stem cells derived from amniotic fluid, adipose tissue, or bone marrow encapsulated in fibrin gels containing TGF-β3. Biomaterials. 2011;32(32):8139–49.
89. Krishnan R, Alexander M, Robles L, Foster CE, Lakey JRT. Islet and stem cell encapsulation for clinical transplantation. Vol. 11, Review of Diabetic Studies. 2014. p. 84–101.
90. Desai TA, Tang Q. Islet encapsulation therapy — racing towards the finish line? Nat Rev Endocrinol. 2018;14(11):630–2.
91. Saenz Del Burgo L, Ciriza J, Espona-Noguera A, Illa X, Cabruja E, Orive G, et al. 3D Printed porous polyamide macrocapsule combined with alginate microcapsules for safer cell-based therapies. Sci Rep. 2018;8(1):1–14.
92. O'Sullivan ES, Vegas A, Anderson DG, Weir GC. Islets transplanted in immunoisolation devices: A review of the progress and the challenges that remain. Vol. 32, Endocrine Reviews. 2011. p. 827–44.

93. An D, Chiu A, Flanders JA, Song W, Shou D, Lu YC, et al. Designing a retrievable and scalable cell encapsulation device for potential treatment of type 1 diabetes. Proc Natl Acad Sci U S A. 2017 Jan 9;115(2):E263–72.
94. Clatworthy JP, Subramanian V. Stem cells and the regulation of proliferation, differentiation and patterning in the intestinal epithelium: Emerging insights from gene expression patterns, transgenic and gene ablation studies. Vol. 101, Mechanisms of Development. 2001. p. 3–9.
95. Wang N, Adams G, Buttery L, Falcone FH, Stolnik S. Alginate encapsulation technology supports embryonic stem cells differentiation into insulin-producing cells. J Biotechnol. 2009;144(4):304–12.
96. Leslie SK, Cohen DJ, Boyan BD, Schwartz Z. Production of osteogenic and angiogenic factors by microencapsulated adipose stem cells varies with culture conditions. J Biomed Mater Res B Appl Biomater. 2020;108(5):1857–67.
97. Leslie SK, Kinney RC, Schwartz Z, Boyan BD. Microencapsulation of stem cells for therapy. In: Methods in Molecular Biology. Humana Press Inc.; 2017. p. 251–9.
98. Wilson JL, Najia MA, Saeed R, Mcdevitt TC. Alginate encapsulation parameters influence the differentiation of microencapsulated embryonic stem cell aggregates. Biotechnol Bioeng. 2014;111(3):618–31.
99. Markusen JF, Mason C, Hull DA, Town MA, Tabor AB, Clements M, et al. Behavior of adult human mesenchymal stem cells entrapped in alginate-GRGDY beads. Tissue Eng. 2006;12(4):821–30.
100. Maguire T, Novik E, Schloss R, Yarmush M. Alginate-PLL microencapsulation: Effect on the differentiation of embryonic stem cells into hepatocytes. Biotechnol Bioeng. 2006;93(3):582–91.
101. Maguire T, Davidovich AE, Wallenstein EJ, Novik E, Sharma N, Pedersen H, et al. Control of hepatic differentiation via cellular aggregation in an alginate microenvironment. Biotechnol Bioeng. 2007;98(3):631–44.
102. Salinas CN, Anseth KS. The enhancement of chondrogenic differentiation of human mesenchymal stem cells by enzymatically regulated RGD functionalities. Biomaterials. 2008;29(15):2370–7.
103. Hwang NS, Varghese S, Zhang Z, Elisseeff J. Chondrogenic differentiation of human embryonic stem cell-derived cells in arginine-glycine-aspartate-modified hydrogels. Tissue Eng. 2006;12(9):2695–706.
104. Moshaverinia A, Ansari S, Chen C, Xu X, Akiyama K, Snead ML, et al. Co-encapsulation of anti-BMP2 monoclonal antibody and mesenchymal stem cells in alginate microspheres for bone tissue engineering. Biomaterials. 2013;34(28):6572–9.
105. Anamizu M, Tabata Y. Design of injectable hydrogels of gelatin and alginate with ferric ions for cell transplantation. Acta Biomater. 2019;100:184–90.

106. Chen B, Wright B, Sahoo R, Connon CJ. A novel alternative to cryopreservation for the short-term storage of stem cells for use in cell therapy using alginate encapsulation. Tissue Eng Part C Methods. 2013;19(7):1–35.
107. Nemati S, Rezabakhsh A, Khoshfetrat AB, Nourazarian A, Biray Avci Ç, Goker Bagca B, et al. Alginate-gelatin encapsulation of human endothelial cells promoted angiogenesis in in vivo and in vitro milieu. Biotechnol Bioeng. 2017;114(12):2920–30.
108. Nemati S, Alizadeh Sardroud H, Baradar Khoshfetrat A, Khaksar M, Ahmadi M, Amini H, et al. The effect of alginate–gelatin encapsulation on the maturation of human myelomonocytic cell line U937. J Tissue Eng Regen Med. 2019;13(1):25–35.
109. Saberianpour S, Karimi A, Nemati S, Amini H, Alizadeh Sardroud H, Khaksar M, et al. Encapsulation of rat cardiomyoblasts with alginate-gelatin microspheres preserves stemness feature in vitro. Biomedicine and Pharmacotherapy. 2019;109:402–7.
110. Amini H, Hashemzadeh S, Heidarzadeh M, Mamipour M, Yousefi M, Saberianpour S, et al. Cytoprotective and cytofunctional effect of polyanionic polysaccharide alginate and gelatin microspheres on rat cardiac cells. Int J Biol Macromol. 2020;161:969–76.
111. Tang M, Chen W, Weir MD, Thein-Han W, Xu HHK. Human embryonic stem cell encapsulation in alginate microbeads in macroporous calcium phosphate cement for bone tissue engineering. Acta Biomater. 2012;8(9):3436–45.
112. Qiao P, Wang J, Xie Q, Li F, Dong L, Xu T. Injectable calcium phosphate-alginate-chitosan microencapsulated MC3T3-E1 cell paste for bone tissue engineering in vivo. Materials Science and Engineering C. 2013;33(8):4633–9.
113. Chan BP, Hui TY, Wong MY, Yip KHK, Chan GCF. Mesenchymal stem cell-encapsulated collagen microspheres for bone tissue engineering. Tissue Eng Part C Methods. 2010 Apr 1;16(2):225–35.
114. Li YY, Cheng HW, Cheung KMC, Chan D, Chan BP. Mesenchymal stem cell-collagen microspheres for articular cartilage repair: Cell density and differentiation status. Acta Biomater. 2014;10(5):1919–29.
115. Chan BP, Hui TY, Yeung CW, Li J, Mo I, Chan GCF. Self-assembled collagen-human mesenchymal stem cell microspheres for regenerative medicine. Biomaterials. 2007;28(31):4652–66.
116. Doetschman TC, Eistetter H, Katz M. The in vitro development of blastocyst-derived embryonic stem cell lines: Formation of visceral yolk sac, blood islands and myocardium. J Embryol Exp Morphol. 1985;87(1):27–45.
117. Kehat I, Kenyagin-Karsenti D, Snir M, Segev H, Amit M, Gepstein A, et al. Human embryonic stem cells can differentiate into myocytes with structural and functional properties of cardiomyocytes. Journal of Clinical Investigation. 2001;108(3):407–14.
118. Jing D, Parikh A, Tzanakakis ES. Cardiac cell generation from encapsulated embryonic stem cells in static and scalable culture systems. Cell Transplant. 2010;19(11):1397–412.

119. Mayfield AE, Tilokee EL, Latham N, McNeill B, Lam BK, Ruel M, et al. The effect of encapsulation of cardiac stem cells within matrix-enriched hydrogel capsules on cell survival, post-ischemic cell retention and cardiac function. Biomaterials. 2014;35(1):133–42.
120. Ban K, Park HJ, Kim S, Andukuri A, Cho KW, Hwang JW, et al. Cell therapy with embryonic stem cell-derived cardiomyocytes encapsulated in injectable nanomatrix gel enhances cell engraftment and promotes cardiac repair. ACS Nano. 2014;8(10):10815–25.
121. Heile A, Brinker T. Clinical translation of stem cell therapy in traumatic brain injury: The potential of encapsulated mesenchymal cell biodelivery of glucagon-like peptide-1. Dialogues Clin Neurosci. 2011;13(3):279–86.
122. Sarnowska A, Jablonska A, Jurga M, Dainiak M, Strojek L, Drela K, et al. Encapsulation of mesenchymal stem cells by bioscaffolds protects cell survival and attenuates neuroinflammatory reaction in injured brain tissue after transplantation. Cell Transplant. 2013;22(SUPPL.1):S67-82.
123. Klinge PM, Harmening K, Miller MC, Heile A, Wallrapp C, Geigle P, et al. Encapsulated native and glucagon-like peptide-1 transfected human mesenchymal stem cells in a transgenic mouse model of Alzheimer's disease. Neurosci Lett. 2011;497(1):6–10.
124. Heile AMB, Wallrapp C, Klinge PM, Samii A, Kassem M, Silverberg G, et al. Cerebral transplantation of encapsulated mesenchymal stem cells improves cellular pathology after experimental traumatic brain injury. Neurosci Lett. 2009;463(3):176–81.
125. Ngoc PK, van Phuc P, Nhung TH, Thuy DT, Nguyet NTM. Improving the efficacy of type 1 diabetes therapy by transplantation of immunoisolated insulin-producing cells. Hum Cell. 2011;24(2):86–95.
126. Han Y, Tao R, Han Y, Sun T, Chai J, Xu G, et al. Microencapsulated VEGF gene-modified umbilical cord mesenchymal stromal cells promote the vascularization of tissue-engineered dermis: An experimental study. Cytotherapy. 2014;16(2):160–9.
127. Meier RPH, Mahou R, Morel P, Meyer J, Montanari E, Muller YD, et al. Microencapsulated human mesenchymal stem cells decrease liver fibrosis in mice. J Hepatol. 2015;62(3):634–41.
128. Shah K. Encapsulated stem cells for cancer therapy. Vol. 3, Biomatter. 2013. p. 24278–85.
129. Martinez-Quintanilla J, He D, Wakimoto H, Alemany R, Shah K. Encapsulated stem cells loaded with hyaluronidase-expressing oncolytic virus for brain tumor therapy. Molecular Therapy. 2015;23(1):108–18.
130. Liu ZC, Chang TMS. Artificial cell microencapsulated stem cells in regenerative medicine, tissue engineering and cell therapy. Adv Exp Med Biol. 2010;670:68–79.
131. Firouzi N, Baradar Khoshfetrat A, Kazemi D. Enzymatically gellable gelatin improves nano-hydroxyapatite-alginate microcapsule characteristics for modular bone tissue formation. J Biomed Mater Res A. 2020;108(2):340–50.
132. Gleeson JP, Plunkett NA, O'Brien FJ. Addition of hydroxyapatite improves stiffness, interconnectivity and osteogenic potential of a highly porous collagen-based scaffold for bone tissue regeneration. Eur Cell Mater. 2010;20:218–30.

133. Wang P, Song Y, Weir MD, Sun J, Zhao L, Simon CG, et al. A self-setting iPSMSC-alginate-calcium phosphate paste for bone tissue engineering. Dental Materials. 2016;32(2):252–63.
134. Shih YR V., Hwang Y, Phadke A, Kang H, Hwang NS, Caro EJ, et al. Calcium phosphate-bearing matrices induce osteogenic differentiation of stem cells through adenosine signaling. Proc Natl Acad Sci U S A. 2014;111(3):990–5.
135. Rezaei S, Shakibaie M, Kabir-Salmani M, Moghaddam MS, Rezvani M, Shahali M, et al. Improving the growth rate of human adipose-derived mesenchymal stem cells in alginate/gelatin versus alginate hydrogels. Iran J Biotechnol. 2016;14(1):1–8.
136. Gao C, Peng S, Feng P, Shuai C. Bone biomaterials and interactions with stem cells. Vol. 5, Bone Research. 2017. p. 17059–166.
137. Shie MY, Ding SJ. Integrin binding and MAPK signal pathways in primary cell responses to surface chemistry of calcium silicate cements. Biomaterials. 2013;34(28):6589–606.
138. Aiyelabegan HT, Sadroddiny E. Fundamentals of protein and cell interactions in biomaterials. Vol. 88, Biomedicine and Pharmacotherapy. 2017. p. 1–27.
139. Rastogi S, Pandey MM, Rawat AKS. Medicinal plants of the genus Betula - Traditional uses and a phytochemical-pharmacological review. Vol. 159, Journal of Ethnopharmacology. 2015. p. 62–83.
140. Park SY, Kim HJ, Kim KR, Lee SK, Lee CK, Park KK, et al. Betulinic acid, a bioactive pentacyclic triterpenoid, inhibits skeletal-related events induced by breast cancer bone metastases and treatment. Toxicol Appl Pharmacol. 2014;275(2):152–62.
141. Yogeeswari P, Sriram D. Betulinic Acid and Its Derivatives: A Review on their Biological Properties. Curr Med Chem. 2010;12(6):657–66.
142. Fulda S. Betulinic acid for cancer treatment and prevention. Vol. 9, International Journal of Molecular Sciences. 2008. p. 1096–107.
143. Lo YC, Chang YH, Wei BL, Huang YL, Chiou WF. Betulinic acid stimulates the differentiation and mineralization of osteoblastic MC3T3-E1 Cells: Involvement of BMP/Runx2 and β-Catenin Signals. J Agric Food Chem. 2010 Jun 9;58(11):6643–9.
144. Mizerska-Kowalska M, Sławinska-Brych A, Kaławaj K, Zurek A, Pawinska B, Rzeski W, et al. Betulin promotes differentiation of human osteoblasts in vitro and exerts an osteoinductive effect on the HfOB 1.19 cell line through activation of JNK, ERK1/2, and mTOR kinases. Molecules. 2019;24(14):2637–53.
145. Fobker M. Stability of glucose in plasma with different anticoagulants. Clin Chem Lab Med. 2014;52(7):1057–60.
146. Fisher SA, Cutler A, Doree C, Brunskill SJ, Stanworth SJ, Navarrete C, et al. Mesenchymal stromal cells as treatment or prophylaxis for acute or chronic graft-versus-host disease in haematopoietic stem cell transplant (HSCT) recipients with a haematological condition. Cochrane Database of Systematic Reviews. 2019. p. 1–90.

147. Luo R, Lu Y, Liu J, Cheng J, Chen Y. Enhancement of the efficacy of mesenchymal stem cells in the treatment of ischemic diseases. Vol. 109, Biomedicine and Pharmacotherapy. 2019. p. 2022–34.
148. Ryan EA, Paty BW, Senior PA, Bigam D, Alfadhli E, Kneteman NM, et al. Five-year follow-up after clinical islet transplantation. Diabetes. 2005;54(7):2060–9.
149. Kumar PV, Jain NK. Suppression of agglomeration of ciprofloxacin-loaded human serum albumin nanoparticles. AAPS PharmSciTech. 2007;8(1):118–23.
150. Giustarini D, Dalle-Donne I, Milzani A, Rossi R. Low molecular mass thiols, disulfides and protein mixed disulfides in rat tissues: Influence of sample manipulation, oxidative stress and ageing. Mech Ageing Dev. 2011;132(4):141–8.
151. Olabisi RM. Cell microencapsulation with synthetic polymers. Vol. 103, Journal of Biomedical Materials Research - Part A. John Wiley and Sons Inc.; 2015. p. 846–59.
152. Maitz MF. Applications of synthetic polymers in clinical medicine. Biosurf Biotribol. 2015;1(3):161–76.
153. Rivera Diaz PA, Gómez Camargo DE, Ondo-Méndez A, Gómez-Alegría CJ. A colorimetric bioassay for quantitation of both basal and insulin-induced glucose consumption in 3T3-L1 adipose cells. Heliyon. 2020;6(2):1–7.
154. Leslie SK, Cohen DJ, Sedlaczek J, Pinsker EJ, Boyan BD, Schwartz Z. Controlled release of rat adipose-derived stem cells from alginate microbeads. Biomaterials. 2013;34(33):8172–84.
155. Ghobashy MM, Bassioni G. pH stimuli-responsive poly(acrylamide-co-sodium alginate) hydrogels prepared by γ-radiation for improved compressive strength of concrete. Advances in Polymer Technology. 2018;37(6):2123–33.
156. Shoichet MS, Li RH, White ML, Winn SR. Stability of hydrogels used in cell encapsulation: An in vitro comparison of alginate and agarose. Biotechnol Bioeng. 1996;50(4):374–81.
157. Hobbs HA, Kendall J, Darrabie M, Opara EC. Prevention of morphological changes in alginate microcapsules for islet xenotransplantation. In: Journal of Investigative Medicine. 2001. p. 572–5.
158. Hou L, Wu P. Exploring the hydrogen-bond structures in sodium alginate through two-dimensional correlation infrared spectroscopy. Carbohydr Polym. 2019;205:420–6.
159. Leslie SK, Nicolini AM, Sundaresan G, Zweit J, Boyan BD, Schwartz Z. Development of a cell delivery system using alginate microbeads for tissue regeneration. J Mater Chem B. 2016;4(20):3515–25.
160. Wataha JC, Hanks CT, Sun Z. Effect of cell line on in vitro metal ion cytotoxicity. Dental Materials. 1994;10(3):156–61.
161. Blázquez-Prunera A, Díez JM, Gajardo R, Grancha S. Human mesenchymal stem cells maintain their phenotype, multipotentiality, and genetic stability when cultured using a defined xeno-free human plasma fraction. Stem Cell Res Ther. 2017;8(1):103–14.
162. Mazza G, Al-Akkad W, Rombouts K, Pinzani M. Liver tissue engineering: From implantable tissue to whole organ engineering. Hepatol Commun. 2018;2(2):131–41.

163. Boonyagul S, Pukasamsombut D, Pengpanich S, Toobunterng T, Pasanaphong K, Sathirapongsasuti N, et al. Bioink hydrogel from fish scale gelatin blended with alginate for 3D-bioprinting application. J Food Process Preserv. 2021;46(8):1–9.
164. Azhar FF, Olad A, Salehi R. Fabrication and characterization of chitosan-gelatin/nanohydroxyapatite- polyaniline composite with potential application in tissue engineering scaffolds. Des Monomers Polym. 2014;17(7):654–67.
165. Lewińska D, Rosiński S, Weryński A. Influence of Process Conditions during Impulsed Electrostatic Droplet Formation on Size Distribution of Hydrogel Beads. Artif Cells Blood Substit Immobil Biotechnol. 2004;32(1):41–53.
166. Koyama R, Hakamata W, Hirano T, Nishio T. Identification of small-molecule inhibitors of human golgi mannosidase via a drug repositioning screen. Chem Pharm Bull (Tokyo). 2018;66(6):678–81.
167. Koyama R, Kano Y, Kikushima K, Mizutani A, Soeda Y, Miura K, et al. A novel Golgi mannosidase inhibitor: Molecular design, synthesis, enzyme inhibition, and inhibition of spheroid formation. Bioorg Med Chem. 2020;28(11):1–7.
168. Granneman JG, Li P, Lu Y, Tilak J. Seeing the trees in the forest: Selective electroporation of adipocytes within adipose tissue. Am J Physiol Endocrinol Metab. 2004;287(3 50-3):574–82.
169. Feng Y, Liu L, Wang J, Liu J, Hu W, Wang X, et al. Integrated refolding techniques for Schistosoma japonicum MTH1 overexpressed as inclusion bodies in Escherichia coli. Protein Expr Purif. 2012;84(2):181–7.
170. Silvestroff L, Franco PG, Pasquini JM. Neural and oligodendrocyte progenitor cells: Transferrin effects on cell proliferation. ASN Neuro. 2013;5(1):43–67.
171. Hellewell AL, Rosini S, Adams JC. A rapid, scalable method for the isolation, functional study, and analysis of cell-derived extracellular matrix. Journal of Visualized Experiments. 2017;2017(119):1–9.

9 CURRICULUM VITAE